U.S. DEPARTMENT OF COMMERCE
National Technical Information Service
PB-284 347

Characterization of Sorbent Resins for Use in Environmental Sampling

Arthur D. Little, Inc, Cambridge, Mass

Prepared for

Industrial Environmental Research Lab, Research Triangle Park, N C

Mar 78

PB 284 347

EPA U.S. Environmental Protection Agency
Office of Research and Development

Industrial Environmental Research
Laboratory
Research Triangle Park, North Carolina 27711

EPA-600/7-78-054
March 1978

CHARACTERIZATION OF SORBENT RESINS FOR USE IN ENVIRONMENTAL SAMPLING

Interagency
Energy-Environment
Research and Development
Program Report

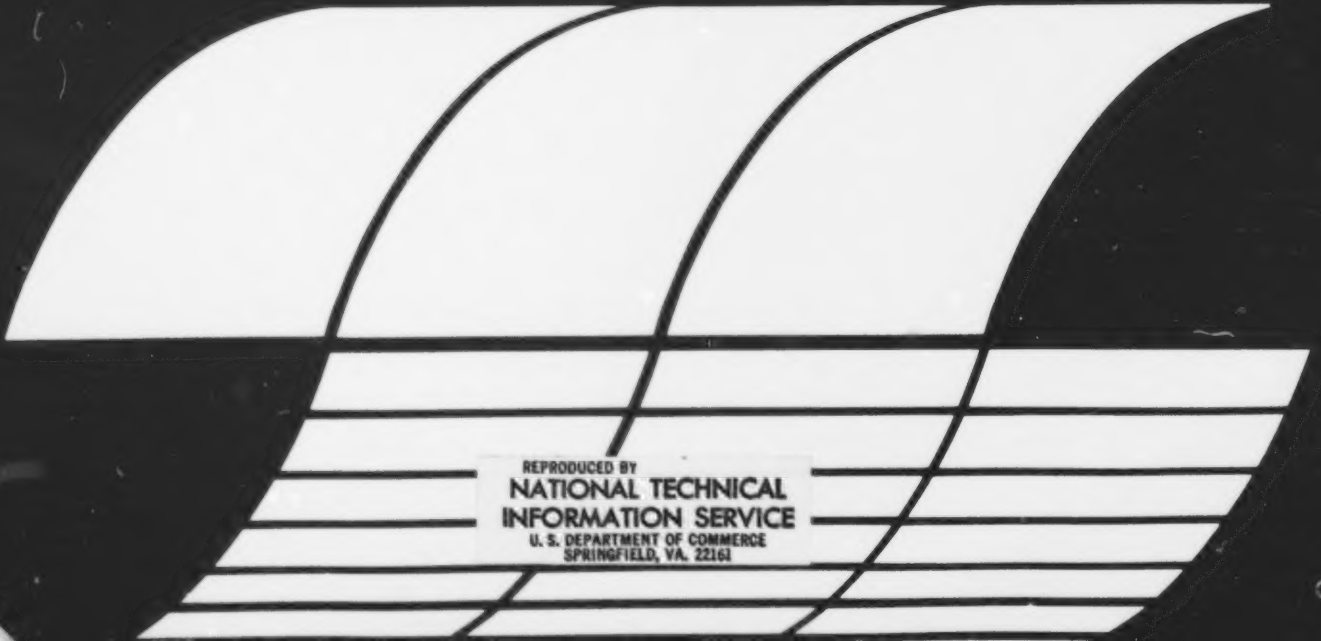

REPRODUCED BY
NATIONAL TECHNICAL
INFORMATION SERVICE
U. S. DEPARTMENT OF COMMERCE
SPRINGFIELD, VA. 22161

RESEARCH REPORTING SERIES

Research reports of the Office of Research and Development, U.S. Environmental Protection Agency, have been grouped into nine series. These nine broad categories were established to facilitate further development and application of environmental technology. Elimination of traditional grouping was consciously planned to foster technology transfer and a maximum interface in related fields. The nine series are:

1. Environmental Health Effects Research
2. Environmental Protection Technology
3. Ecological Research
4. Environmental Monitoring
5. Socioeconomic Environmental Studies
6. Scientific and Technical Assessment Reports (STAR)
7. Interagency Energy-Environment Research and Development
8. "Special" Reports
9. Miscellaneous Reports

This report has been assigned to the INTERAGENCY ENERGY-ENVIRONMENT RESEARCH AND DEVELOPMENT series. Reports in this series result from the effort funded under the 17-agency Federal Energy/Environment Research and Development Program. These studies relate to EPA's mission to protect the public health and welfare from adverse effects of pollutants associated with energy systems. The goal of the Program is to assure the rapid development of domestic energy supplies in an environmentally-compatible manner by providing the necessary environmental data and control technology. Investigations include analyses of the transport of energy-related pollutants and their health and ecological effects; assessments of, and development of, control technologies for energy systems; and integrated assessments of a wide range of energy-related environmental issues.

EPA REVIEW NOTICE

This report has been reviewed by the participating Federal Agencies, and approved for publication. Approval does not signify that the contents necessarily reflect the views and policies of the Government, nor does mention of trade names or commercial products constitute endorsement or recommendation for use.

This document is available to the public through the National Technical Information Service, Springfield, Virginia 22161.

TECHNICAL REPORT DATA

(Please read Instructions on the reverse before completing)

1. REPORT NO.
EPA-600/7-78-054

2.

3. RECIPIENT'S ACCESSION NO.
PB284347

4. TITLE AND SUBTITLE
Characterization of Sorbent Resins for Use in Environmental Sampling

5. REPORT DATE
March 1978

6. PERFORMING ORGANIZATION CODE

7. AUTHOR(S)
R. F. Gallant, J. W. King, P. L. Levins*, and J. F. Piecewicz

8. PERFORMING ORGANIZATION REPORT NO.

9. PERFORMING ORGANIZATION NAME AND ADDRESS
Arthur D. Little, Inc.
Acorn Park
Cambridge, Massachusetts 02140

10. PROGRAM ELEMENT NO.
EHB537

11. CONTRACT/GRANT NO.
68-02-2150, Task 10601

12. SPONSORING AGENCY NAME AND ADDRESS
EPA, Office of Research and Development
Industrial Environmental Research Laboratory
Research Triangle Park, NC 27711

13. TYPE OF REPORT AND PERIOD COVERED
Task Final; 3/77-1/78

14. SPONSORING AGENCY CODE
EPA/600/13

15. SUPPLEMENTARY NOTES IERL-RTP task officer is Larry D. Johnson, Mail Drop 62, 919/541-2557.

16. ABSTRACT
The report describes the use of chromatographic techniques to characterize resins which are used to trap vapors in environmental sampling schemes. It describes two such techniques (frontal and elution analysis) which have been applied to characterize sorbent cartridges packed with Tenax-GC and XAD-2 sorbents, two synthetic polymeric resins commonly used as sampling media. Three diverse adsorbate groups, consisting of eight distinct chemical classes, were studied as potential pollutants. Elution analysis of these vapors yielded specific retention volumes which can be directly related to the breakthrough characteristics of the sorbent resins under a diversity on sampling conditions. Adsorption coefficients, derivable from the specific retention volumes, vield the weight capacity of the sorbent at challenge concentrations in the Henry's Law region. Frontal analysis results confirm the elution data for sorbate uptake of resins. A slight flow rate dependence for sorbate uptake is noted for XAD-2. Specific retention volume data extrapolated to ambient conditions correlate well with adsorbate boiling point and molecular polarizability. These correlations allow breakthough and weight capacity to be estimated for a variety of adsorbate types.

17. KEY WORDS AND DOCUMENT ANALYSIS

a. DESCRIPTORS		b. IDENTIFIERS/OPEN ENDED TERMS	c. COSATI Field/Group
Air Pollution	Chromatography	Air Pollution Control	13B
Sampling	Vapors	Stationary Sources	14B
Analyzing	Elution	Frontal Analysis	07A
Polymers			07D
Sorbents			11G
Properties			

18. DISTRIBUTION STATEMENT Unlimited	19. SECURITY CLASS *(This Report)* Unclassified	21. NO. OF PAGES 163
	20. SECURITY CLASS *(This page)* Unclassified	22. PRICE PCA08 MFA01

EPA Form 2220-1 (9-73)

EPA-600/7-78-054
March 1978

CHARACTERIZATION OF SORBENT RESINS FOR USE IN ENVIRONMENTAL SAMPLING

by

R. F. Gallant, J. W. King, P. L. Levins,*
and J. F. Piecewicz

Arthur D. Little, Inc.
Acorn Park
Cambridge, Massachusetts 02140

Contract No. 68-02-2150
Task 10601
Program Element No. EHB537

EPA Task Officer: Larry D. Johnson

Industrial Environmental Research Laboratory
Office of Energy, Minerals and Industry
Research Triangle Park, N.C. 27711

Prepared for

U.S. ENVIRONMENTAL PROTECTION AGENCY
Office of Research and Development
Washington, D.C. 20460

ii

TABLE OF CONTENTS

Page

LIST OF FIGURES v

LIST OF TABLES viii

ACKNOWLEDGEMENT x

SUMMARY xi

I. INTRODUCTION 1

II. APPROACH 4

A. Frontal and Elution Analysis Methods . . . 4

B. Relation of Chromatographic Data to Sorbent-Based Collection Devices 7

III. EXPERIMENTAL TECHNIQUE AND APPARATUS 10

A. Experimental Apparatus 10

B. Choice of Adsorbates and Adsorbents 14

C. Discussion of Experimental Conditions . . . 18

IV. RESULTS AND DISCUSSION 21

A. Specific Retention (Elution) Volume Data . . 21

1. Comparison of Experimental V_g^T Values with Other Chromatographic Literature Values 26

2. Correlation of V_g^T with Adsorbate Physical Properties 28

3. Flow Rate Effects on V_g^T 59

B. Adsorption Coefficients 69

C. Heats of Adsorption 76

D. Frontal Analysis 79

E. Adsorption Isotherms 93

V. CONCLUSIONS AND RECOMMENDATIONS 103

continued....

TABLE OF CONTENTS (continued)

Page

VI. REFERENCES 105

APPENDIX A 109

APPENDIX B 133

LIST OF FIGURES

Figure No. Page

1 Relationship Between Frontal Breakthrough Curve and Elution Peak 5

2 Relationship Between Initial Retention Volume (V_I), V_g^T and Levels of Frontal Analysis Breakthrough 8

3 Gas Chromatographic Apparatus Used to Determine V_g^T and Adsorption Isotherms 11

4 Chemical Structure of Sorbent Resins 16

5 Log V_g^{20} vs Adsorbate Boiling Point for Tenax-GC . . 30

6 Log V_g^{20} vs Adsorbate Boiling Point for XAD-2 31

7 Log V_g^{20} vs Boiling Point for Individual Adsorbate Groups on XAD-2 33

8 Log V_g^{20} vs Boiling Point for Individual Adsorbate Groups on Tenax-GC 34

9 Log V_g^{20} vs Boiling Point of Adsorbate n-Alkanes on Tenax-GC 36

10 Log V_g^{20} vs Boiling Point of Adsorbate Aromatic Hydrocarbons on Tenax-GC 37

11 Log V_g^{20} vs Boiling Point of Adsorbate Halogenated Hydrocarbons on Tenax-GC 38

12 Log V_g^{20} vs Boiling Point of Adsorbate Ketones on Tenax-GC 39

13 Log V_g^{20} vs Boiling Point of Adsorbate Amines on Tenax-GC 40

14 Log V_g^{20} vs Boiling Point of Adsorbate Aliphatic Alcohols on Tenax-GC 41

15 Log V_g^{20} vs Boiling Point of Adsorbate Phenols on Tenax-GC 42

16 Log V_g^{20} vs Boiling Point of Adsorbate Aliphatic Acids on Tenax-GC 43

17 Log V_g^{20} vs Boiling Point of Adsorbate n-Alkanes on XAD-2 44

continued....

LIST OF FIGURES (continued)

Figure No. Page

18 Log V_g^{20} vs Boiling Point of Adsorbate Aromatic Hydrocarbons on XAD-2 45

19 Log V_g^{20} vs Boiling Point of Adsorbate Halogenated Hydrocarbons on XAD-2 46

20 Log V_g^{20} vs Boiling Point of Adsorbate Ketones on XAD-2 47

21 Log V_g^{20} vs Boiling Point of Adsorbate Amines on XAD-2 48

22 Log V_g^{20} vs Boiling Point of Adsorbate Aliphatic Alcohols on XAD-2 49

23 Log V_g^{20} vs Boiling Point of Adsorbate Phenols on XAD-2 50

24 Log V_g^{20} vs Boiling Point of Adsorbate Aliphatic Acids on XAD-2 51

25 Specific Retention Volume (20°C) vs Adsorbate Total Polarizability for Tenax-GC 57

26 Dependence on Electronic Polarizability α for Chromatographic Characteristics Deduced with Small Samples for the Porous Polymer Chromosorb 102 58

27 V_g^T vs Flow Rate - Ethylbenzene 60

28 V_g^T vs Flow Rate - n-Hexylamine 61

29 Incremental Surface Area Distribution (Desorption): XAD-2 63

30 Incremental Surface Area Distribution (Desorption): Tenax-GC 64

31 V_g^T vs Flow Rate - Pentanoic Acid 67

32 Frontal and Elution Chromatograms for n-Hexane at Approximately 90°C on XAD-2 80

33 Frontal and Elution Chromatograms for n-Octane at 94.7°C on XAD-2 82

continued....

LIST OF FIGURES (continued)

Figure No. Page

34 Frontal Chromatograms for n-Octane at 87.8°C on XAD-2 83

35 Frontal Chromatograms for n-Octane at 87.8°C on XAD-2 84

36 Adsorption Isotherm of Toluene on XAD-2 Derived from Frontal Analysis Results 96

37 Comparison of Adsorption Isotherms for Different Types of Adsorbates 97

38 Comparison of Sorption Isotherms Generated by Different Chromatographic Techniques at High Challenge Concentration 98

39 Comparison of Sorption Isotherms Generated by Different Chromatographic Techniques for Low Challenge Concentrations 99

40 Adsorption Isotherm Dependence on Flow Rate of Carrier Gas 101

LIST OF TABLES

Table No. Page

1 Adsorbate Group and Classification 17

2 Resin Capacity for n-Butylamine at 93.2°C on XAD-2 and a Challenge Concentration of 130 ppm (v/v) 20

3 Specific Retention Volumes (V_g) for Adsorbate Vapors on Sorbent Resins (20°C) 22

4 Comparison of V_g^T Values with Previously Reported Breakthrough Volumes on Tenax-GC . . . 25

5 Comparison of Log V_g^T Values for Selected Sorbates 27

6 Comparison of Log V_g^T Values with Values Determined by Janak (8) at 20°C on Tenax-GC 29

7 Linear Regression Parameters for Log V_g^{20} vs Boiling Point (°C) Plots of Adsorbate Classes on Tenax-GC Resin 52

8 Linear Regression Parameters for Log V_g^{20} vs Boiling Point (°C) Plots of Adsorbate Classes on XAD-2 Resin 53

9 Total Polarizability Values (α) for Adsorbates. . 55

10 Adsorption Coefficients, K_A, for Adsorbate Vapors on Sorbent Resins (20°C) 70

11 Equilibrium Sorption Capacities, q_g, for n-Alkanes and Aromatics on Sorbent Resins at 20°C and 1 ppm (v/v) Challenge Concentrations . 73

12 Weight Capacities of Adsorbates on XAD-2 Calculated from Adsorption Coefficients 74

13 Comparison of Differential Heats of Adsorption, ΔH_A, for Adsorbates on Sorbent Resins with Heat of Liquefaction, $\Delta \overline{H}_L$ 77

14 Comparison of Specific Retention Volumes Determined via Elution Chromatography with Those Determined by Frontal Analysis for n-Butylamine at 93.2°C on XAD-2 86

LIST OF TABLES (continued)

Table No. Page

15 Comparison of V_g^T and Weight Capacities for Sorbates on XAD-2 from Elution and Frontal Analysis (Gow-Mac) 87

16 Comparison of V_g^T and Weight Capacities for n-Octane on XAD-2 from Elution and Frontal Analysis 89

17 Comparison of V_g^T and Weight Capacities for Sorbates on XAD-2 from Elution and Frontal Analysis (Varian) 92

18 Comparison of the V_g^T (adsorption)/V_g^T (desorption) with Weight Capacity (adsorption)/Weight Capacity (desorption) Ratio 94

ACKNOWLEDGEMENT

This report has been submitted in partial fulfillment of the requirements on EPA Contract No. 68-02-2150, Technical Directive 10601. The authors wish to acknowledge the support and encouragement of Drs. Larry Johnson, Project Officer and Raymond Merrill, Assistant Project Officer, and thank them for their suggestions and review of the work. Thanks are also given to Dr. Charles Lochmüller, Duke University, for his encouragement and review of the work.

SUMMARY

The contents of this technical report pertain to the use of chromatographic techniques to characterize resins which are used to trap vapors in environmental sampling schemes. Two chromatographic techniques are described, frontal and elution analysis, which have been applied to characterize sorbent cartridges packed with Tenax-GC and XAD-2 sorbents. These are synthetic polymeric resins commonly used as sampling media.

Three diverse adsorbate groups, consisting of eight distinct chemical classes, were studied as potential pollutants. Elution analysis of these vapors yielded specific retention volumes, V_g^T , which can be directly related to the breakthrough characteristics of the sorbent resins under a diversity of sampling conditions. Adsorption coefficients, K_A, derivable from V_g^T, yield the weight capacity of the sorbent at challenge concentrations in the Henry's Law region.

Frontal analysis results confirm the elution data for sorbate uptake of resins. A slight flow rate dependence for sorbate uptake is noted for XAD-2. Specific retention volume data extrapolated to ambient conditions correlate well with adsorbate boiling point and molecular polarizability. These correlations allow breakthrough and weight capacity to be estimated for a variety of adsorbate types.

A definite specificity for non-polar adsorbates is exhibited by both resins. Tenax-GC and XAD-2 are approximately equivalent in their capacity to trap sorbate vapors at a given challenge concentration. This interaction is due predominantly to non-specific dispersion forces between adsorbent and adsorbate yielding Type I, Langmuir isotherms. Good agreement is observed between chromatographically-predicted breakthrough volumes and actual breakthrough in sampling experiments.

I. INTRODUCTION

In the past decade, adsorbent-filled cartridges have found increased use in the sampling of volatile and relatively non-volatile organic compounds. Among the media to which this method has been applied are ambient air and stack sampling, the characterization of water for organic compounds, and the sampling of industrial worker atmospheres for potential carcinogenic vapors. The adsorbent loaded device is generally "challenged" by the medium of interest by inducing a well-defined flow across the sorbent bed, either by the application of a sampling pump or superimposition of vacuum. Hence, by knowing the flow rate and sampling time precisely, the concentration of the species of interest can be determined.

Sorbent modules are frequently employed as one of a number of collection devices or stages in a multi-purpose sampling device, such as the EPA-SASS train (57). The SASS train sorbent trap is primarily designed to capture organic species that have sufficient volatility to pass through particulate filters upstream from the sorbent bed.

For several reasons, care must be taken in designing experiments and interpreting results with sorbent traps. Very volatile gases are retained poorly by most sorbent resins currently used in sampling devices. Other species will "break through" the trap if the sampled volume exceeds the volume or weight capacity of the sorbent.

The availability of data which describe the quantitative relationship between sorbent, chemical species and sampling volumes allows the sampling conditions to be specified so that reliable results may be obtained. The studies described in this report were designed to obtain those data.

One of the more common methods of characterizing adsorbents is the use of gas chromatography. Several reviews (1,2) attest to the popularity of this technique for thermodynamic and kinetic characterization of solid surfaces. As will be shown later, the retention time (volume) in a gas chromatography experiment is directly related to the breakthrough volume observed for an organic adsorbate in a sorbent sampler. Thus, tabulations of chromatographic retention data have intrinsic value to the chemist or engineer designing a sampling experiment involving sorbent resins. The data allow an estimate to be made as to the suitability of a particular adsorbent for the source to be sampled, the time required until breakthrough has occurred, and the amount of sorbent required to collect a sufficient amount of analyte for analytical or biological testing.

Characteristic data may be obtained by both elution analysis and frontal analysis methods. In the elution method a small quantity of sorbate is introduced to the sorbent in a short time. In the frontal method the sorbent is continuously challenged with a steady state concentration of sorbate. Research employing the gas chromatography methods for the above purposes has already been reported by several investigators (3,4,5,6). These include: studies to screen sorbent media for their appropriateness in sampling (7); the effect of other agents, such as water vapor, on the breakthrough and retention volume (8); and investigations relating the specific retention volume, V_g^T, to the breakthrough volume exhibited by the sorbent device for a particular vapor at a specified challenge concentration (9).

In an earlier report, it was shown that chromatographic retention volume data could be correlated with frontal analysis results generated by a sorbent trap exposure apparatus (10). This report expands upon the previously reported studies by examining the following factors:

1. The retention characteristics exhibited by two specific sorbent resins, XAD-2 and Tenax-GC, for a large variety of compound types, each type representing a distinct sorbate class.

2. The relationship between the equilibrium adsorption isotherm and the retention volume results obtained in the low surface coverage region (i.e., Henry's Law region), and its application to sorbent sampling device design.

3. The advantages and disadvantages of several chromatographic based methods for determining V_g^T, breakthrough curves (adsorption and desorption branches), adsorption isotherms, and weight capacity of the sorbent trap.

4. The effect of flow rate on retention volume, particularly at face velocities similar to those corresponding to actual sampling conditions.

5. The correlation of elution volume (V_g^T) data with sorbate physical properties to aid in the prediction of breakthrough volumes of other organic species.

6. The relationship between elution and frontal chromatographic approaches; an elution volume V_g^T value corresponds to the 50% breakthrough volume on a frontal breakthrough curve.

II. APPROACH

A. Frontal and Elution Analysis Methods

Several chromatographic methods have been used in this study to produce the data on specific retention volumes, adsorption isotherms, etc. The theoretical relationships unifying these approaches are given in detail in Appendix A.

The underlying principle of the experimental approach is that the specific retention volume, V_g^T, for an analyte, on a sorbent is related in a simple manner to the equilibrium adsorption coefficient, K_A, so long as the experiments are carried out at low analyte concentrations (the Henry's Law region). Under these conditions

$$V_g^T = K_A^* A_s^\circ$$

where V_g^T = specific retention volume

K_A^* = equilibrium adsorption coefficient

A_s° = adsorbent specific surface area

The experiments were conducted using both elution and frontal analysis techniques. The primary difference between frontal and elution analysis is in the method of sample introduction. In elution analysis, a small quantity of adsorbate is injected onto the sorbent cartridge in a short time. For the frontal analysis case, the sample introduction time is long and continuous. The mode of sample introduction in no way affects the appearance of the frontal boundary curve or the elution peak maxima. Both are determined by the equation given above and theoretically should appear as pictured in Figure 1.

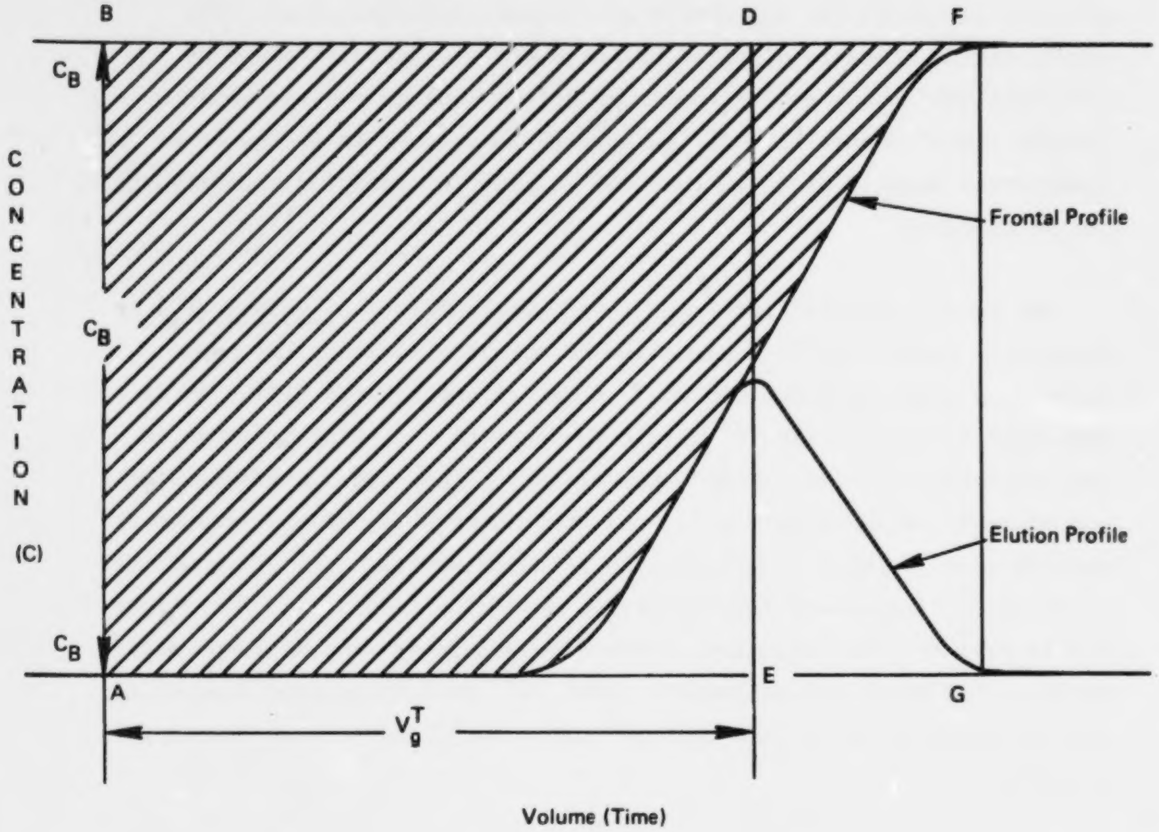
B
D
F
C_B
C_B
C_B
CONCENTRATION
(C)
Frontal Profile
Elution Profile
A
E
G
V_g^T
Volume (Time)

FIGURE 1 RELATIONSHIP BETWEEN FRONTAL BREAKTHROUGH CURVE AND ELUTION PEAK

In the frontal analysis technique, a gas containing a specified concentration of sorbate is continuously fed into the sorbent cartridge. The experimenter waits for the appearance of the boundary profile and continues to monitor the "breakthrough" of sorbate until it equilibrates with the cartridge for the challenge concentration specified. The equilibration stage is signaled by the onset of a concentration vs. time "plateau" which can be continued for as long as one wishes in a "steady state" condition. If the breakthrough curve is sharp, or a symmetrical sigmoid profile, then the equilibrium sorption capacity, q, can be computed.

The relationship of the specific retention (elution) volume (V_g^T) to measurable parameters in a gas chromatographic experiment has been derived in many standard treatises on gas chromatography (12). It is important to realize that V_g^T is the fundamental retention constant in gas chromatography and reflects the effect of flow rate, pressure drop, temperature, column void volume, and stationary phase weight (volume or surface area) on the retention of an injected solute. Knowledge of the value of V_g^T [frequently for convention corrected to 0°C (273°K)] allows one to estimate the retention volume of a solute at another temperature or for a different column length. Thus, V_g^T determined from conventional gas chromatographic columns can aid in the design of sorbent sampling modules.

The specific retention volume is also directly relatable to fundamental phase distribution constants, such as the partition coefficient, K_L, or K_A, the equilibrium adsorption coefficient. Thus if certain physical characteristics (such as A_s°) of the stationary phase are known, then K_A values can be obtained which allow calculation of sorbate distribution for sorption systems larger than analytical scale devices. Further details on specific calculation procedures and explanation of other terms used in the study are given in Appendix A.

B. Relation of Chromatographic Data to Sorbent-Based Collection Devices

The specific retention volume allows one to determine whether an organic compound is retained by a given weight of adsorbent at a specified flow rate and sampling temperature and time. If V_g^T is greater than the volume of gas passed through a sorbent during any specified time period, then the sorbate will be retained by the trap. This statement must be qualified somewhat since V_g^T actually corresponds to 50% breakthrough in an elution chromatography experiment.

This concept is illustrated in Figure 2, where the actual breakthrough of the sorbent begins to occur after V_I volumes of gas have passed over the sorbent bed. The difference between this V_I value and V_g^T can be considerable, however, there are several reasons why V_I is not routinely determined. For one, the value of V_I is dependent upon the dispersion of the chromatographic peak in the sorbent bed, thus V_I is flow rate dependent, shows a dependence on the packing structure of the sorbent column, and is difficult to precisely locate on the chromatogram. The specific retention volume V_g^T, on the other hand, is easily located and is the only point on the chromatographic band corresponding to true thermodynamic equilibrium. Provided that it is understood that V_g^T represents the 50% breakthrough volume on a corresponding breakthrough curve, a safety factor can be built into any calculation of breakthrough volume to account for the disparity between V_g^T and V_I.

Specific retention volume data in this report have been obtained at higher temperatures than the normal operation of the sorbent trap module of the SASS sampling train. Thus to obtain V_g^T data applicable to SASS train conditions requires extrapolation to a typical ambient temperature value (20°C). This is normally done by plotting the log V_g^T vs $1/T_c$ relationship and extrapolating to the desired temperature. The values of V_g^T thus obtained by extrapolation should be highly accurate if good linear regression coefficients have been obtained in fitting the experimental

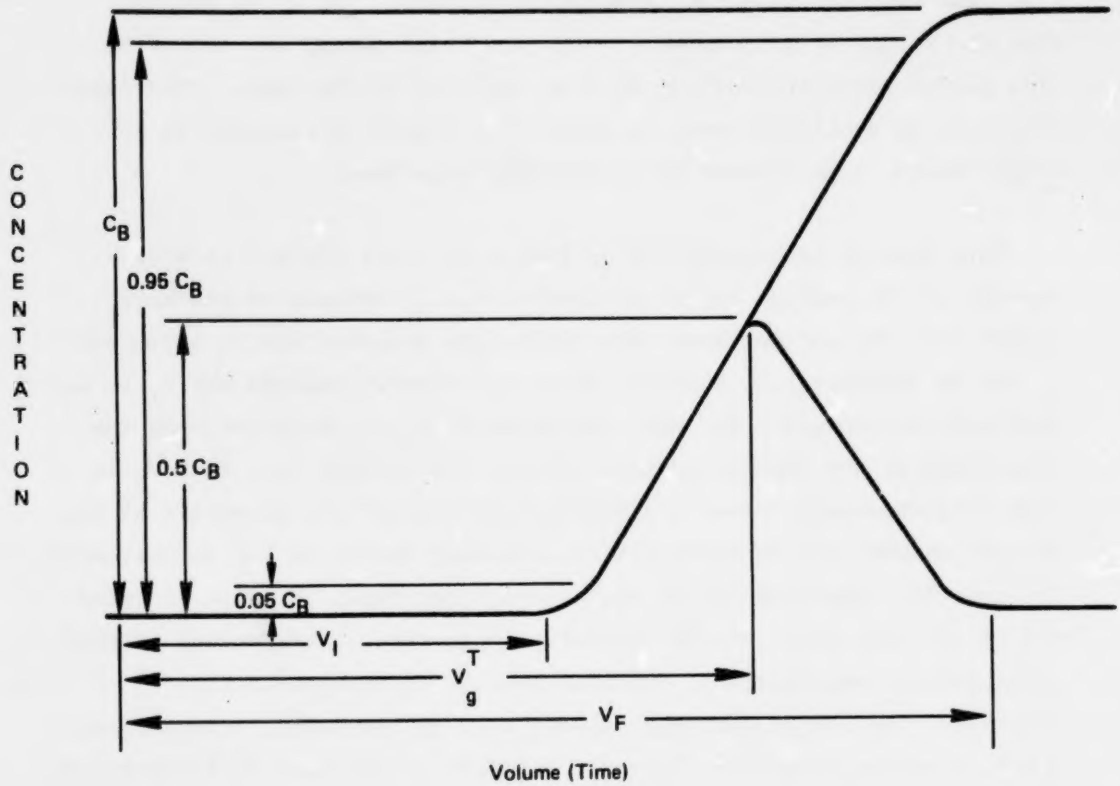

FIGURE 2 RELATIONSHIP BETWEEN INITIAL RETENTION VOLUME (V_I), V_g^T AND LEVELS OF FRONTAL ANALYSIS BREAKTHROUGH

data. A number of investigators (26,27) have employed this approach in characterizing sorbent media for environmental sampling.

A logical concern is the validity of extrapolating log V_g^T vs $1/T_c$ data to temperatures considerably lower than those upon which the regression equation is fitted. Naturally, V_g^T data should be taken as close as possible to the temperature desired but this may not be possible due to the limited volatility of the adsorbate.

A study of the temperature dependence of the adsorption isotherm is of value since q values can be obtained at constant c, challenge concentration, for a number of values of c. Unfortunately such experiments require the gathering of considerable experimental data to generate isosteres (plots of log c vs 1/T for constant c values).

The primary purpose in generating isotherms in these studies was to confirm the validity of V_g^T data in accurately predicting breakthrough from sorbent cartridges. Note, however, that the isotherm data presented here can be of value in other sampling and analysis contexts. For example, knowledge of the desorption characteristics could be of value in the thermal desorption of sorbent cartridges for chemical analyses.

III. EXPERIMENTAL TECHNIQUE AND APPARATUS

A. Experimental Apparatus

Figure 3 is a schematic of the type of apparatus used to determine elution volumes, V_g^T, and adsorption isotherms on sorbent cartridges. A commercially available gas chromatograph was modified to include a column inlet pressure gauge. The temperature of the column oven was read with a thermocouple/potentiometer. Samples were injected via microliter syringe for elution analysis while frontal analysis steady state sorbent vapor challenge concentrations were generated using a syringe-drive pump.

All concentrations cited in this report are given in ppm calculated on a volume/volume basis.

The sorbent cartridges were proportionately scaled down from the typical cross section of an SASS train sorbent resin canister. Stainless steel tubing 9 cm long, 0.45 to 0.51 cm I.D., and 0.64 cm O.D. was used to contain the resin. The internal volume of tubing was found to hold 0.40 g of 35/60 mesh Tenax-GC packing and 0.53-0.73 g of XAD-2 resin, depending upon the I.D. of the tubing.

The sorbent cartridge was connected to two 0.64 cm x 0.16 cm (1/4 in x 1/16 in) reducing unions drilled out to minimize dead volume. The resin was retained in the trap by stainless steel frits at the end of the tubing. Connections to the chromatograph were made with 0.16 cm tubing.

The weight of the resin in the cartridge was determined by difference after packing. Resins were changed frequently during the course of this study to allow the collection of data on fresh sorbent. However, our studies showed little variation in specific retention volume with use.

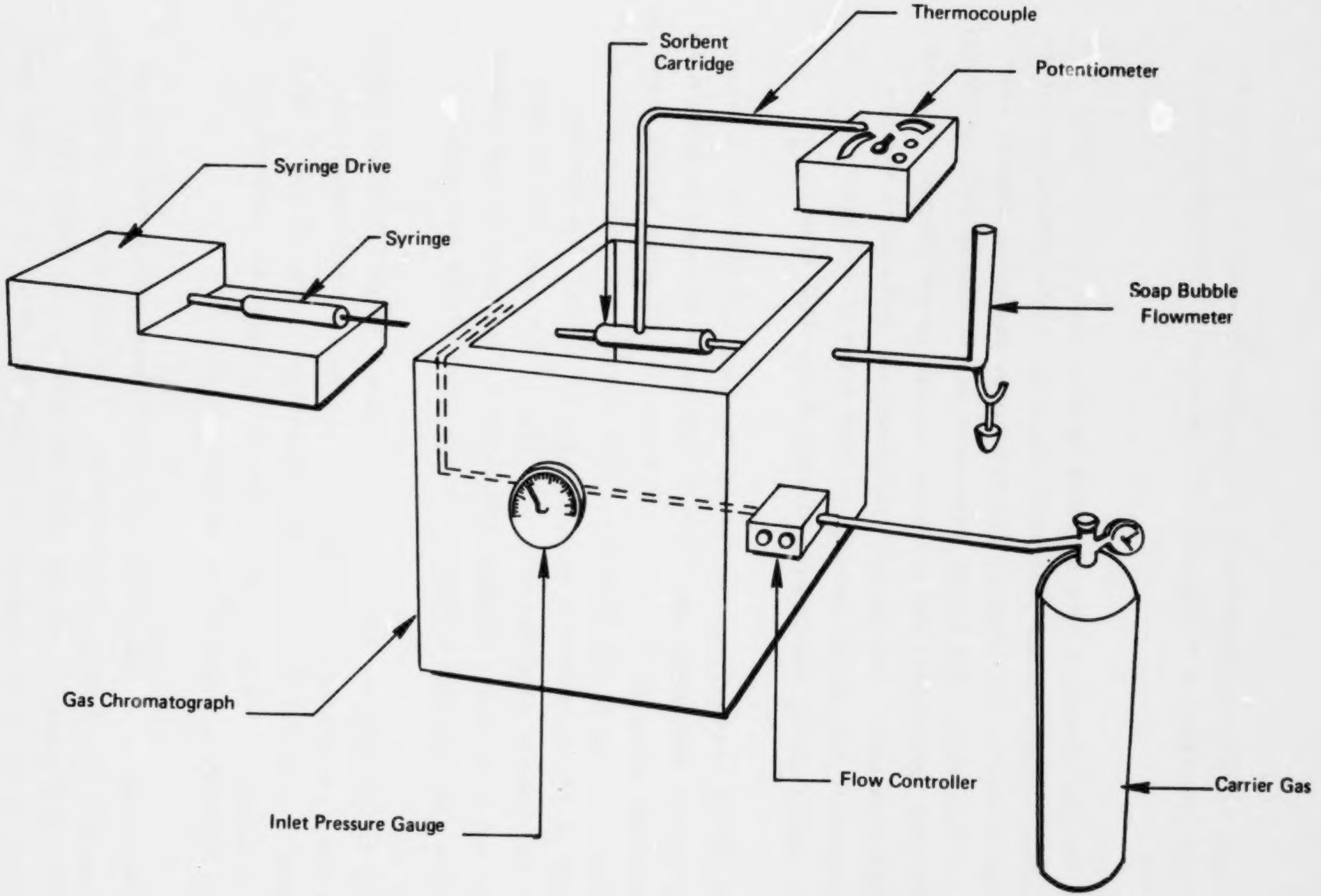
Thermocouple
Sorbent Cartridge
Potentiometer
Syringe Drive
Syringe
Soap Bubble Flowmeter
Gas Chromatograph
Flow Controller
Carrier Gas
Inlet Pressure Gauge

FIGURE 3 GAS CHROMATOGRAPHIC APPARATUS USED TO DETERMINE V_g^T AND ADSORPTION ISOTHERMS

This result is also complemented by the results obtained by Pellizzari (28) on the constancy of collection efficiency with repeated cycling of the resin.

The two gas chromatographs employed in this study were a Varian Model 1200, a single column instrument employing flame ionization detection, and a Gow-Mac 550, dual column instrument employing thermal conductivity detection. The latter instrument was outfitted with two Porter VCD 1000 flow controllers and a special Gow-Mac 10-454 thermal conductivity diffusion cell. The Gow-Mac instrument was employed to measure chromatographic fronts and peaks up to flow rates of one liter per minute, equivalent to the linear velocity in the SASS train.

The column head pressure on the Gow-Mac unit was read with a U-tube, mercury-filled manometer, the pressure reading being taken by puncturing the injection septum with a Becton-Dickinson No. 22 gauge needle connected via plastic tubing to the manometer. The thermal conductivity cell was operated at 200 milliamperes input current and at full sensitivity, due to the limited sensitivity of this type of detector and the high carrier gas flow rates. Frontal chromatograms obtained on this instrument were recorded with a Hewlett-Packard Model 17501A recorder.

The Varian 1200 was fitted with a Wallace & Tiernan pressure gauge (0-34 psig) to measure the column inlet pressure. Flow control was provided by a Brooks Model 8743 flow controller. Most of the V_g^T data were collected at maximum electrometer sensitivity and recorded on a Linear Instruments Model 355 potentiometric recorder.

The column temperatures for both gas chromatographs were measured with the aid of a Rubicon potentiometer. Iron-constantan thermocouples (No. 20) were placed in contact with the sorbent cartridges and connected to the potentiometer. To offset the effect of a "line" room temperature EMF generating junction, a second thermocouple was connected in series with the oven thermocouple at room temperature. The other end of the thermocouple was immersed in an ice bath whose temperature was read with a Fisher-ASTM calibrated thermometer. The EMF corresponding to the temperature of the bath (0.2-0.4°C) was then added to the originally measured EMF. The injector and detector temperature were usually kept 50°C higher than the highest boiling point of the injected solutes. During the frontal analysis experiments on the thermal conductivity gas chromatograph, the injection port heater was frequently turned off since the solute was injected directly onto the column in the oven proper.

Total gas flow rates were measured using a soap bubble flow meter (100 mL or 250 mL capacity) with bubble transient times being recorded with a Meyhan Model 228 stopwatch (resolution - 0.1 sec). The infusion rates for the syringe pump were also measured by the above technique using a 10.0 mL burette. The slow flow rates (0.05 to 0.5 mL/min) of gas sample infused into the sorbent column by the syringe required the use of smaller capacity soap bubble flow meters for these measurements.

Sample introduction technique varied considerably depending on whether elution or frontal analysis was being performed. The technique used in the elution analysis studies consisted of withdrawing a small amount (<1 μl) of liquid sorbate in a 10 μl syringe, expelling the liquid and pumping the syringe 50 times. This would generate a reproducible dilute sorbate vapor concentration. With these low concentration samples the experiments were able to be conducted in the Henry's Law region and symmetrical peaks were obtained. For solid sorbates (i.e., phenols) samples were obtained from the headspace in a sealed vial. Typically, a 2.5 mL Hamilton gas-tight syringe was used for these studies. Frontal analysis chromatograms were generated using a Harvard Apparatus Model 944 infusion/withdrawal pump.

A typical laboratory procedure for introducing the vapor contained in a finite gaseous volume into the sorbent bed consisted of withdrawing a known concentration of vapor into a gas-tight syringe from a gas-tight sampling bag. The contents of the syringe (Precision Scientific Series A-2, 5 cc Pressure Lok) were then metered in through the injection port of the gas chromatograph using the infusion syringe pump. An 8-inch, 20-gauge hypodermic needle was employed to allow direct injection of the gas samples onto the sorbent cartridge.

A 5-liter sampling bag from Calibrated Instruments, Inc., was partially filled with a precisely measured quantity of He, the latter being measured by a Singer Dry Gas Meter, with appropriate corrections for temperature and pressure. The required amount of liquid sample was added via syringe into the bag through a septum to give a particular vapor concentration. To assure that the saturation vapor pressure of the organic solute was not exceeded, vapor pressures were calculated by use of the Antoine equation and the saturation concentration of the vapor determined in the sampling bag. All concentrations were kept below this limit.

Determination of the appropriate chromatographic conditions (infusion rate, flow rate, attenuation, etc.) for the solute was done using elution chromatography as a preliminary scanning technique. In addition, running elution chromatograms also allowed a comparison between V_g^T at the level of the plateau concentration and that corresponding to the maximum of the elution peak. Three to four replicate frontal chromatograms were run per compound. The amount of gas delivered via the syringe drive was measured 4-5 times using a 10.0 mL soap bubble flow meter. Typical infusion rates of 0.3-0.6 mL/min were used.

B. Choice of Adsorbates and Adsorbents

As noted in the introduction, two adsorbents have been investigated in this study, Tenax-GC and XAD-2. These sorbents differ in several of their physical properties. Some key properties of these resins are listed below.

Sorbent	Mesh Size	Bulk Density (g/cc)	BET Surface Area (m^2/g)	Pore Volume (cc/g)
XAD-2	20 - 50	0.38	364	0.854
Tenax-GC	35 - 60	0.14	23.5	0.053

The surface area of XAD-2 is about 15 times larger than Tenax-GC. The pore size distribution of both resins as determined by mercury porosimetry allows both sorbents to be classified as microporous in character (29). XAD-2 does contain a small fraction of its total pores in the range of 170-325Å.

The XAD-2 used in these studies was cleaned according to the EPA Level 1 procedures by serial extraction with water, methanol and methylene chloride. Tenax-GC, obtained from Applied Science Laboratories, Inc., State College, Pa., was used as received. The polymers differ in chemical structure, XAD-2 being a cross-linked styrene-divinylbenzene polymer while Tenax-GC is poly (p-2,6-diphenyl-phenylene oxide). The chemical structures of both porous polymers are given in Figure 4. Tenax-GC is stable at temperatures up to 400°C. XAD-2 darkens at temperatures above 150°C, hence the taking of retention data was limited to temperatures below 190°C. A complete summary of the physical properties of the two resins was given in the earlier report (10).

Tenax-GC and XAD-2 are both classified as weak Type III adsorbants according to the classification scheme of Kiselev (30). The basis for this classification is that localized negative charges are available for interaction with the adsorbate molecules. For XAD-2, the aromatic π electrons are the negative charged moiety, while for Tenax-GC, both aromatic π electrons and the ether oxygen lone pair electrons are available for nonspecific and specific interaction with the adsorbate.

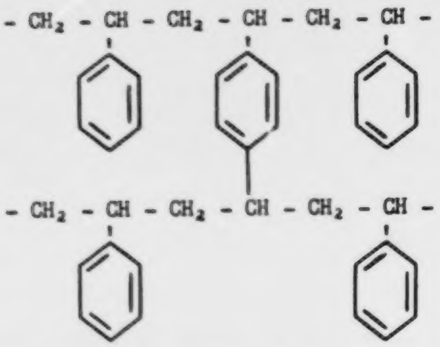

XAD-2

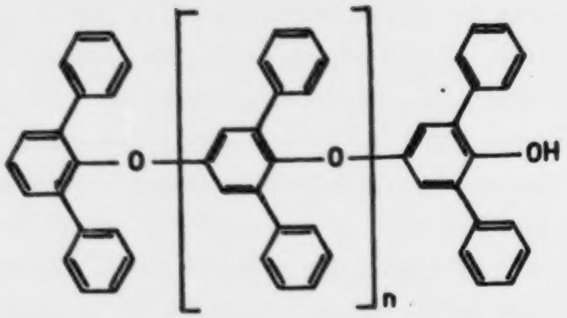

Tenax-GC

Figure 4. Chemical Structure of Sorbent Resins

In order to measure the specificity of the resin for a particular class of adsorbates and to provide a data base of V_g^T values for general use, adsorbates were chosen to represent three of four sorbate classes* specified by Kiselev (Table 1). The adsorbate groups chosen for this study and their classification were as follows:

Table 1

Adsorbate Group	Group Classification
n-Alkanes	A
Aromatic Hydrocarbons	B
Halogenated Hydrocarbons	B
Ketones	B
Tertiary Amines	B
Primary Amines	D
Secondary Amines	D
Phenols	D
Aliphatic Alcohols	D
Aliphatic Acids	D

The n-alkanes represent Group A, while aromatic hydrocarbons, ketones, and tertiary amines fall into a Group B category according to Kiselev. Group D sorbates include such chemical moieties as primary and secondary amines, alcohols and acids, all compounds capable of specific interactions with Type III adsorbents.

In general, the adsorbent and adsorbate physical properties, particularly vapor pressure of the sorbate, determined the temperature range in which the experiments were run. Such factors as elution time and sharpness of the boundary or peak determined the upper and lower temperature over which V_g^T data could be recorded.

---

*Kiselev's category C, which includes for example organo-metallics, was omitted.

C. Discussion of Experimental Conditions

In order to obtain symmetrical elution peaks corresponding to sorbate vapor concentrations in the Henry's Law region, great care had to be taken to obtain as small a sample as possible. Unfortunately, even with the dilute vapor samples obtained by consecutively pumping the vapor space of the syringe, some skewing of the chromatogram was observed. Other investigators (9,31) have also noted this phenomena. In general, the small amount of asymmetry does not have a significant effect on the V_g^T data.

Elution experiments run on the thermal conductivity gas chromatograph required maximum detector sensitivity and extremely small samples (sometimes resulting in only 1% full-scale recorder response) to approach the Henry's Law region. This approach was extremely challenging for the high flow rate experiments done on that unit since the sample was further diluted by the high volume of carrier gas passing through the cell.

Several experiments were conducted to see if the V_g^T obtained by sequential vapor space pumping of the injection syringe compared well with a method using dilute solutions of the solute in CS_2. The latter technique had been employed in the earlier studies (10). Some improvement was noted, but the improved precision obtained was in part due to the improved experimental apparatus used to determine V_g^T. For example, the relative standard deviation in V_g^T for n-octane at 135°C was 0.0199 compared to 0.112 previously recorded for this solute. A similar trend was also apparent at 109°C (0.0331 compared to 0.112 for the previous chromatographic apparatus) for n-octane.

In addition, it was noted that the V_g^T values for n-octane were somewhat higher than those obtained earlier (10). To determine whether the presence of CS_2 had affected V_g^T, an n-octane sample was spiked with a finite volume of CS_2. The specific retention volume obtained was lower than that found for a vapor sample introduced by the successive pumping technique.

The reproducibility of the frontal analysis curves can best be ascertained by noting the precision associated by integrating the curves representing vapor uptake in front of the boundary curve. Table 2 is an example of some resin sorbent capacities calculated for n-butylamine at a challenge concentration of 130 ppm (v/v) on XAD-2. The precision of the technique is excellent as judged from reproducibility shown in Table 2.

The temperature dependence of V_g^T was obtained via a linear regression fit of log V_g^T vs $1/T_c$ plots. Cursory examination of the correlation coefficients tabulated in Appendix B for these data indicates that very acceptable correlation was obtained and that extrapolated V_g^T values may be used with confidence.

Table 2

Resin Capacity for n-Butylamine at 93.2°C on XAD-2 and a Challenge Concentration of 130 ppm (v/v)

Run		Resin Sorption Capacity
1		0.249 mg/g of resin
2		0.238 mg/g of resin
3		0.221 mg/g of resin
4		0.242 mg/g of resin
	Average	0.238 mg/g of resin
	Standard Deviation	0.012

IV. RESULTS AND DISCUSSION

A. Specific Retention (Elution) Volume Data

Experimentally determined V_g^T data for each temperature are presented in Appendix B. These are entered for each adsorbate class on the specified resin. The listed V_g^T represent the average of these experimentally determined V_g^T values for each compound at the specified temperature. For each sorbate, the regression constants (slope, intercept) and the resultant correlation coefficient are tabulated. These data should easily permit the extrapolation or interpolation to obtain V_g^T at any desired temperature.

The regression equations for the log V_g^T vs $1/T_c$ plots have been used to tabulate V_g^T values at 20°C for all the sorbates investigated. These are presented in Table 3 for both XAD-2 and Tenax-GC resins. Examination of the data in Table 3 shows that, for most sorbates, the V_g^T values on XAD-2 and Tenax-GC are comparable, within an order of magnitude. The quantitative differences between the values may, of course, be very significant in the design of sampling equipment.

For the 39 adsorbates tested on both resins, 25 of the V_g^T's on Tenax-GC are greater than those on XAD-2. Three sorbate classes, the n-alkanes, halogenated hydrocarbons, and ketones, showed greater V_g^T's on Tenax-GC than XAD-2 for all the individual members of those classes. A decided preference is shown for XAD-2 by the aliphatic alcohols (four out of six) and by the four phenolic solutes investigated.

It is interesting to note that two of the lower members of a homologous series (the aliphatic alcohols and aliphatic acids) have V_g^T's that are greater on XAD-2 than Tenax-GC. An opposite trend is noted for the sorbates in these series having a carbon number of three or higher. For the three aliphatic amines examined, the V_g^T's are greater

Table 3

Specific Retention Volumes (Vg)* for Adsorbate Vapors on Sorbent Resins (20°C)

Adsorbate	Tenax-GC	XAD-2
n-Hexane	2.58×10^4	4.14×10^3
n-Octane	1.89×10^5	6.45×10^4
n-Decane	3.08×10^6	5.06×10^5
n-Dodecane	2.19×10^8	---
Benzene	6.09×10^4	5.24×10^4
Toluene	7.88×10^5	2.58×10^5
p-Xylene	3.81×10^5	9.05×10^5
Ethylbenzene	8.36×10^5	5.64×10^5
n-Propylbenzene	1.53×10^6	4.61×10^6
1,2-Dichloroethane	2.32×10^4	1.96×10^4
Fluorobenzene	8.82×10^4	3.13×10^4
1,1,2-trichloroethylene	8.82×10^4	3.06×10^4
Chlorobenzene	2.36×10^6	2.43×10^5
Bromobenzene	8.41×10^6	6.39×10^5
1,4-Dichlorobenzene	1.73×10^7	2.33×10^6
2-Butanone	2.21×10^4	4.39×10^3
2-Heptanone	5.55×10^6	1.49×10^6
4-Heptanone	3.22×10^6	1.52×10^6
Cyclohexanone	1.36×10^6	3.66×10^5
3-Methyl-2-butanone	6.46×10^4	2.53×10^4
3,3-Dimethyl-2-butanone	--	8.59×10^4
2,6-Dimethyl-4-heptanone	--	1.61×10^7
Acetophenone	1.23×10^7	7.70×10^6
n-Butylamine	2.67×10^4	1.80×10^4
n-Amylamine	1.96×10^5	1.29×10^5
n-Hexylamine	7.35×10^5	4.80×10^5
Benzylamine	1.58×10^6	7.87×10^6
Di-n-butylamine	1.91×10^6	6.90×10^6
Tri-n-butylamine	4.85×10^5	--

continued...

Table 3 (continued)

Specific Retention Volumes (Vg)* for Adsorbate Vapors on Sorbent Resins (20°C)

Adsorbate	Tenax-GC	XAD-2
Ethanol	9.08×10^2	1.75×10^3
n-Propanol	5.71×10^3	9.31×10^3
n-Butanol	4.34×10^4	2.07×10^4
2-Butanol	1.86×10^4	2.04×10^4
2-Methyl-2-propanol	7.08×10^2	1.60×10^3
2-Methyl-1-propanol	2.88×10^4	1.28×10^4
Phenol	2.47×10^6	3.68×10^6
o-Cresol	1.00×10^7	1.33×10^7
p-Cresol	1.40×10^7	1.51×10^7
m-Cresol	1.18×10^7	1.55×10^7
Acetic Acid	3.20×10^3	7.07×10^3
Propionic Acid	1.73×10^4	4.00×10^4
n-Butanoic Acid	1.04×10^5	7.74×10^4
n-Pentanoic Acid	5.53×10^5	2.89×10^5

---

* In units of mL/g.

on Tenax-GC than on XAD-2.

The design of sampling experiments based on these data is relatively simple. The sample volume divided by the weight of the sorbent resin should be less than V_g^T. To allow for some margin of safety, the gas volume sampled per gram of resin should be not more than one-half of the relevant V_g^T value. This is important particularly in cases where the elution peak profile is extremely broad.

For example, two solutes, 2,6-dimethyl-4-heptanone and 3,3-dimethyl-4-heptanone, were difficult to chromatograph on Tenax-GC due not only to their short retention times, but resultant skewed peak profile. These observations are consistent with literature reports (32) of anomolous peak broadening of methyl-branched ketones on porous polymer packing, which in part may be due to the restricted diffusion of the sorbate in the pores of the polymeric substrate.

The V_g^T values obtained in this study have been compared (Table 4) with breakthrough volumes reported by Pellizzari (28) in his study, which included five of the sorbates included in this report. The breakthrough volumes obtained by Pellizzari are listed in the last column on Table 4. For several sorbates--methyl ethyl ketone, toluene, and 1,1,2-trichloroethylene--the agreement is excellent. In all the comparisons listed, the V_g^T and breakthrough volume are never different by more than an order of magnitude. In all but one case the V_g^T is greater than the cartridge breakthrough volumes. This confirms earlier statements that V_g^T will probably be greater than actual breakthrough volumes, since V_g^T is determined at the actual peak maxima and not V_I. However, the V_g^T still allows for a reliable estimate to be made of the sample parameters to minimize loss of collected sample.

Table 4

Comparison of V_g^T Values with Previously Reported Breakthrough Volumes on Tenax-GC

Adsorbate	V_g^T (This Study)	Breakthrough Volume (Pellizari, Ref. 28)
2-Butanone	2.21×10^4	2.0×10^4 (1)
Acetophenone	1.23×10^7	1.34×10^6 (2)
Toluene	7.88×10^5	8.23×10^5 (3)
1,1,2-Trichloroethylene	8.82×10^4	4.84×10^4 (4)
Chlorobenzene	2.36×10^6	3.27×10^5 (5)
1,1,2-Trichloroethylene	8.82×10^4	5.16×10^4 (6)
Chlorobenzene	2.36×10^6	3.26×10^5 (7)

Notes: All values in mL/g.

(1) Table 3, p. 15, Ref. 28, figures at sampling rate of 4 L/min.

(2) Table 15, p. 34, Ref. 28, volume required to elute 1/2 of the adsorbed vapor @ 25°C.

(3) Table 18, p. 38, Ref. 28, breakthrough for field sampling study, assumed cartridge contains ∿2.15 g based on geometric considerations, sampling time = 150 mins, 1,770 L - volume air sampled.

(4) Table 19, p. 39, Ref. 28, breakthrough study, assumed cartridge length ∿ weight of resin, so 1.5 cm I.D. x 3 cm in length cartridge should contain 1.075 g Tenax-GC breakthrough volume represents 50% pt.

(5) Same as (4)

(6) Table 20, p.46, Ref. 28, breakthrough volume

(7) Same as (6)

1. Comparison of Experimental V_g^T Values with Other Chromatographic Literature Values

In order to determine the accuracy of the V_g^T data presented in this report, an extensive review of the literature was conducted for published retention volume data on the two substrates, XAD-2 and Tenax-GC. Although a reference compendium of the chromatographic applications of porous polymers is available, relatively little temperature dependent V_g^T data exists.

One particular reference appropriate for comparison purposes is the work of Butler and Burke (9) who used 6.40 to 30.7 cm long, 1.6 mm and 3.2 mm O.D. sorbent packed tubes filled with Tenax-GC and Chromosorb 102, an XAD-2 analog. Table 5 compares the results obtained by Butler and Burke with the data obtained in this study. The agreement is excellent for benzene on both resins and for methyl ethyl ketone and t-butanol on Tenax-GC.

V_g^T values for the ketone and alcohol on XAD-2 are in serious disagreement. There is no apparent explanation for the difference between the V_g^T values for methyl ethyl ketone. The value for t-butanol reported by Burke *et al*. seems inconsistent with the other trends observed in their data (note how similar V_g^T is for both the Tenax-GC and Chromosorbs for MEK and benzene).

Burke's data was obtained by extrapolation of V_g^T vs. $1/T_c \times 10^3$ plots up to 200°C. Burke notes that the correlation coefficient for this relationship for the Tenax-GC/t-butanol combination was poor due to the sample size being in the non-linear region of the sorption isotherm. Still the values obtained in this study agree well with those of Burke.

Table 5

Comparison of Log V_g^T Values for Selected Sorbates

	---------------- Log V_g^{20} ----------------		
Adsorbent/Adsorbate	t-Butanol	Methly Ethyl Ketone	Benzene
Literature Results			
Tenax-GC	2.867	4.612	4.921
Chromosorb 101	2.843	4.762	4.749
Chromosorb 102	4.763	4.833	4.954
This Study			
Tenax-GC	2.850	4.345	4.785
XAD-2	3.203	3.643	4.719

Additional confirmation of the accuracy of reported V_g^T's are provided by a comparison of the results reported by Janak and coworkers (8) for solutes: ethanol, propanol and benzene on Tenax-GC. Table 6 shows that the agreement is excellent for these three sorbates. It should be noted that one log V_g^T value for n-propanol is at 25°C (since listed regression coefficients gave values both at 25°C and 20°C that were in conflict with the values reported in the text).

2. Correlation of V_g^T with Adsorbate Physical Properties

The determination of a large number of V_g^T values for potential pollutants is at best a laborious task, hence a correlation scheme which would permit V_g^T to be ascertained from the physical properties of the adsorbate would be of immense value. In the previous work (10), it was noted that a possible correlation might exist between log V_g^T of the sorbate and its boiling point at atmospheric pressure. This assumed relationship was based on a correlation between log V_g^T and boiling point for a limited number of adsorbates, and on literature data (33). The correlations obtained showed a linear dependence between log V_g^T and boiling point; thus making predictions of V_g^T and therefore sorbate breakthrough times and capacities on adsorbates readily available for a large number of compounds. However, it was also noted that some sorbates deviated from this relationship, particularly on XAD-2.

Figures 5 and 6 depict the relationship between log V_g^T and atmospheric boiling points (34,35) for all sorbates in all chemical classes chromatographed on Tenax-GC and XAD-2, respectively. The V_g^T values are for 20°C. The linear regression coefficients for all of the data are quite low--0.800 for Tenax-GC and 0.849 for XAD-2 resin. The dashed lines represent a typical SASS train sampling limit (4-hour sampling time at 4 scfm) for resin charges of 130 g (XAD-2) and 29 g (Tenax-GC) in the SASS train sorbent trap.

Table 6

Comparison of Log V_g^T Values with Values Determined by Janak (8) at 20°C on Tenax-GC

	--------------Laboratory----------------	
Adsorbate	Janak	This Study
Ethanol	3.061	2.958
n-Propanol	3.761*	3.757
Benzene	4.667	4.785

*Value at 25°C.

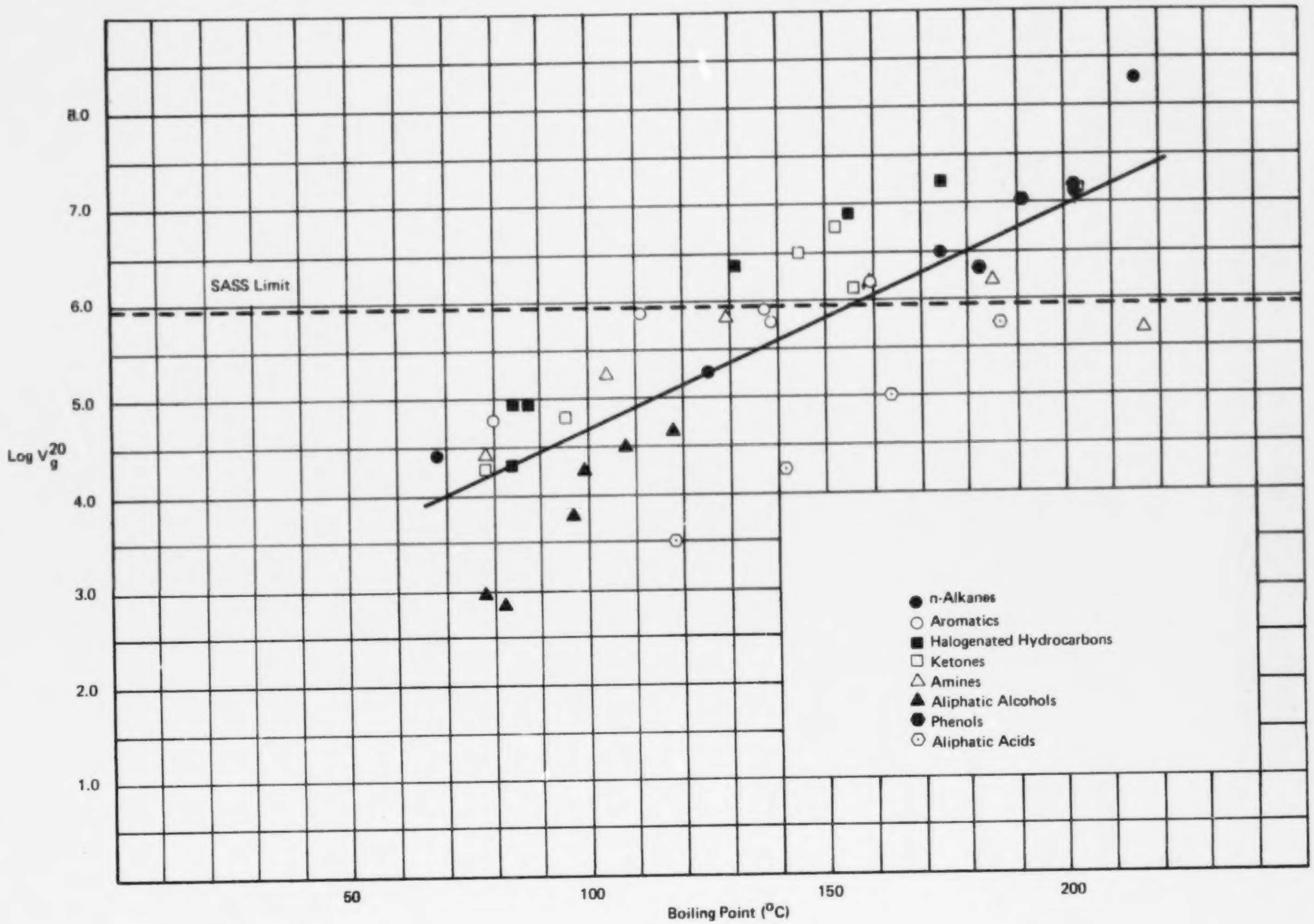

FIGURE 5 LOG V_g^{20} VS. ADSORBATE BOILING POINT FOR TENAX–GC

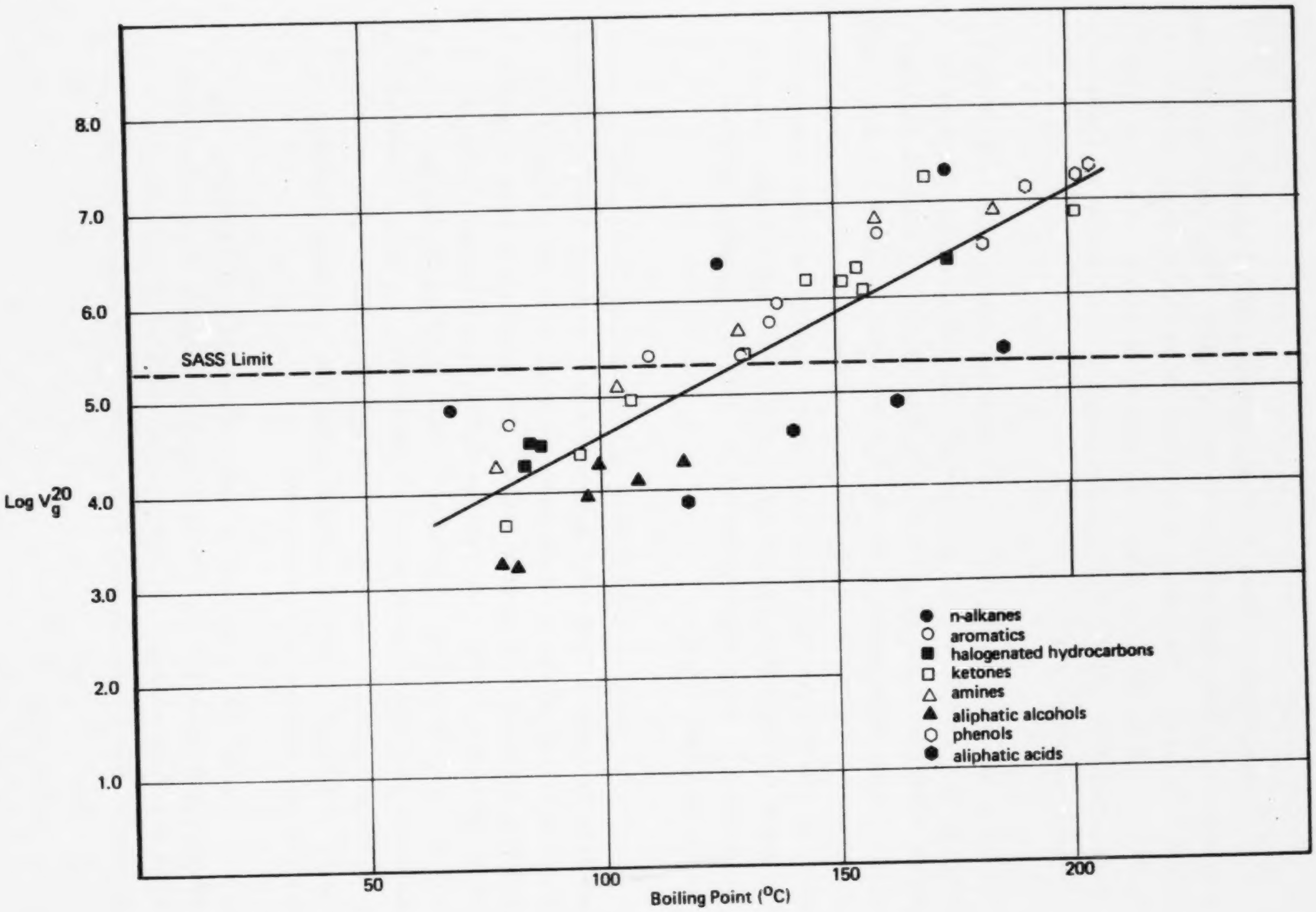

FIGURE 6 LOG V_g^{20} VS. ADSORBATE BOILING POINT FOR XAD-2

The sorbates lying above the dashed line would be adequately retained under the sampling conditions used while those below would break through the trap. The cutoff point seems to be for solutes having a boiling point of 130°C on XAD-2 and 150°C on Tenax-GC. Different sampling conditions and/or resins might permit the collection of the more volatile and polar adsorbates.

Matching of the data points with the legend code in Figures 5 and 6 indicates that within a single chemical class there frequently exists a better linear relationship between V_g^T and the sorbate boiling point. These relationships are plotted in Figures 7 and 8 for each class of sorbates. The parallel relationship between these classes, particularly on XAD-2 resin, has been observed by a number of other researchers. The lines have not been extrapolated beyond the range of experimentally determined V_g^T. Each line represents the linear regression relationship for the compound class.

The vertical displacement of each sorbate class reflects the specificity shown by the resin matrix for that class of adsorbates. There is a clear preference for non-polar adsorbates (such as n-alkanes and aromatic hydrocarbons) on both resins. The more polar, Group D adsorbates, such as aliphatic alcohols and acids, are retained the least. This selectivity pattern is similar to that observed by Kiselev (36), and indicates that, although Tenax-GC and XAD-2 are both Type III adsorbents with the potential for nonspecific and specific interactions, the nonspecific, dispersion forces are dominating the retentive interactions between both resins and the sorbates.

Certain exceptions in these trends do exist however. For example, halogenated hydrocarbons are preferentially retained on Tenax-GC as opposed to XAD-2. Increased selectivity of n-aliphatic hydrocarbons on XAD-2 resin is also found. The V_g^T for phenols on Tenax-GC

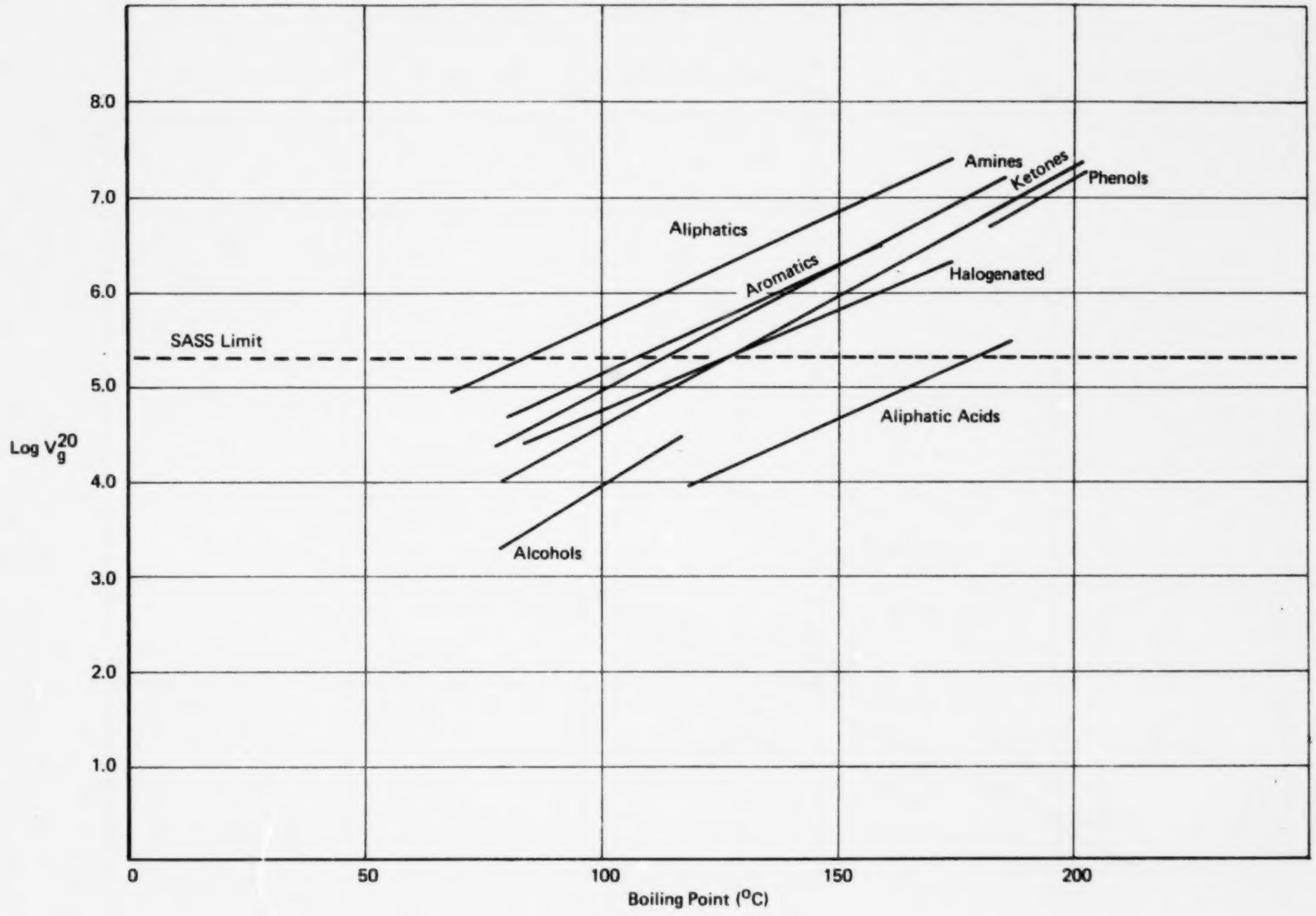

FIGURE 7 LOG V_g^{20} VS. BOILING POINT FOR INDIVIDUAL ADSORBATE GROUPS ON XAD–2

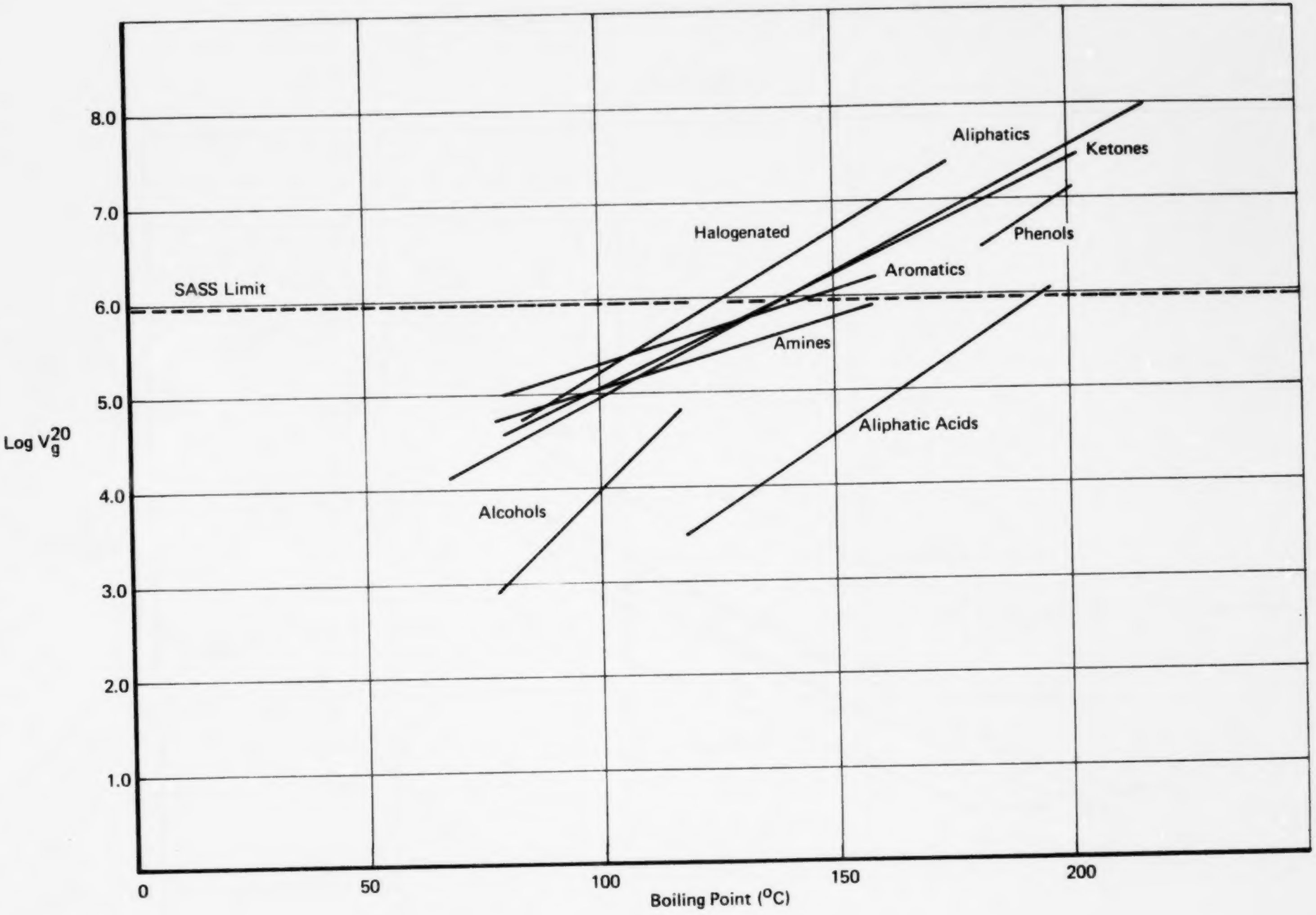

FIGURE 8 LOG V_g^{20} VS. BOILING POINT FOR INDIVIDUAL ADSORBATE GROUPS ON TENAX – GC

seems to be an extension of the V_g^T trend observed for the aromatic hydrocarbons on this sorbent. However, the phenols on XAD-2 resin are aligned with the V_g^T vs boiling point trend observed for the aliphatic alcohols.

Figures 9-16 and Figures 17-24 are the individual V_g^T data vs. boiling point curves for each sorbate class. Linear regression has been applied to these data and the slope, intercept and regression coefficients for the fitted line are included in Table 7 for Tenax-GC elution and in Table 8 for XAD-2. These parameters were used for the lines in Figures 7 and 8.

In general, considering that the adsorbate classes do not always consist of members of a homologous series, the correlations are adequate for predictive purposes. On Tenax-GC the n-alkanes (Figure 9), halogenated hydrocarbons (Figure 11), ketones (Figure 12), aliphatic alcohol (Figure 14), and aliphatic acids (Figure 16) all show good linearity when the log V_g^T vs. boiling points relationships are plotted. It could appear that the value for toluene in Figure 10 is in error and accounts for the regression coefficient found for this particular set of data. The data for the amines (Figure 13) had a correlation coefficient of 0.71 when all of the data were used. The correlation was considerably improved when the data point corresponding to tri-n-butylamine was omitted. This has been done for the regression line shown in the figure (correlation coefficient 0.91). It is interesting to note that of the amines in Figure 13, tri-n-butylamine is the only member which is not a Group D type adsorbate. Even the phenols exhibit a regression coefficient above 0.90, which is rather remarkable considering the limited variation in structure studies in this class of sorbates.

It is worth noting that even higher correlation coefficients can be obtained in some cases (for the n-alkylamines and n-alcohols), if only the members of a homologous series in the adsorbate class are

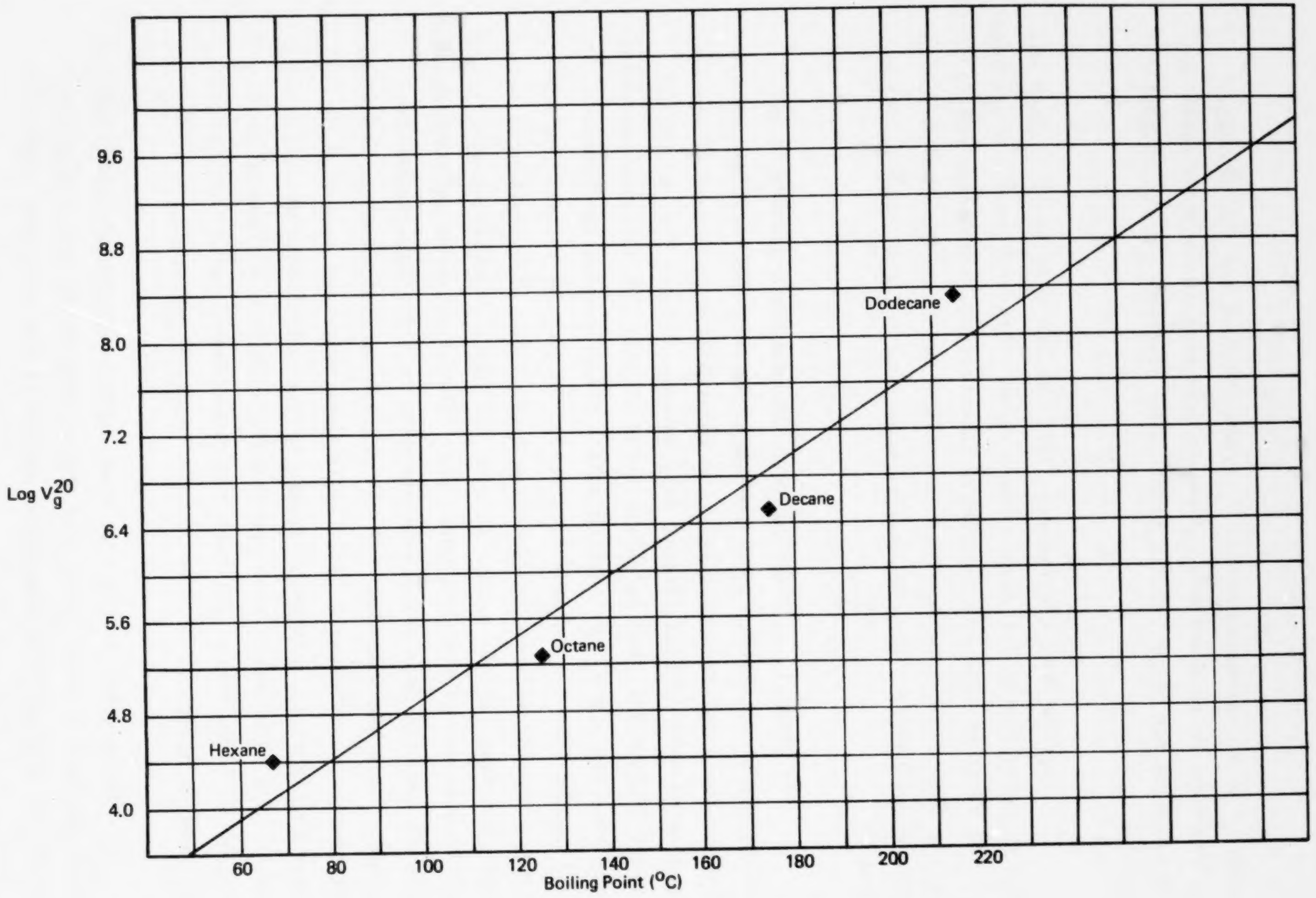

FIGURE 9 LOG V_g^{20} VS. BOILING POINT OF ADSORBATE n-ALKANES ON TENAX–GC

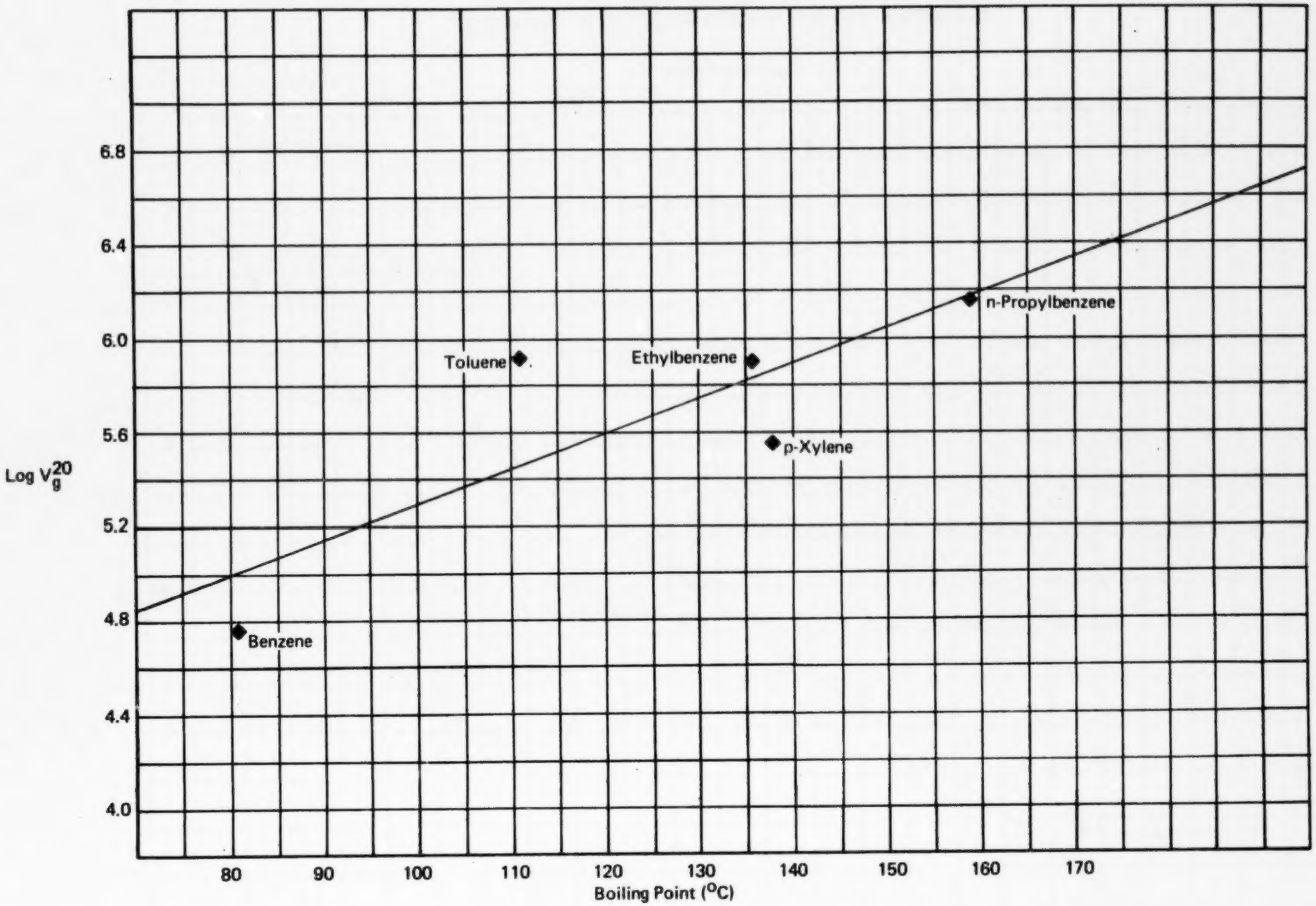

FIGURE 10 LOG V_g^{20} VS. BOILING POINT OF ADSORBATE AROMATIC HYDROCARBONS ON TENAX–GC

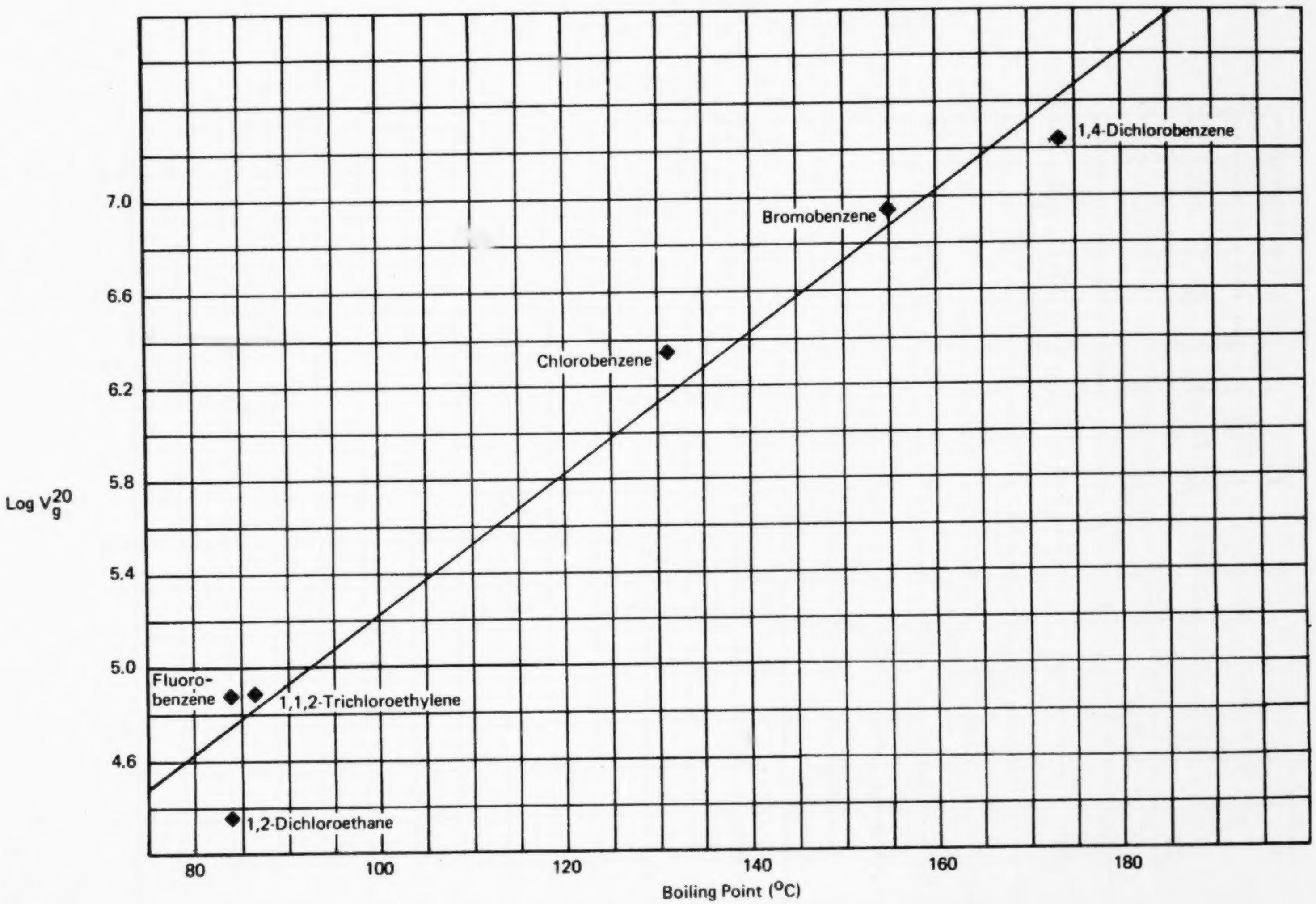

FIGURE 11 LOG V_g^{20} VS. BOILING POINT OF ADSORBATE HALOGENATED HYDROCARBONS ON TENAX–GC

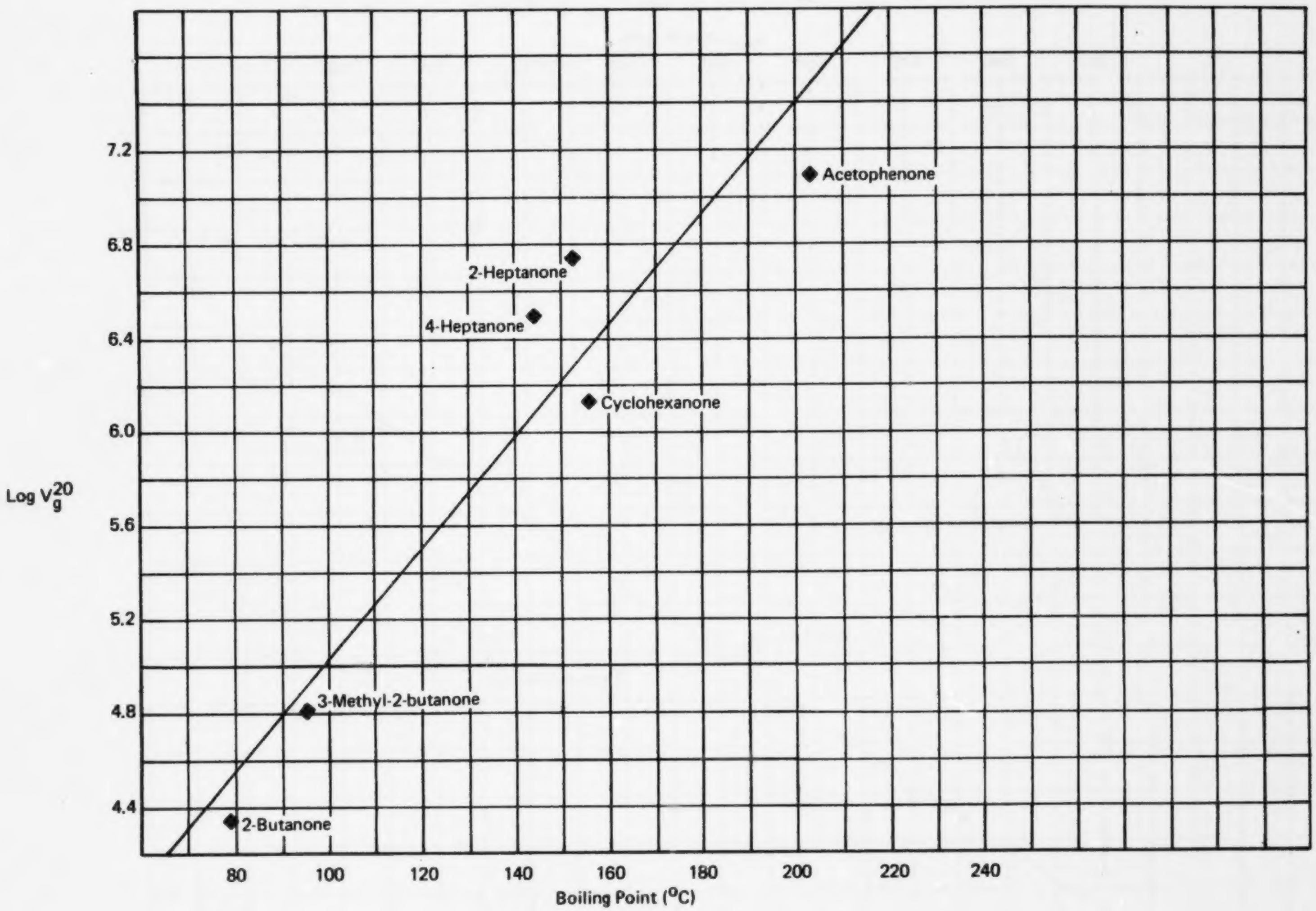

FIGURE 12 LOG V_g^{20} VS. BOILING POINT OF ADSORBATE KETONES ON TENAX–GC

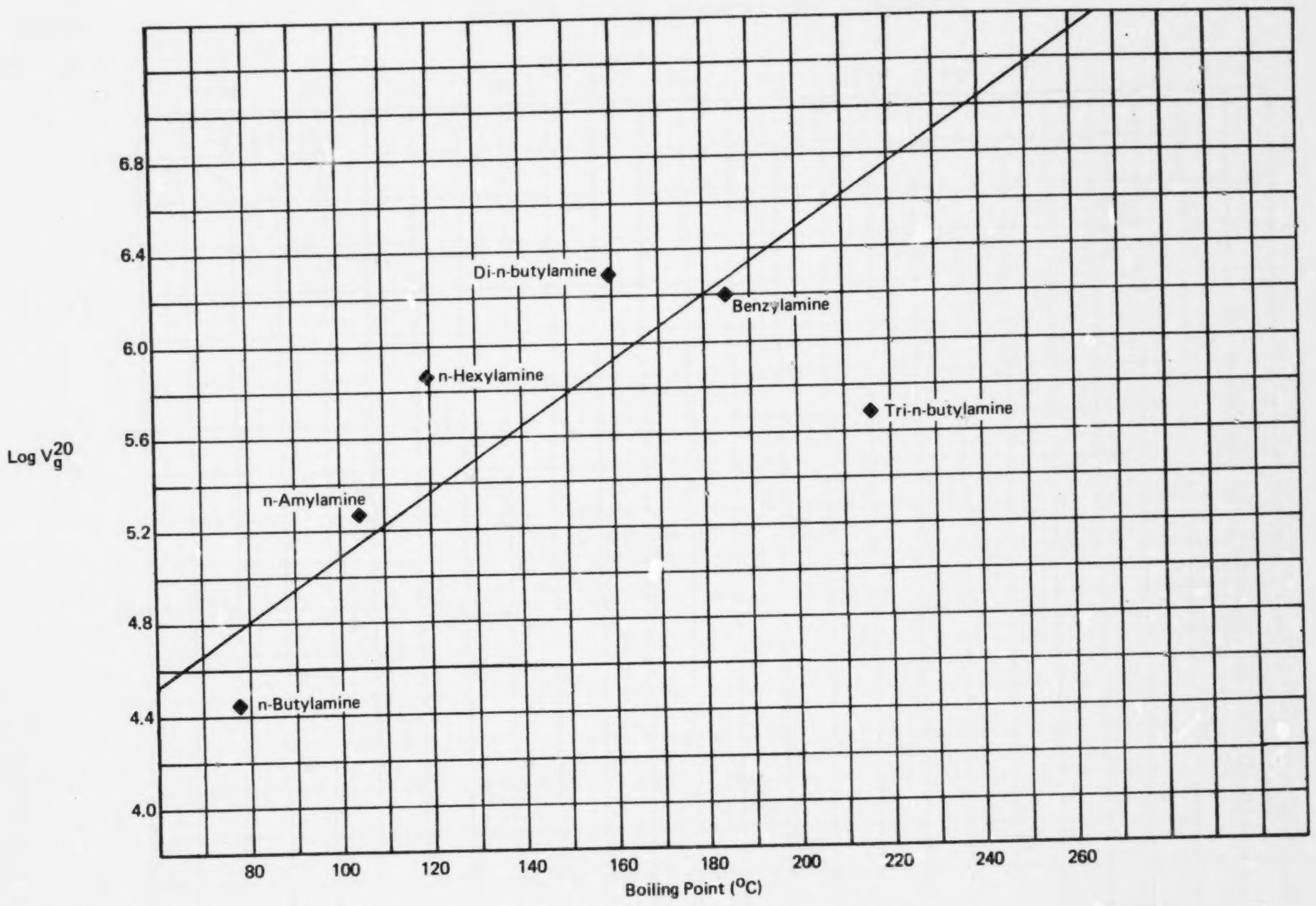

FIGURE 13 LOG V_g^{20} VS. BOILING POINT OF ADSORBATE AMINES ON TENAX–GC

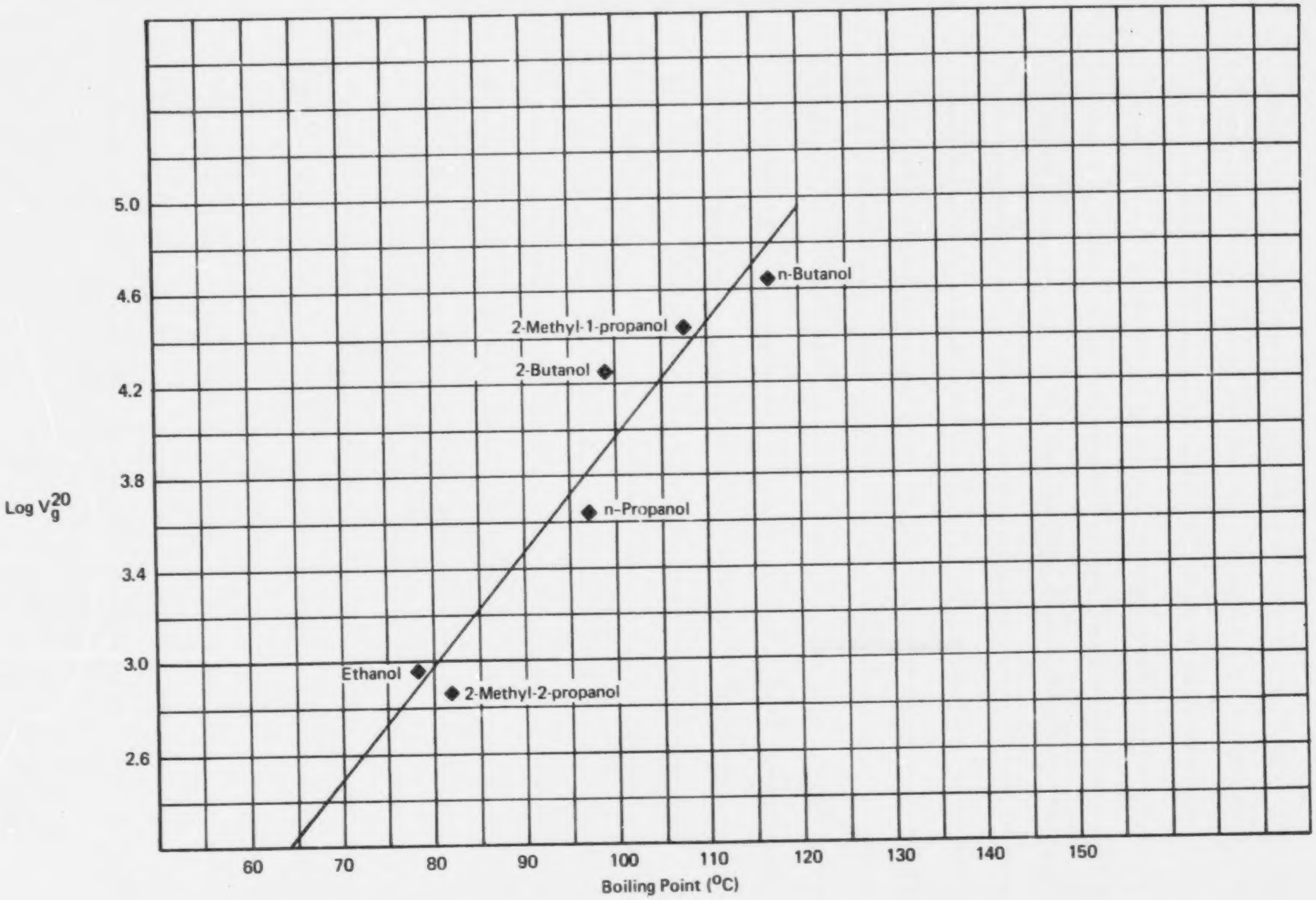

FIGURE 14 LOG V_g^{20} VS. BOILING POINT OF ADSORBATE ALIPHATIC ALCOHOLS ON TENAX–GC

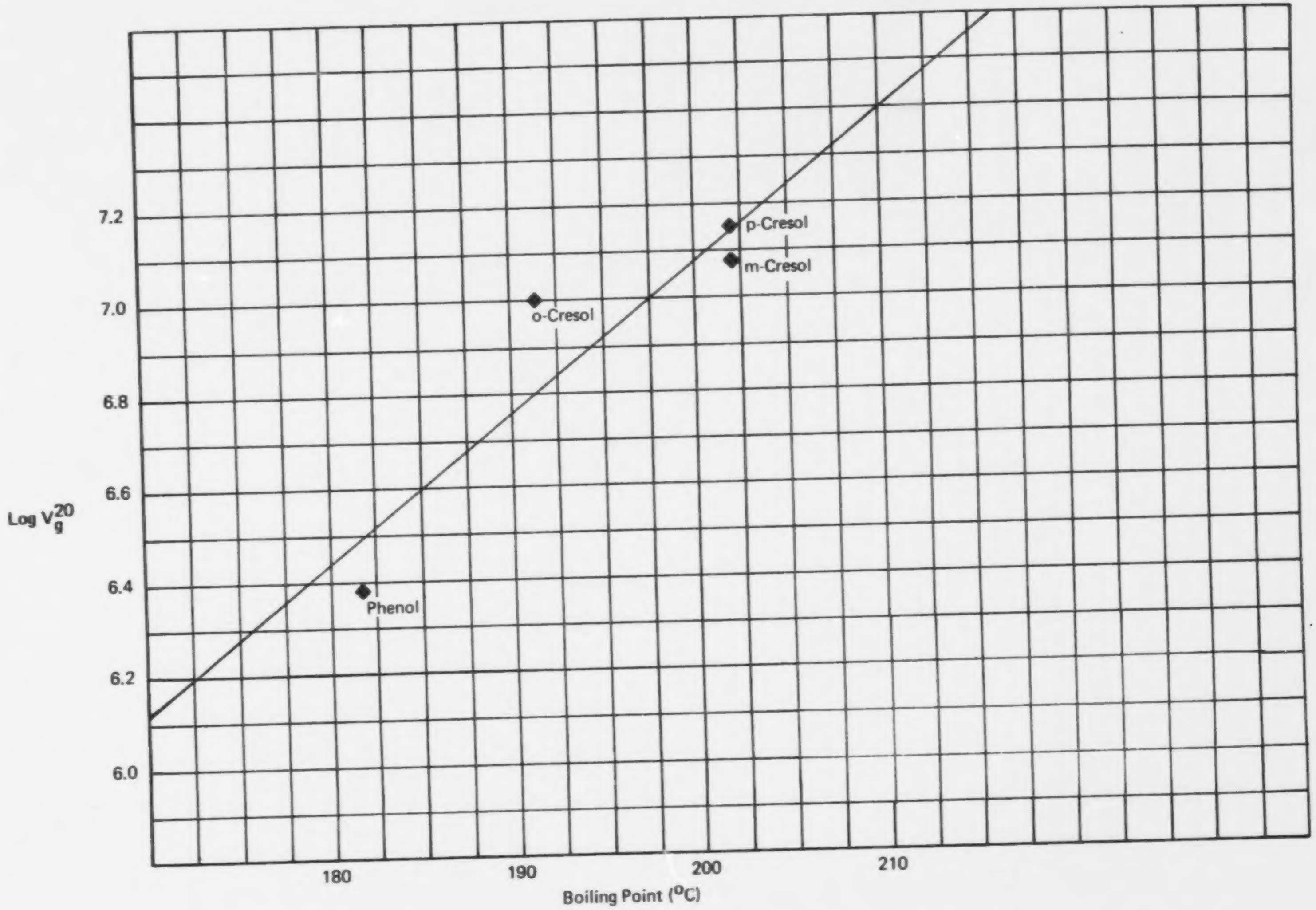

FIGURE 15 LOG V_g^{20} VS. BOILING POINT OF ADSORBATE PHENOLS ON TENAX–GC

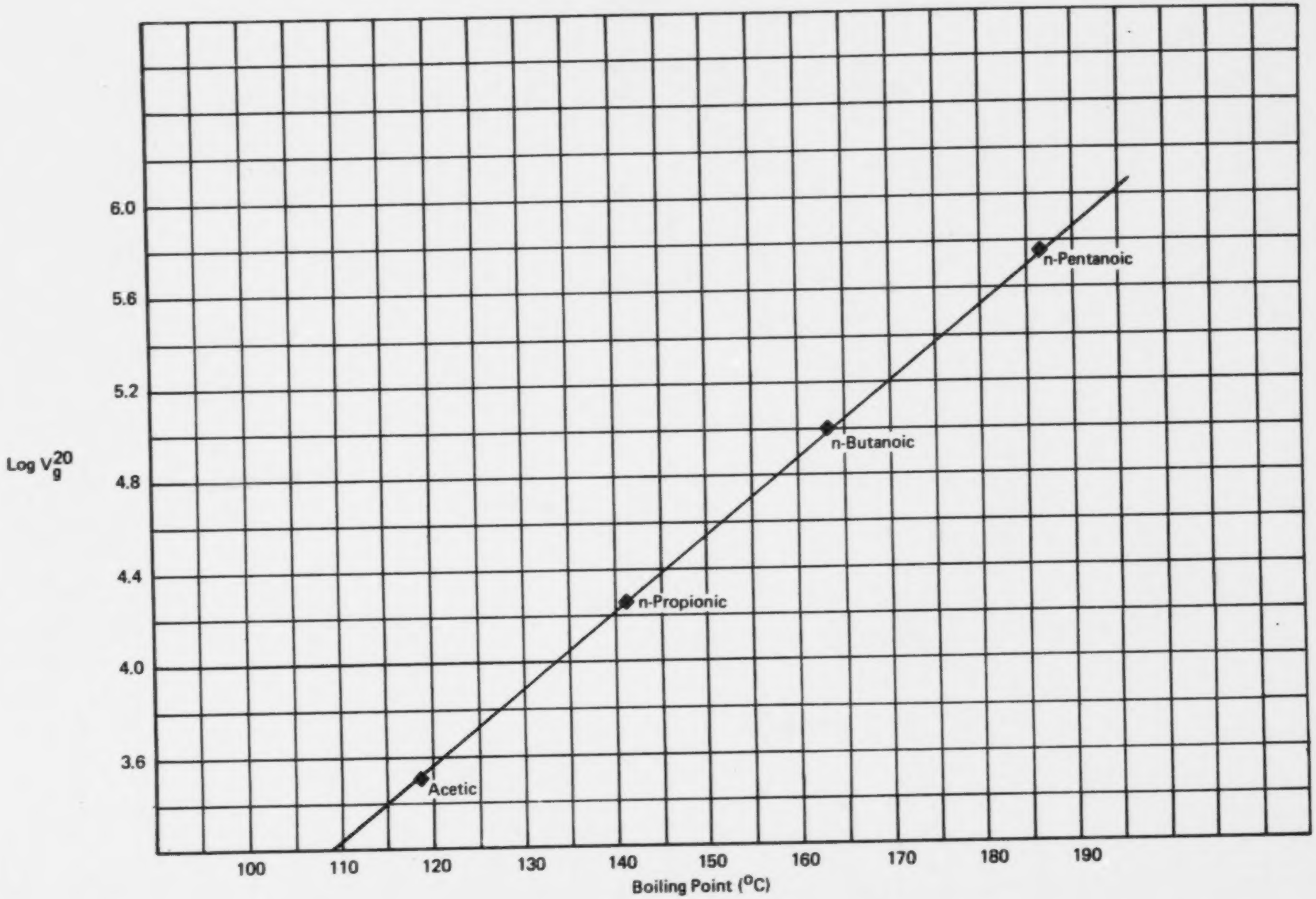

FIGURE 16 LOG V_g^{20} VS. BOILING POINT OF ADSORBATE ALIPHATIC ACIDS ON TENAX–GC

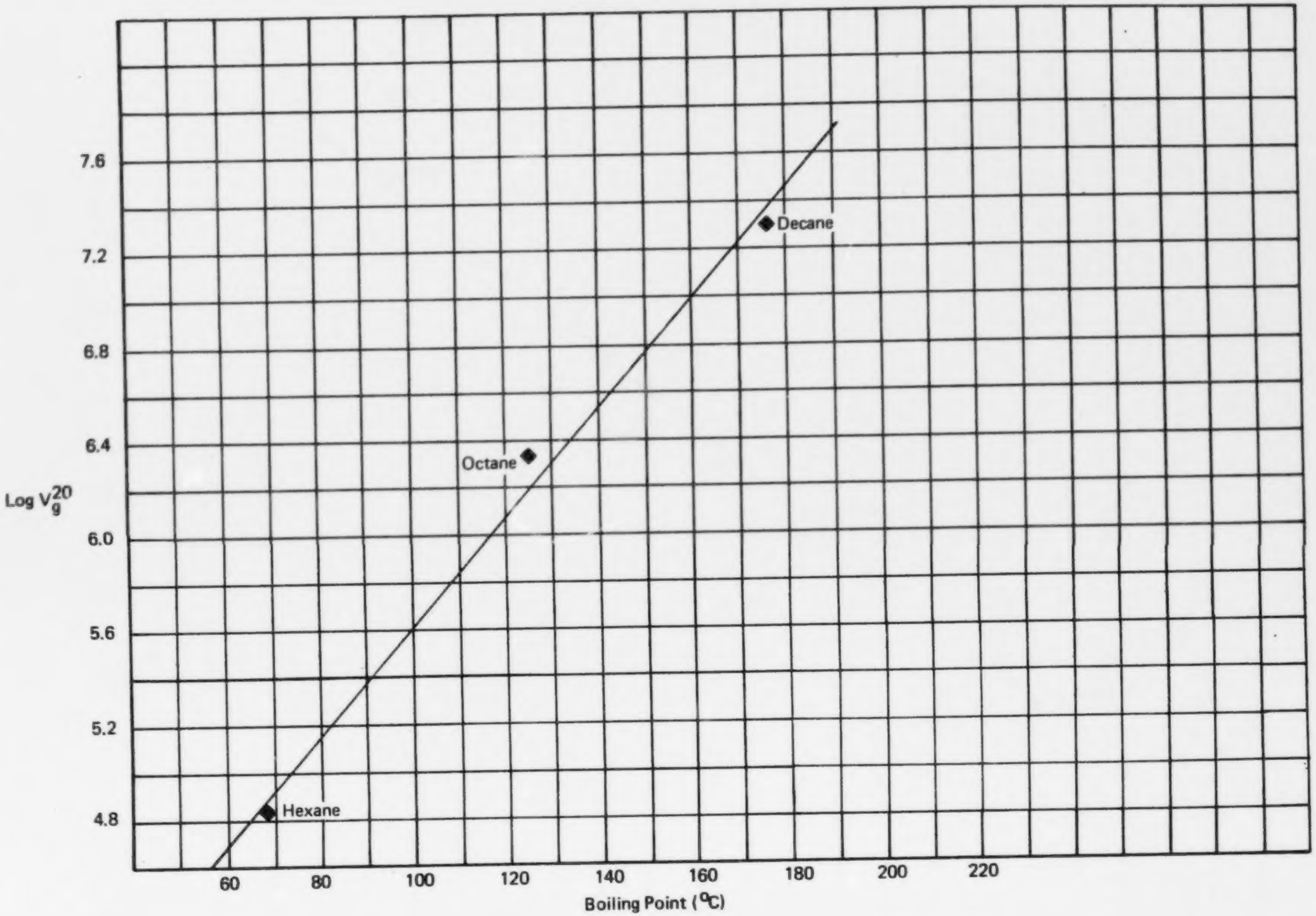

FIGURE 17 LOG V_g^{20} VS. BOILING POINT OF ADSORBATE n-ALKANES ON XAD–2

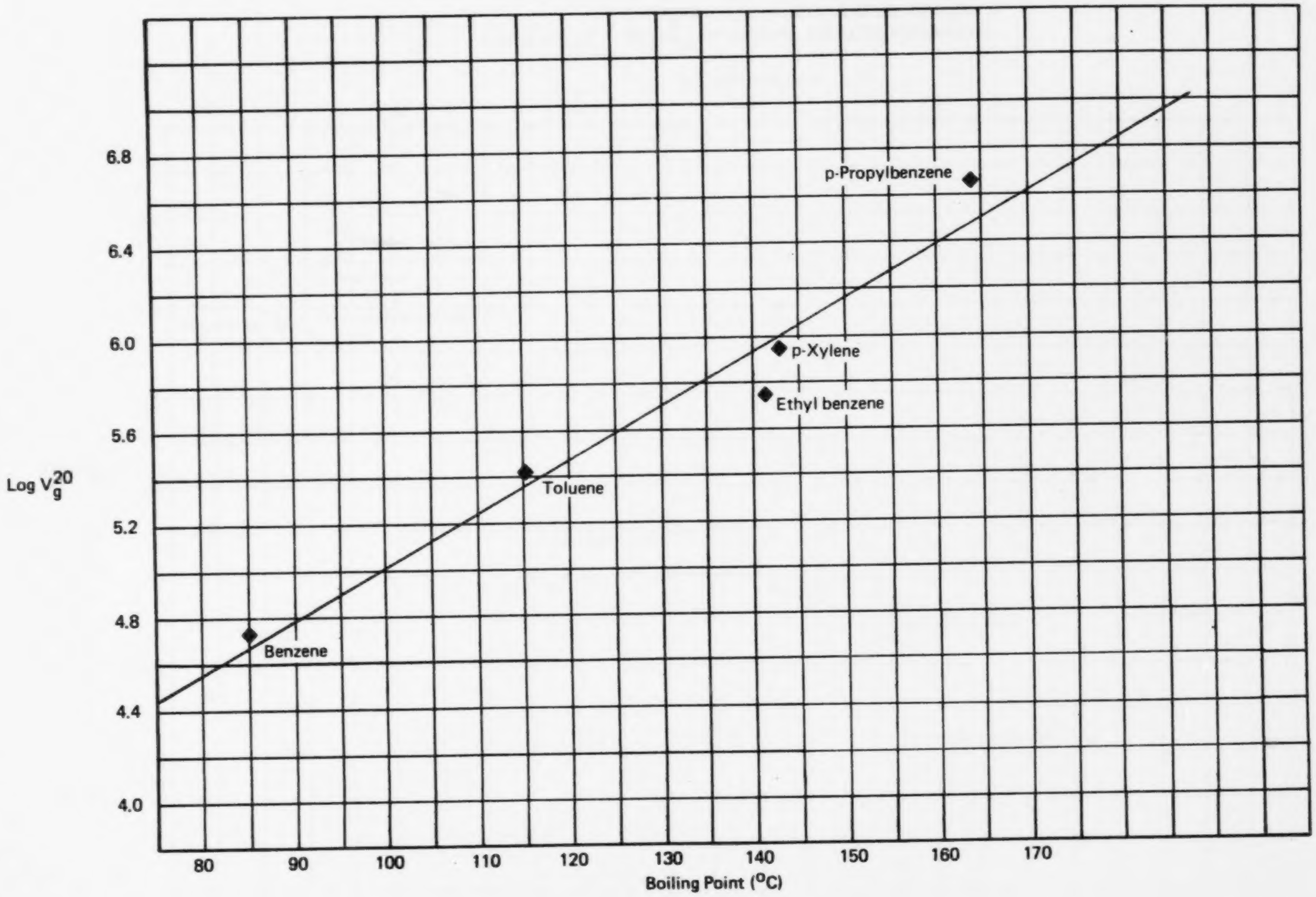

FIGURE 18 LOG V_g^{20} VS. BOILING POINT OF ADSORBATE AROMATIC HYDROCARBONS ON XAD–2

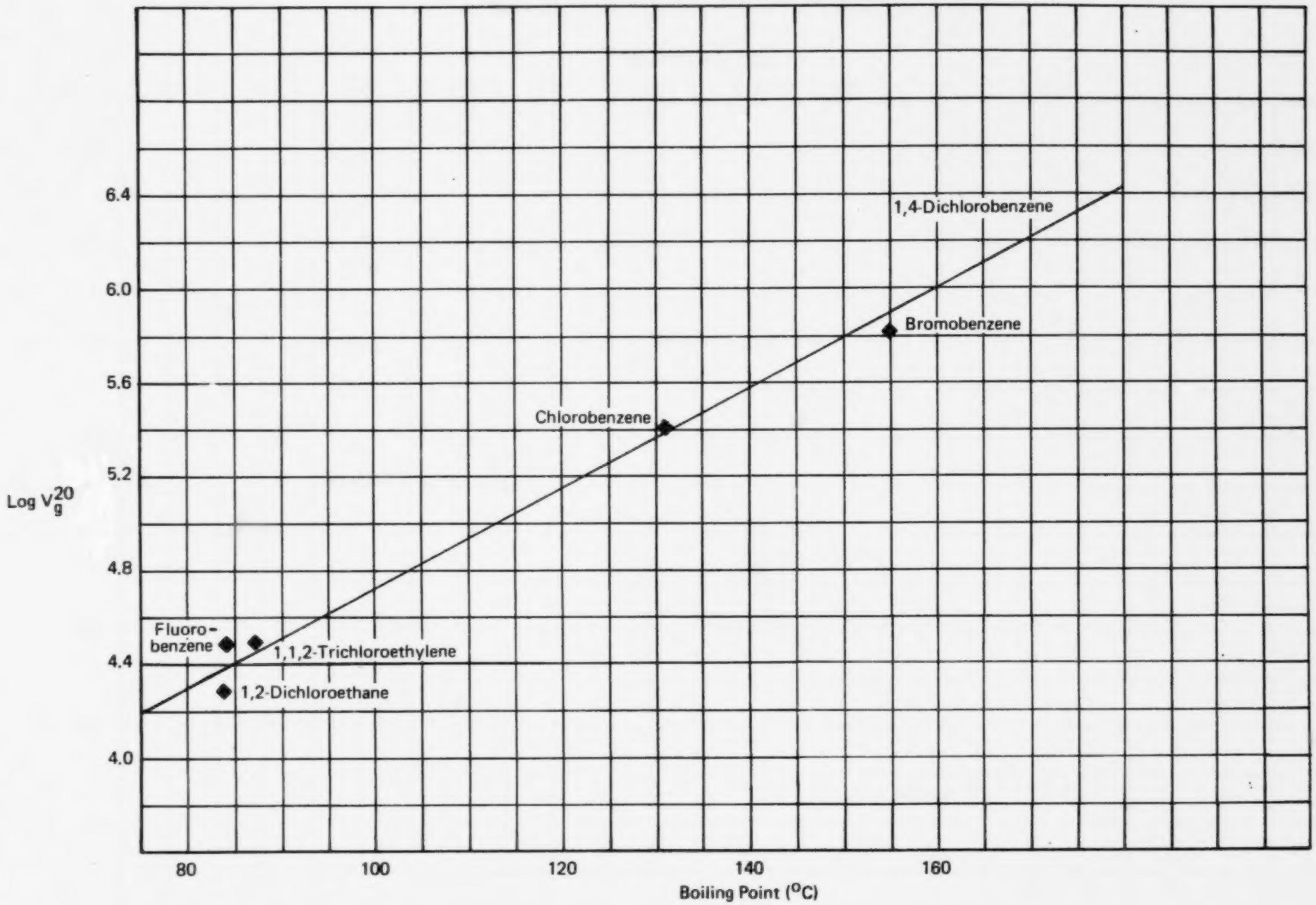

FIGURE 19 LOG V_g^{20} VS. BOILING POINT OF ADSORBATE HALOGENATED HYDROCARBONS ON XAD–2

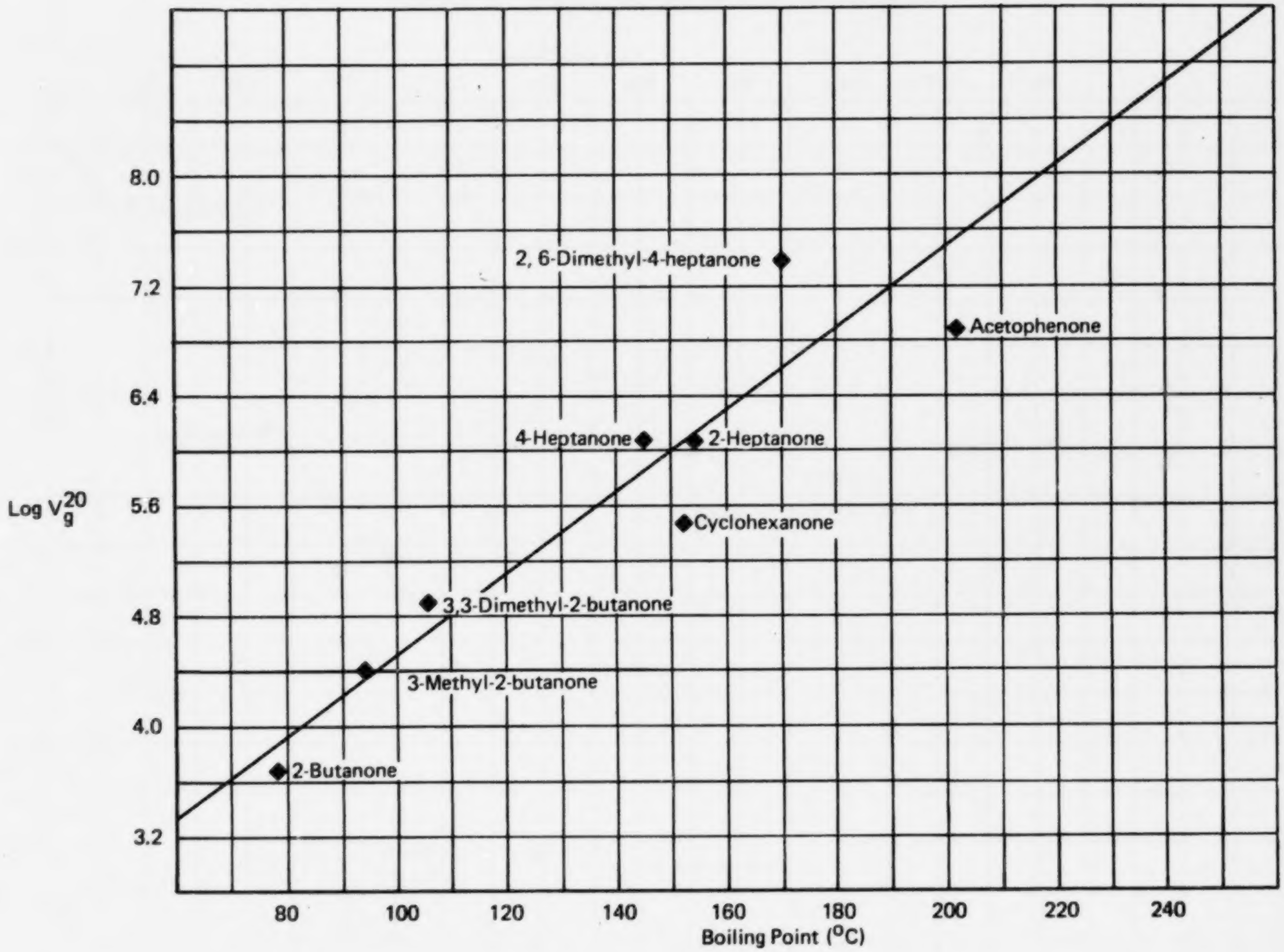

FIGURE 20 LOG V_g^{20} VS. BOILING POINT OF ADSORBATE KETONES ON XAD–2

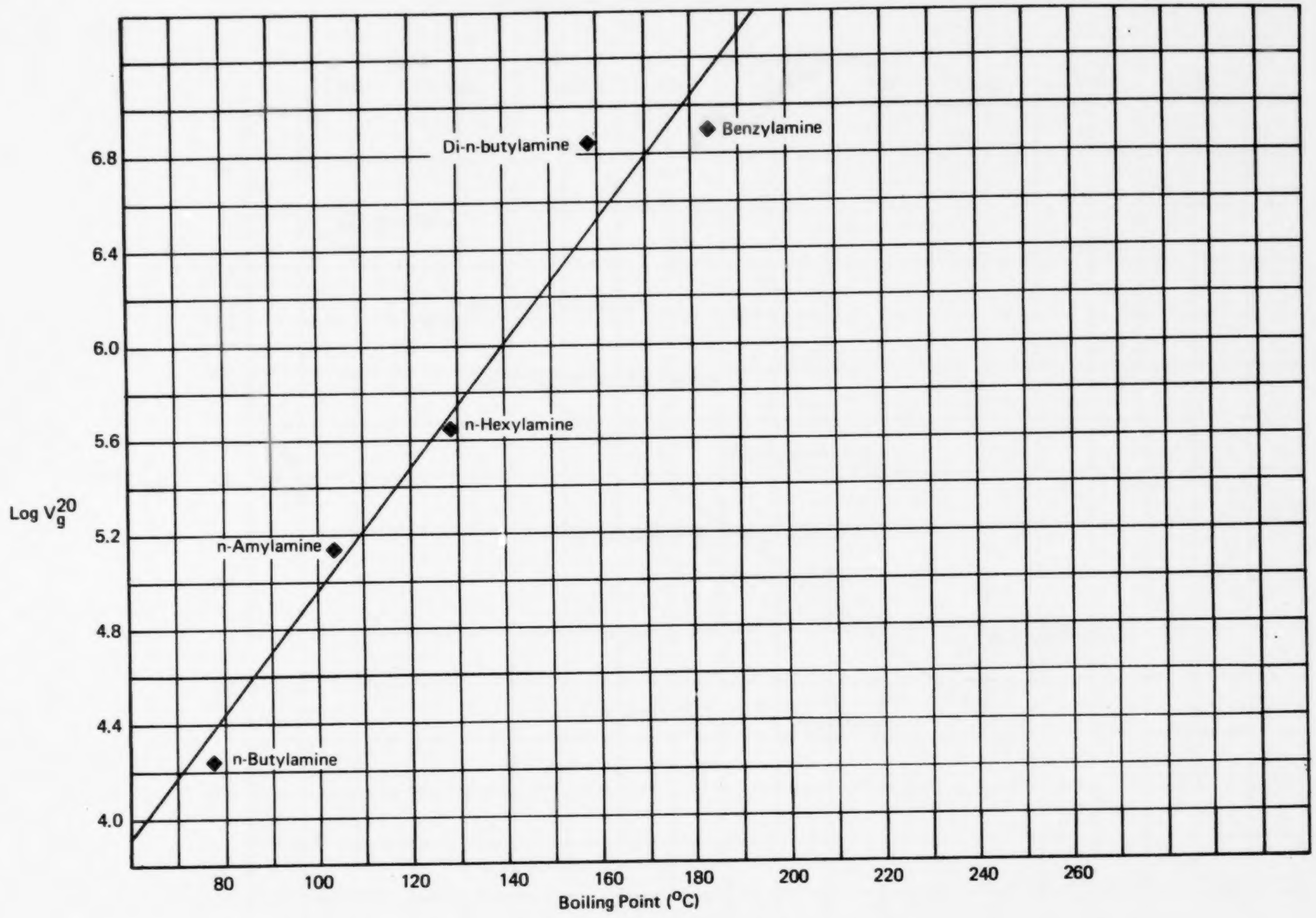

FIGURE 21 LOG V_g^{20} VS. BOILING POINT OF ADSORBATE AMINES ON XAD–2

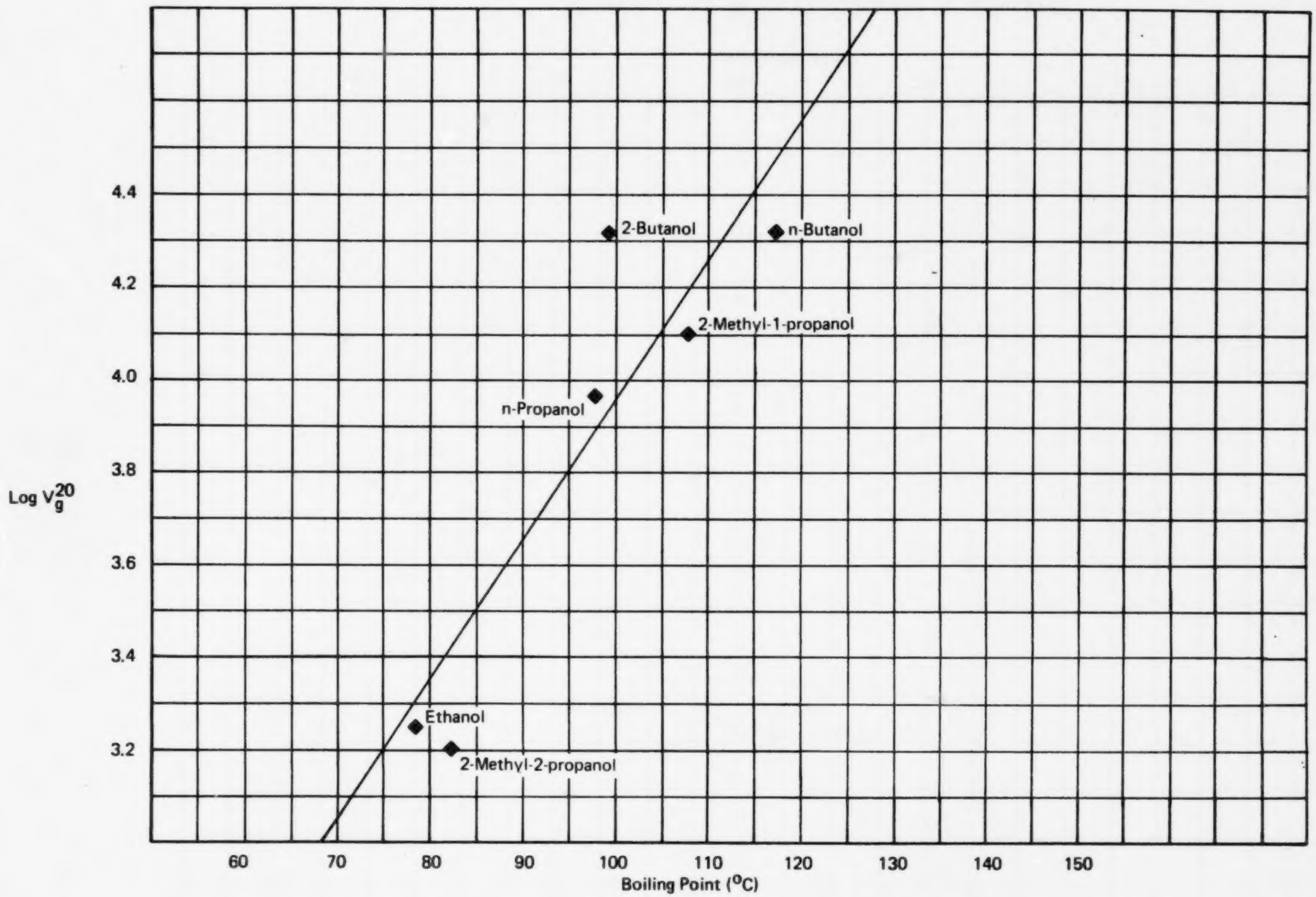

FIGURE 22 LOG V_g^{20} VS. BOILING POINT OF ADSORBATE ALIPHATIC ALCOHOLS ON XAD–2

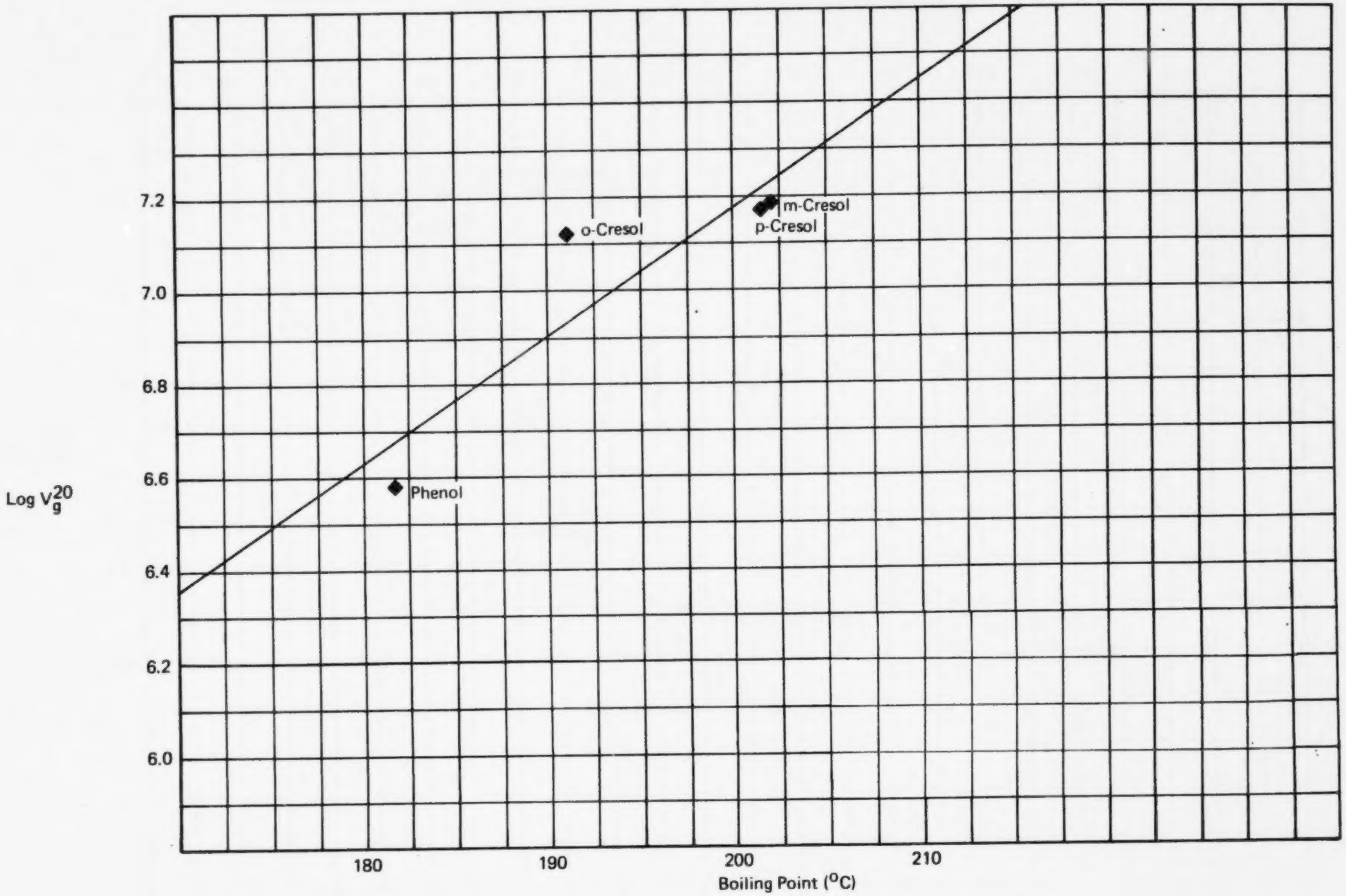

FIGURE 23 LOG V_g^{20} VS. BOILING POINT OF ADSORBATE PHENOLS ON XAD–2

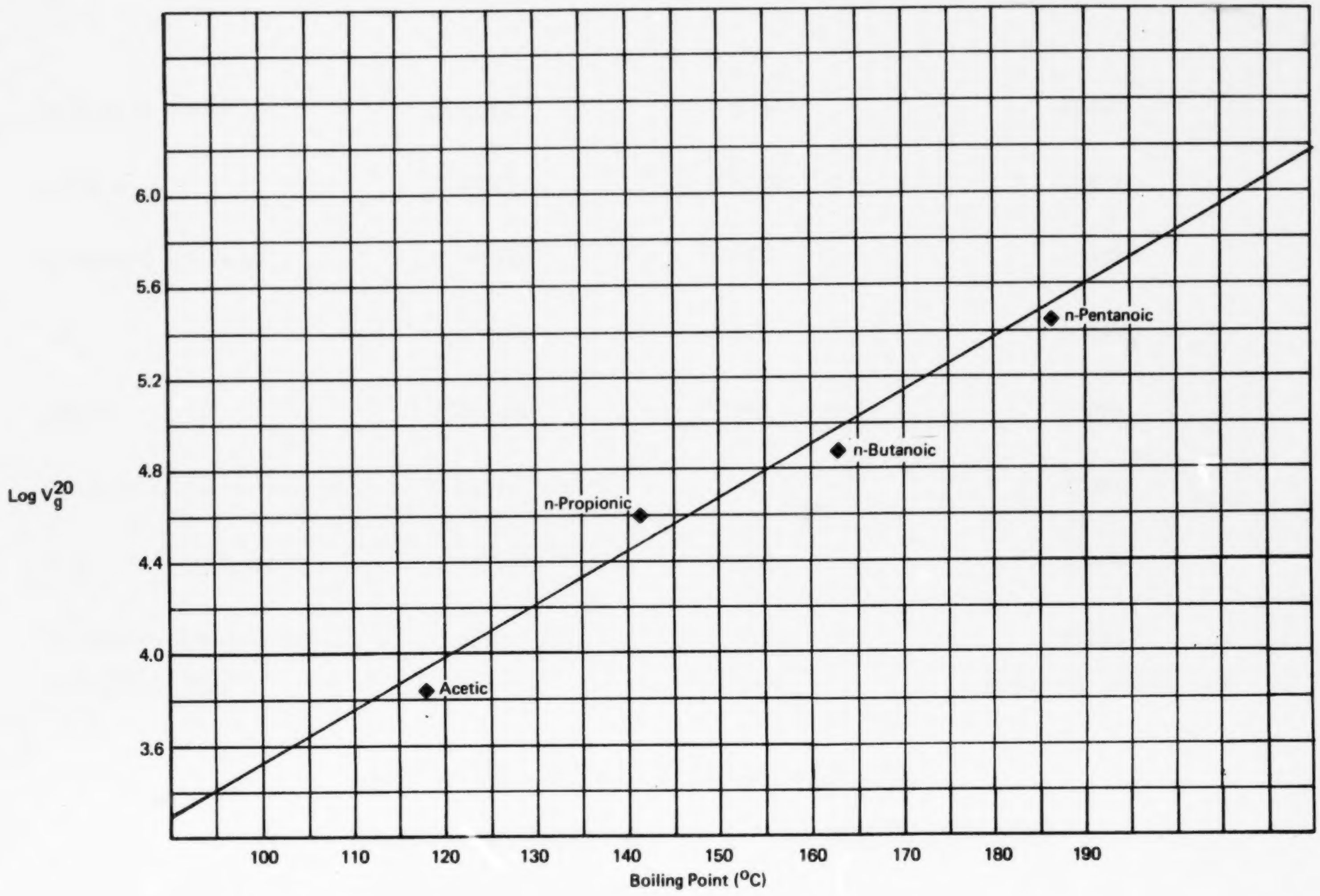

FIGURE 24 LOG V_g^{20} VS. BOILING POINT OF ADSORBATE ALIPHATIC ACIDS ON XAD–2

Table 7

Linear Regression Parameters for log V_g^{20} vs Boiling Point (°C)

Plots of Adsorbate Classes on Tenax-GC Resin

Adsorbate Class	Slope	Intercept	Correlation Coefficient
Aliphatic Hydrocarbons	0.02591	2.348	0.972
Aromatic Hydrocarbons	0.01513	3.786	0.848
Halogenated Hydrocarbons	0.02952	2.280	0.981
Ketones	0.02356	2.687	0.945
Amines	0.01449	3.597	0.906
Aliphatic Alcohols	0.04975	-1.012	0.963
Phenols	0.03206	0.6767	0.913
Aliphatic Acids	0.03308	-0.4162	1.000

Table 8

Linear Regression Parameters for log V_g^{20} vs Boiling Point (°C) Plots of Adsorbate Classes on XAD-2 Resin

Adsorbate Class	Slope	Intercept	Correlation Coefficient
Aliphatic Hydrocarbons	0.02309	3.349	0.997
Aromatic Hydrocarbons	0.02308	2.820	0.981
Halogenated Hydrocarbons	0.02115	2.618	0.996
Ketones	0.02765	1.805	0.928
Amines	0.02613	2.337	0.980
Aliphatic Alcohols	0.03089	0.8567	0.905
Phenols	0.02734	1.706	0.893
Aliphatic Acids	0.02263	1.251	0.987

plotted. The literature abounds in experimental data verifying this trend. (See references 33,55,56).

Similar trends and success in correlating V_g^T with boiling point have been observed for the results on XAD-2 resin. Inspection of Figures 17-24 and Table 8 indicate that for the same adsorbate classes, there is even a greater correspondence to linearity when log V_g^T vs. boiling point is plotted than was observed for Tenax-GC.

A number of other linear relationships have been found to hold when such parameters as molecular weight, carbon number, and electron polarizability of the sorbate are plotted vs log V_g^T (38). Again, for each sorbate class, the lines are vertically displaced from each other, but of similar slope for each sorbate class. In an attempt to find a physicochemical adsorbate parameter that might induce coincidence of all the sorbates on one single generalized line, total molecular polarizability, α, was examined. Values of α are given for a selected number of adsorbates in Table 9. The large polarizability exhibited by the n-alkanes can readily be contrasted with the low values for polar adsorbates and water, which is minimally retained by the porous polymer resin. Note that α also increases with chain length, thus a potential relationship could exist between log V_g^T and α.

The values of α given in Table 9 were obtained from a number of sources and represent both experimental values (38-40) as well as calculated molar refractions (41,42) which have been converted to total polarizabilities via

$$\alpha = 0.3964\ R$$

where R = molar refraction in cc/mole.

Table 9

Total Polarizability Values (α)* for Adsorbates

Adsorbate	α*
n-Hexane	11.78
n-Octane	15.53
n-Decane	19.22
Benzene	10.32
Toluene	12.15
p-Xylene	14.2
Acetic Acid	5.05
Propionic Acid	6.80
n-Butanoic Acid	8.58
Ethanol	5.06
n-Propanol	6.89
n-Butanol	8.72
Benzylamine	11.6
Water	1.49

* In units of $\mathring{A}^3$

and

$$R = \left(\frac{n_r - 1}{n_r - 2}\right)\left(\frac{mw}{d}\right)$$

where n_r = refractive index of adsorbate

mw = molecular weight of adsorbate

d = density of adsorbate

The second equation is the classical Lorentz-Lorenz equation relating R to n_r Hence, values of α should be readily obtainable since tables of n_r, mw, and d are readily available and n_r can be experimentally determined with a refractometer.

Figure 25 shows log V_g^T for the solutes listed in Table 9 vs α. At first the correlative value looks no better than the log V_g^T vs. boiling point relationship; however, the acids, alcohols and single amine (benzylamine) do appear to follow a single line. The aromatic sorbates are between the n-alkane line and the polar sorbates. This suggests that a single monotonic relationship between α and log V_g^T may not be possible, but that various groups of molecules do tend to correlate in terms of log V_g^T vs α.

Data presented by Kiselev (43) indicate the validity of the above approach. Figure 26 shows the log t_R (retention time) vs α relationship for various sorbates on Chromosorb 102. Note that a linear relation exists for the alcohols (Group D sorbates) and separately for Groups A and B molecules. This is similar to what is observed in Figure 25 and indicates that V_g^T is not totally dependent on boiling point or dipole moment, but is affected by α (48). In addition, this supports the classification of Tenax-GC and XAD-2 as Type III adsorbents (weakly specific), although it does not preclude that porous polymers having specific adsorbing surfaces grafted into the copolymerized matrix

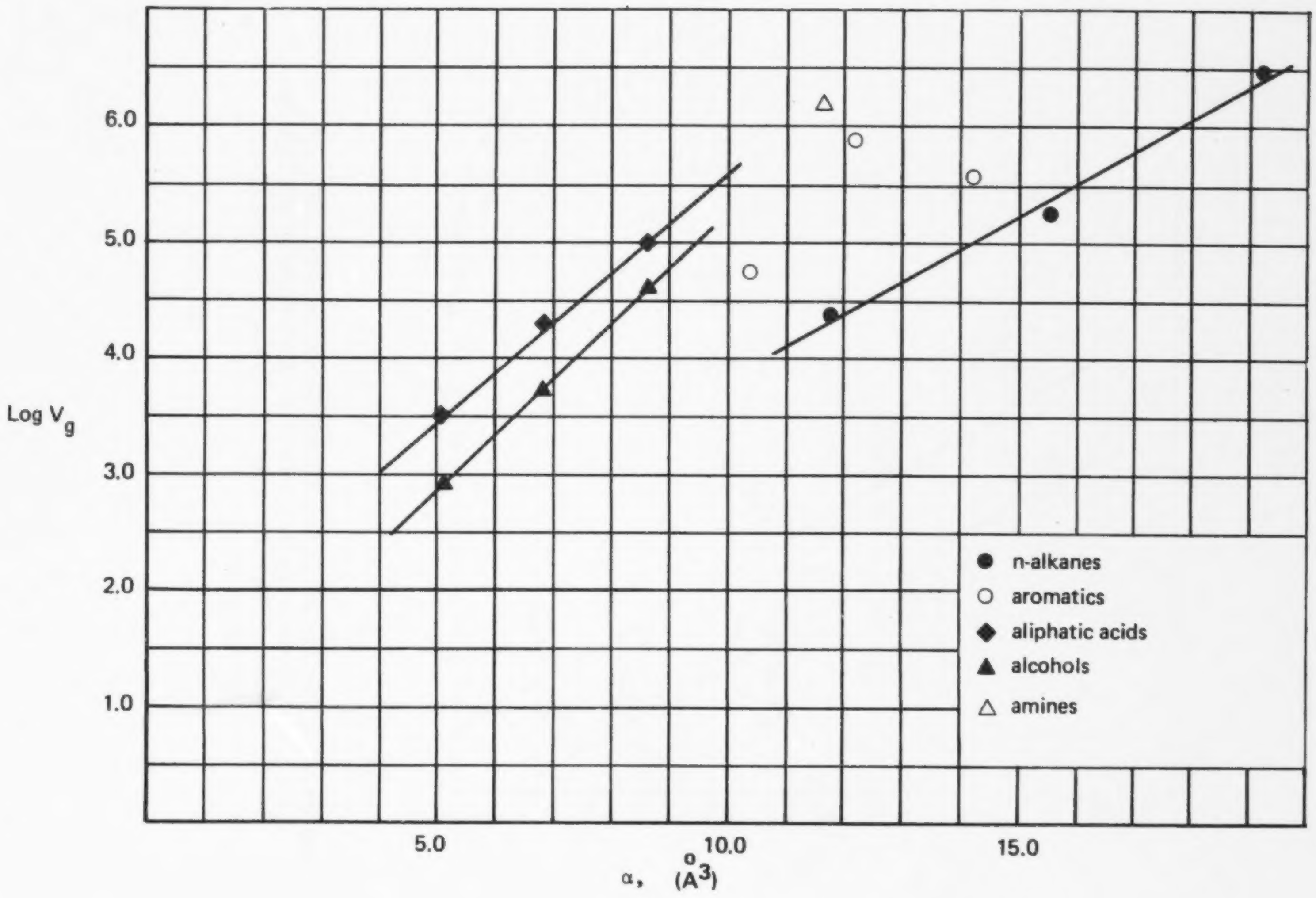

FIGURE 25 SPECIFIC RETENTION VOLUME (20°C) VS. ADSORBATE TOTAL POLARIZABILITY FOR TENAX-GC

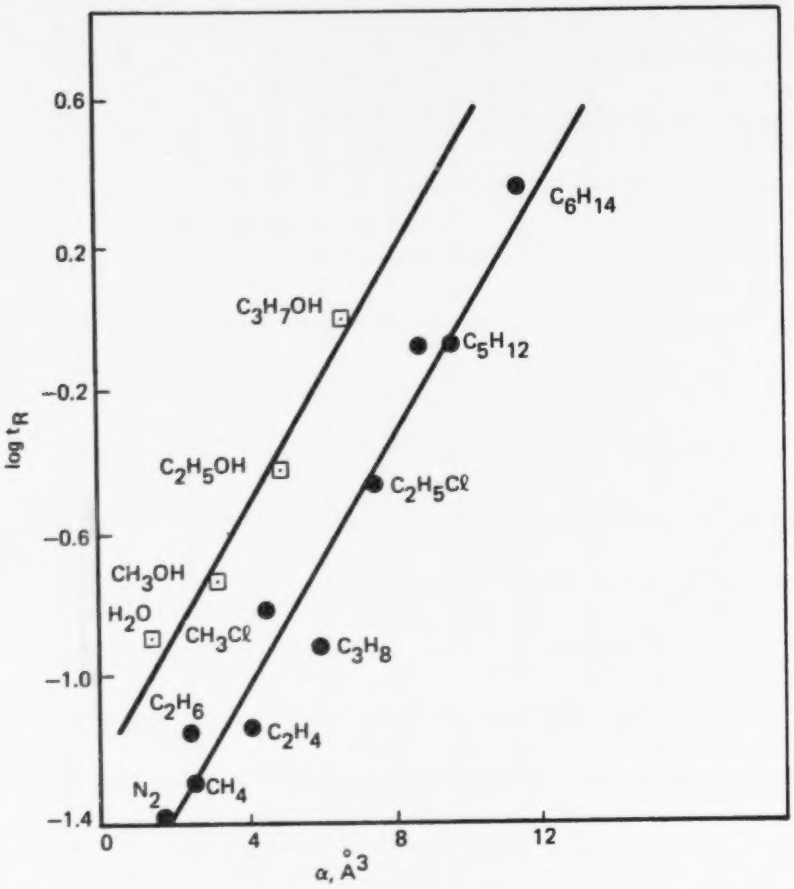

FIGURE 26 DEPENDENCE ON ELECTRONIC POLARIZABILITY α FOR CHROMATOGRAPHIC CHARACTERISTICS DEDUCED WITH SMALL SAMPLES FOR THE POROUS POLYMER CHROMOSORB 102 (REFERENCE 43)

may exhibit other types of more specific adsorption activity.

3. Flow Rate Effects on V_g^T

The V_g^T values computed in earlier sections were determined using a flow rate range of 60-150 mL/min--flow rates considerably below the equivalent flow rate experienced in SASS train sorbent traps. The 60-150 mL/min flow rate range in the 0.5 cm I.D. sorbent columns corresponds to a linear velocity of 6-16 cm/sec. The SASS train sorbent module operates at about 46 cm/sec. In order to determine whether flow rate has any significant effect on V_g^T and thus the breakthrough of the sorbate, several experiments were conducted with a limited number of sorbates to determine V_g^T at flow rates up to one liter/minute (106 cm/sec).

These experiments were accomplished using the thermal conductivity gas chromatograph which overcame the problem of flame blow-out on the flame ionization detector; however the larger volume of gas flowing through the thermal conductivity cell also decreased its response to the sorbate vapor.

Figures 27 and 28 show the trends in V_g^T with flow rate for ethylbenzene and n-hexylamine, respectively on Tenax-GC and XAD-2. As will be shown later, these two compounds have similar adsorption coefficients determined at low flow rates, hence any effect flow may have on V_g^T may be attributed to a loss in effective surface area. The symbols in Figures 27 and 28 represent the average V_g^T value of from 3 to 8 separate determinations of V_g^T, while the brackets represent the extremes in V_g^T. Although the precision of this data is not as high as might be desired, due to the experimental difficulties, definite trends are observable with flow rate.

The results obtained for both adsorbates on XAD-2 seem to indicate a gradual decrease in V_g^T up to flow rates of 400 mL/min (43 cm/sec). Similar trends have been noted by Janak and coworkers for n-heptane

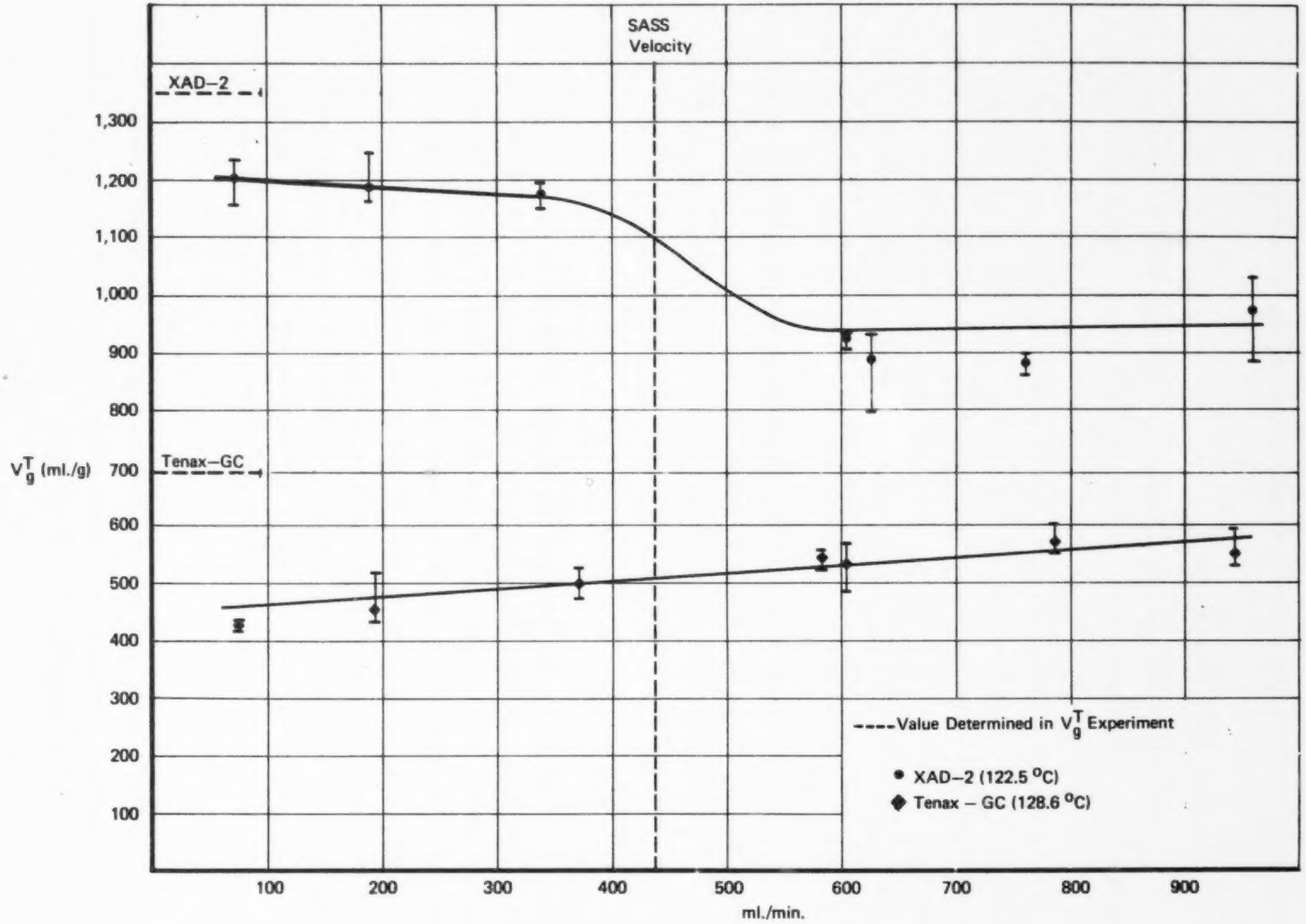

FIGURE 27 V_g^T VS. FLOWRATE – ETHYLBENZENE

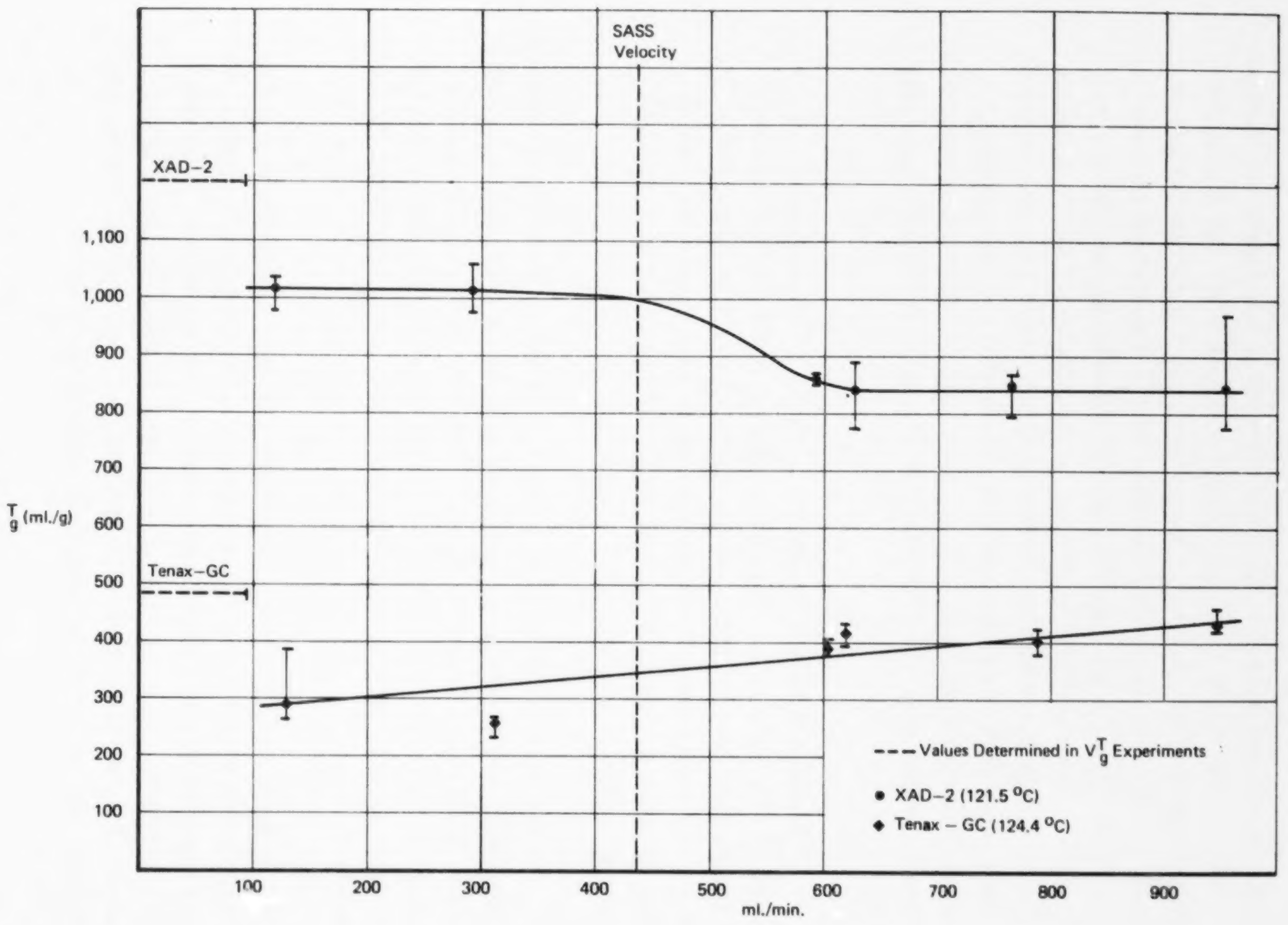

FIGURE 28 V_g^T VS. FLOWRATE – n-HEXYLAMINE sorption on Porapak polymers (44), by Oberholtzer and Rogers for methane and ethane retention by molecular sieve 4A and 5A (45), and in gel permeation chromatography (46,47). Between 400 and 600 mL/min (43 and 64 cm/sec), there is a significant decrease in V_g^T, compared to the limiting low velocity V_g^T value (79% in the case of ethylbenzene and 82% for n-hexylamine). Reductions of this order of magnitude (up to 75% decrease in V_g^T) have also been observed by Moreland and Rogers in a continuation of their studies on slow mass transfer in gas-solid chromatography (molecular sieves) (48), particularly with solutes which could penetrate the porous sorbent structure totally or partially at low gas phase velocities.

Beyond 600 mL/min (64 cm/sec), there is a leveling off in the drop in V_g^T with flow rate. This trend was also observed by Moreland and Rogers (48) and, in fact, some of their V_g^T vs. flow rate curves bear a close resemblance to those obtained in this study. Similar curves to those obtained in Figures 27 and 28 have also been obtained for n-hexylamine on XAD-2 at 80°C and 100°C.

The results obtained for both adsorbates on Tenax-GC as depicted in Figures 27 and 28 are quite different than those for sorption on XAD-2. There is a gradual increase in V_g^T with flow rate indicating a slight increase in uptake of the sorbate by the resin at higher gas velocities. This trend is also observable at 80°C and 100°C for n-hexylamine on Tenax-GC.

As noted previously, the trends observed on XAD-2 are probably related to the effect of slow mass transfer of the organic solute in and out of the porous structure of the adsorbent. A comparison of surface area distribution as a function of pore size in XAD-2 (Figure 29) and Tenax-GC (Figure 30) indicates the presence of some macropore structure (170-325Å) in XAD-2 that is completely missing in Tenax-GC.

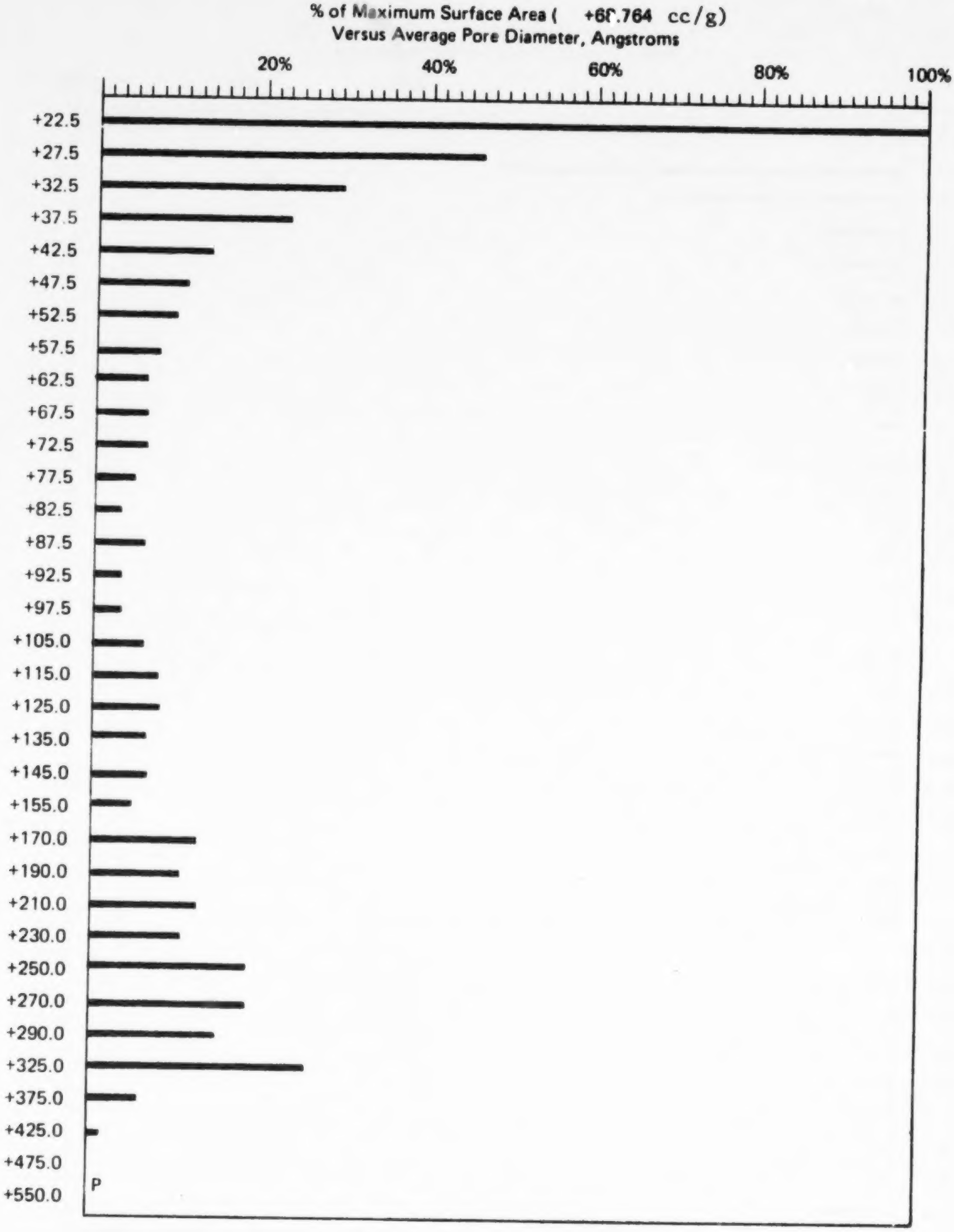

FIGURE 29 INCREMENTAL SURFACE AREA DISTRIBUTION (DESORPTION): XAD–2

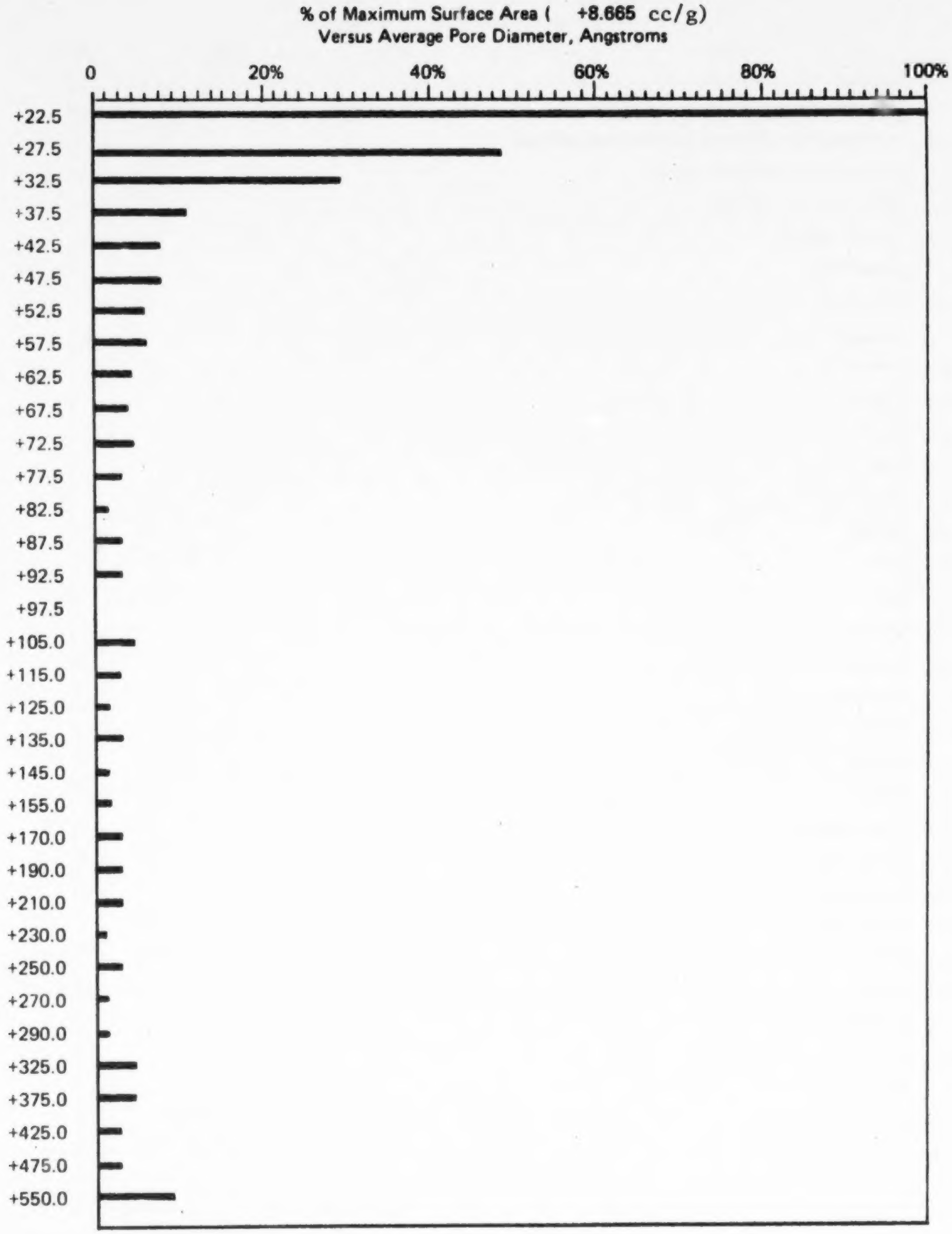

FIGURE 30 INCREMENTAL SURFACE AREA DISTRIBUTION (DESORPTION): TENAX-GC

Hence the reduction in V_g^T on XAD-2 is probably directly related to a loss in interfacial surface area available for sorption (45). It should be emphasized again at this point, that the loss in surface area is kinetically based as has been shown by Janak, et al (49, 50). Hence, minimization of the observed dependence of V_g^T on flow can be accomplished by raising the temperature of the sampling tube or lowering of the flow rate, both which facilitate diffusion into the porous structure of the resin.

Janak's (44) results for V_g^T dependence on carrier gas flow rates bear some additional comment since they are highly relevant to the results presented here. Janak found extremely small drops in V_g^T over a relatively modest change in flow rate for non-extracted Porapak Q and P; however a 14% loss in V_g^T was observed for benzene-extracted Porapak P. It may well be that the methylene chloride-extracted XAD-2 corresponds in a similar manner to Janak's results and that results on non-extracted XAD-2 might show a completely different behavior, although such a treatment would not be acceptable for sampling because of contamination.

Janak's paper also notes results similar to those observed in this study for Tenax-GC. There is no apparent explanation for this phenomena with the possible exception that there might be unremoved liquid in the pores of the Tenax-GC which is retaining the sorbate. Since the sample of Tenax-GC used in this study has undergone no extraction, its post-polymerization history might be suspect.

These results raise the question of what is really being measured by V_g^T for these sorbent trap experiments. Giddings (51) has noted that the conservation-of-mass equations normally used to relate phase distribution of the solute in chromatography depend on the "long-term approximation,", i.e., "that the location and profile of a chromatographic zone is approximated by a limiting mathematical form which is exact only when the elution time is infinitely larger than the time of equilibration.

between phases." In the transient situation we are dealing with, this approximation is probably not valid. Where severe mobile phase mass transfer control exists, as in this case, the elution time of the chromatographic peak is no longer dictated by K_A, but represents the equilibruim uptake at a definite $K_A\mathring{A}_S$ product. Hence the problem is not knowing K_A, which can be obtained from a low velocity experiment, but in knowing what is the "effective surface area" seen by the adsorbate.

One disturbing aspect of the data presented in Figures 27 and 28 is the lack of agreement between the limiting value of V_g^T in the low flow rate region and previous V_g^T values determined for those same compounds in the earlier V_g^T elution studies. The latter values were obtained from regression equations of log V_g^T vs. $1/T$ plots and their values are plotted as dotted lines on the left-hand side in Figures 27 and 28 of this report. These V_g^T values had been determined at flow rates between 80-120 mL/min and considerably smaller sorbate sample sizes. The matter was examined with further studies using n-pentanoic acid.

The third sorbate, n-pentanoic acid, was studied taking precautions to inject very small sample sizes (just above the limit of detectability) into the thermal conductivity gas chromatograph. The results are plotted in Figure 31. Note the good agreement between the V_g^T values obtained via the regression equations and those in the region of $\sim$100 mL/min. This suggests that the discrepancies noted for the two other sorbates were related to differences in sample size between the two types of experiments. For the n-pentanoic acid, the trend of V_g^T with flow rate on XAD-2 is the same as previously recorded for ethylbenzene and n-hexylamine. The drop in V_g^T's absolute value with flow is 21% of its initial value which compares with 21% loss in V_g^T found for ethylbenzene and a figure of 18% for n-hexylamine on the same sorbent.

For n-pentanoic acid adsorbing on Tenax-GC, there is a slight upward trend in V_g^T with flow rate. This parallels similar trends in

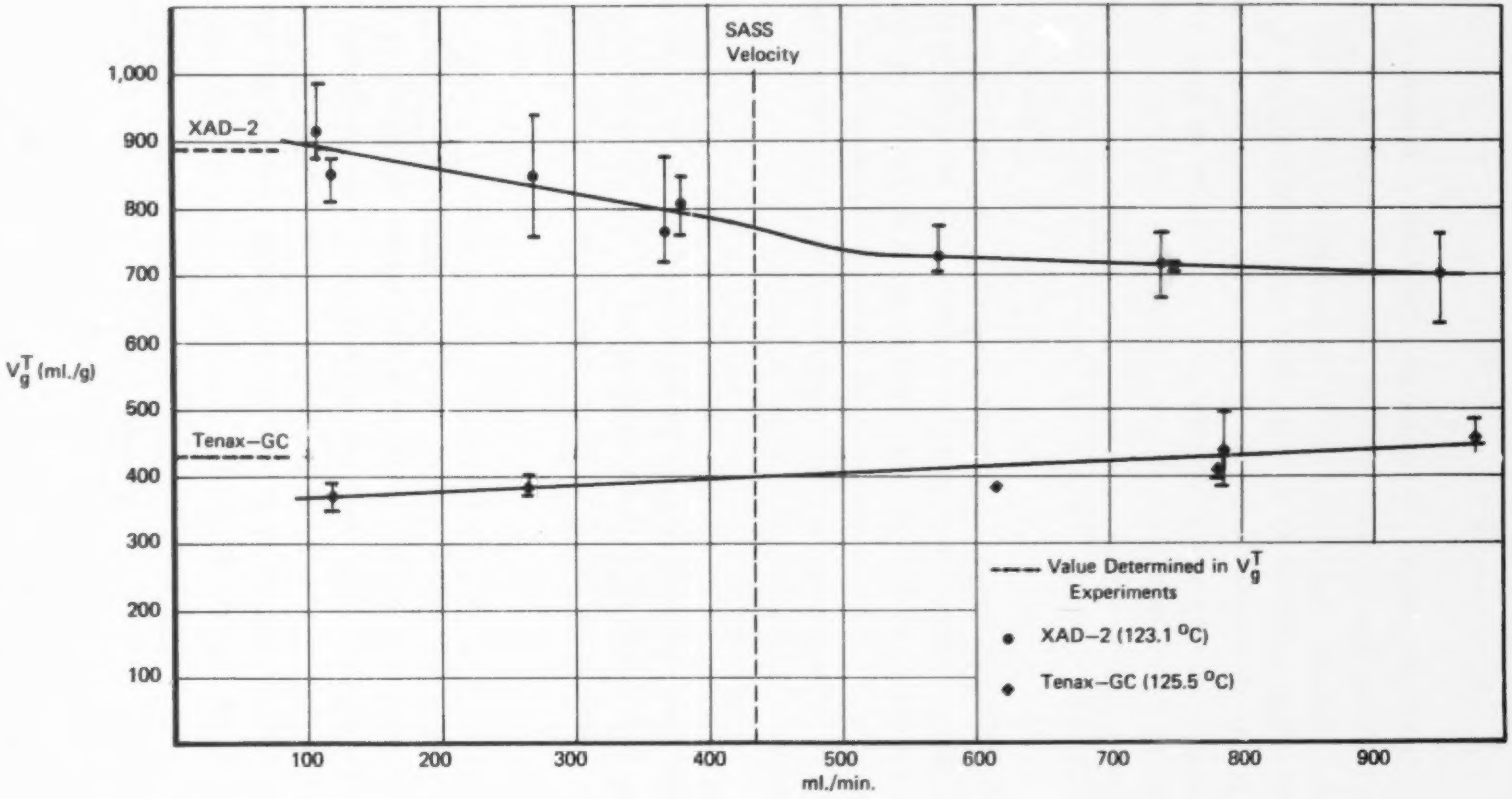

FIGURE 31 V_g^T VS. FLOWRATE – PENTANOIC ACID

V_g^T found for the other two solutes used in this study. However it is interesting to note that V_g^T approaches at high flow rates the V_g^T value obtained via regression analysis of earlier determined data. This suggests that there probably is no true flow rate dependence of V_g^T on Tenax-GC and that the effect noted is again one of sample size (i.e., the solute signal is very small and difficult to observe at high flow rates due to the dilution effect of the carrier gas. The highest flow rates are probably at a sample size comparable to that used with the FID chromatograph).

The results comparing chromatographic V_g^T and experimental breakthrough volumes on Tenax-GC presented in Table 4 seem to confirm the small variation in V_g^T with flow rate depicted in Figures 27, 28 and 31. If V_g^T did vary with flow appreciably, the agreement between the V_g^T's in Table 4 and the breakthrough volumes (determined at much higher flow rates) probably would not be as good as observed.

In summary, there appears to be a small drop in sorption capacity with flow rate for various sorbates on XAD-2 resin. The magnitude of this loss would seem to be independent of the sorbate type. For Tenax-GC the capacity is fairly constant over a wide velocity range and sorbate type.

The data discussed in this section present for the first time, V_g^T values measured over such a large velocity range, invalidating a conclusion by DeLigny (52) that such measurements were experimentally unattainable. Some comparison as to the magnitude of the velocities encountered in the study is given by comparing the linear velocity of the carrier gas, v, as calculated by

$$v = \frac{F_c}{\varepsilon \delta}$$

where: F_c = volumetric carrier gas flow rate

ε = packing porosity

δ = cross-sectional area of the empty column

Assuming a value of 0.8 for ε and a δ value of 0.196 cm^2 for the sorbent tube, v = 106 cm/sec which is considerably higher than the value of 18 cm/sec reported by Janak (44) in his low velocity studies involving V_g^T variance.

B. Adsorption Coefficients

The equilibrium adsorption coefficient can readily be calculated from the specific retention volume data given in Table 3 if the specific surface area of the sorbent resin is known, using equation (23) (Appendix A). A surface area of 364 m^2/g for XAD-2 and 23.5 m^2/g for Tenax-GC were used in these calculations. The values of K_A for each of the adsorbates used in this study are presented in Table 10.

The values of K_A for every adsorbate used in this study are greater on Tenax-GC than on XAD-2. This pronounced difference ranges from similar values of K_A on both resins for the n-alkanes as a sorbate class, to two orders of magnitude difference for such adsorbate groups as aromatic hydrocarbons, halogenated hydrocarbons, and ketones.

Within a number of adsorbate classes there exists a homologous series for which K_A increases with carbon number, for both XAD-2 and Tenax-GC resins. The trend is in part due to the volatility differences in the sorbates as well as the preferred adsorption of the more hydrophobic species.

The weight capacity in grams of sorbate/gram of adsorbates can be calculated from a knowledge of K_A using equation (24) (Appendix A), for sorbents of the same chemical identity but slightly different surface

Table 10

Adsorption Coefficients*, K_A, for Adsorbate Vapors on Sorbent Resins (20°C)

	Resins	
Adsorbate	Tenax-GC	XAD-2
n-Hexane	6.01×10^{-5}	1.12×10^{-5}
n-Octane	4.40×10^{-4}	3.38×10^{-4}
n-Decane	7.17×10^{-3}	3.08×10^{-3}
n-Dodecane	5.10×10^{-1}	--
Benzene	1.42×10^{-4}	7.88×10^{-6}
Toluene	1.84×10^{-3}	3.88×10^{-5}
p-Xylene	8.87×10^{-4}	1.36×10^{-4}
Ethylbenzene	1.95×10^{-3}	8.48×10^{-5}
n-Propylbenzene	3.56×10^{-2}	6.93×10^{-4}
1,2-Dichloroethane	5.41×10^{-5}	2.95×10^{-6}
Fluorobenzene	2.05×10^{-4}	4.71×10^{-6}
1,1,2-trichloroethylene	2.05×10^{-4}	4.61×10^{-6}
Chlorobenzene	5.50×10^{-3}	3.65×10^{-5}
Bromobenzene	1.96×10^{-2}	9.61×10^{-5}
1,4-dichlorobenzene	$4.03\ z\ 10^{-2}$	3.51×10^{-4}
2-Butanone	5.15×10^{-5}	6.60×10^{-7}
2-Heptanone	1.29×10^{-2}	2.24×10^{-4}
4-Heptanone	7.50×10^{-3}	2.29×10^{-4}
Cyclohexanone	3.17×10^{-3}	5.50×10^{-5}
3-Methyl-2-butanone	1.50×10^{-4}	3.80×10^{-6}
3,3-Dimethyl-2-butanone	--	1.29×10^{-5}
2,6-Dimethyl-4-heptanone	--	2.42×10^{-3}
Acetophenone	2.86×10^{-2}	1.08×10^{-3}
n-Butylamine	6.22×10^{-5}	2.71×10^{-6}
n-Amylamine	4.57×10^{-4}	1.94×10^{-5}
n-Hexylamine	1.71×10^{-3}	7.22×10^{-5}
Benzylamine	3.68×10^{-3}	1.18×10^{-3}
Di-n-butylamine	4.45×10^{-3}	1.04×10^{-3}
Tri-n-butylamine	1.13×10^{-3}	--

continued......

Table 10 (continued)

Adsorption Coefficients*, K_A, for Adsorbate Vapors on Sorbent Resins (20°C)

Adsorbate	Tenax-GC	XAD-2
Ethanol	2.11×10^{-6}	2.63×10^{-7}
n-Propanol	1.33×10^{-5}	1.40×10^{-6}
n-Butanol	1.01×10^{-4}	3.11×10^{-6}
2-Butanol	4.33×10^{-5}	3.06×10^{-6}
2-Methyl-2-propanol	1.65×10^{-6}	1.92×10^{-7}
2-Methyl-1-propanol	6.71×10^{-5}	1.92×10^{-6}
Phenol	5.76×10^{-5}	5.53×10^{-4}
o-Cresol	2.33×10^{-3}	2.01×10^{-3}
p-Cresol	3.27×10^{-2}	2.27×10^{-3}
m-Cresol	2.75×10^{-2}	2.33×10^{-3}
Acetic Acid	7.45×10^{-6}	1.06×10^{-6}
Propionic Acid	4.03×10^{-5}	6.01×10^{-6}
n-Butanoic Acid	2.42×10^{-4}	1.16×10^{-5}
n-Pentanoic Acid	1.29×10^{-3}	4.35×10^{-5}

*In units of moles/mm-m^2, derived from $K_A = \frac{V_g^T}{A_s^\circ RT}$

areas. In addition, if the gas phase concentration or challenge concentration is in the Henry's Law region where K_A is applicable, then q_g, the equilibrium sorption capacity, can be computed for various challenge concentrations, C_g.

For example, for a 1 ppm (v/v) challenge concentration, the q_g values have been tabulated for the n-alkanes and aromatic hydrocarbons on Tenax-GC and XAD-2, respectively, in Table 11. The q_g value for the n-alkanes are larger in all cases on XAD-2. For the aromatic hydrocarbons, q_g is greater on Tenax-GC than for XAD-2 in all but one case (p-xylene).

It should be noted that many of the adsorption coefficient values on Tenax-GC are sufficiently greater than on XAD-2, that the equilibrium sorption capacity of Tenax-GC for certain vapors approaches that of XAD-2 despite the much lower surface area of the Tanax-GC. An excellent case in point is the data provided in Table 11. The K_A's for the n-alkanes are of similar magnitude--hence the principal factor in the greater sorption capacity of XAD-2 over Tenax-GC lies in the greater surface area. For the aromatic series, the K_A's on Tenax-GC are an order of a magnitude greater on XAD-2, thus this offsets the effect of the XAD-2 surface area. Thus, one should consider the individual magnitudes of the adsorption coefficients and resin surface areas in selecting the resin for use.

It is interesting to use the tabulated K_A values to calculate q_g values at typical frontal analysis challenge concentrations for comparison with q_g values computed via graphical integration of the frontal analysis curves. Such data exist from some frontal analysis experiments to be described in Part C of this section. Table 17 (p 92) from that part contains weight capacity data (q_g) for challenge concentrations between 0-10 ppm (v/v) as determined via frontal analysis. Table 12 lists the calculated values of q_g. These values can be compared with the q_g in

Table 11

Equilibrium Sorption Capacities*, q_g, for n-Alkanes and Aromatics on Sorbent Resins at 20°C and 1 ppm (v/v) Challenge Concentrations

	Resin	
Adsorbate	**Tenax-GC**	**XAD-2**
n-Hexane	9.26×10^{-5}	2.67×10^{-4}
n-Octane	8.98×10^{-4}	1.07×10^{-2}
n-Decane	1.82×10^{-2}	1.21×10^{-1}
n-Dodecane	1.55	---
Benzene	1.98×10^{-4}	1.70×10^{-4}
Toluene	3.03×10^{-3}	9.89×10^{-4}
p-Xylene	1.68×10^{-3}	3.99×10^{-3}
Ethylbenzene	3.70×10^{-3}	2.49×10^{-4}
n-Propylbenzene	7.64×10^{-2}	2.30×10^{-2}

---

*In units of grams adsorbate/grams of sorbent

Table 12

Weight Capacities of Adsorbates on XAD-2 Calculated From Adsorption Coefficients

Adsorbate	C(ppm) *	T_c(°C)	V_g^T(mℓ/g)	K_A $\frac{\text{moles}}{\text{mm-m}^{-2}}$	q_g $\frac{\text{g-adsorbate}}{\text{g-adsorbent}}$
n-Butylamine	7.76	101.6	367	4.33×10^{-8}	6.79×10^{-6}
3,3-Dimethyl-2-butanone	8.21	115.0	555	6.31×10^{-8}	1.43×10^{-5}
n-Hexane	8.11	87.9	810	9.88×10^{-8}	1.91×10^{-5}
n-Octane	3.08	142.6	364	3.85×10^{-8}	3.74×10^{-6}

* ppm by volume (v/v)

Table 17 for both adsorption and desorption frontal analysis traces. The q_g in Table 12 was calculated by obtaining a V_g^T from the regression equation constants given in Appendix B at the temperatures specified in Table 17. The adsorption coefficient was calculated employing equation (23) (Appendix A), while q_g was obtained at the same challenge concentration values given for the sorbates in Table 17, by using equation (24) (Appendix A).

Examination of Table 12 reveals that K_A is considerably lower than the K_A's tabulated at 20°C (Table 10), a result commensurate with the higher temperature of collection. Cross comparison of q_g in Table 12 with those for the corresponding solutes in Table 17 indicates agreement within a factor of two for n-hexane and 3,3-dimethyl-2-butanone and slightly higher disagreement for n-octane and n-butylamine. The agreement however is very encouraging considering the data came from two different sets of experiments and that the possibility still exists that the challenge concentrations quoted may not be in Henry's Law range.

Equation (24) (Appendix A) can be rearranged to allow calculation of the initial concentration in ppm (v/v) of the pollutant in the gas stream flowing over the sample cartridge bed from the measured uptake q_g, provided K_A is known and that the gas plume concentration of the pollutant is in the Henry's Law region. It is the latter factor which makes a knowledge of the adsorption isotherm of value. For example, if an uptake of n-octane on Tenax-GC at 20°C is 7.50×10^{-4} grams sorbate/gram of adsorbent, then C_g is

$$C_g = \frac{q_g \; 10^6}{K_A A_s^\circ \; (760 \text{ mm Hg}) \; (\text{MW})} = 0.81 \text{ ppm (v/v)}$$

where $K_A = 4.40 \times 10^{-4}$ moles adsorbate/mm Hg-m^2

$A_s^\circ = 23.5$ m^2/g

$q_g = 7.50 \times 10^{-4}$ grams sorbate/grams of adsorbent

MW = 114.23 g sorbate/moles sorbate

ppm = volume/volume basis

It is unfortunate that Tenax-GC is not available in a higher surface area form since thermodynamically, the K_A values exhibited by many adsorbate vapors make it inherently a superior sorbent to XAD-2.

C. Heats of Adsorption

As noted in the theory section (Appendix A), the magnitude and sign of the differential heat of adsorption provides a measure of the interaction between the resin matrix and the sorbate molecule. Although not totally germaine to the design of sorbent trap experiments $\Delta\overline{H}_A$ can readily be calculated using equation (27) (Appendix A), and the slope of the regression equation listed for the individual adsorbates in Appendix B.

The differential heats of adsorption for the sorbates on XAD-2 and Tenax-GC are tabulated in Table 13. In addition, for each sorbate, the heat of liquefaction, $\Delta\overline{H}_L$, is listed. There are some interesting trends in this data which support intuitive concepts of preferential adsorption already gained from the inspection of V_g^T data. For example, thirty out of thirty-eight sorbates have larger $\Delta\overline{H}_A$ on Tenax-GC than on XAD-2. For some groups of adsorbates, such as the phenols, ketones and halogenated hydrocarbons, every member follows this trend. With respect to the reverse trend, only the aliphatic acids show as a class marginally greater $\Delta\overline{H}_A$ on XAD-2 than on Tenax-GC.

The magnitude of the difference between $\Delta\overline{H}_A$ for the individual adsorbates on Tenax-GC and XAD-2 can be marginal (0-1 Kcal/mole) for some sorbate classes, such as n-alkanes, aliphatic alcohols, and the phenols, or as large as 3-5 Kcal/mole for other classes, such as halogenated hydrocarbons and the ketones. The magnitude of the $\Delta\overline{H}_A$ difference between the two resins for the ketones and halogenated hydrocarbons may

Table 13

Comparison of Differential Heats of Adsorption*, $\Delta\bar{H}_A$, for Adsorbates on Sorbent Resins with Heat of Liquefaction*, $\Delta\bar{H}_L$

	-------- ΔH_A on ------		
Adsorbate	Tenax-GC	XAD-2	ΔH_L**
n-Hexane	14.0	14.0	7.5
n-Octane	14.9	17.3	9.9
n-Decane	18.4	18.0	12.3
n-Dodecane	24.3	--	--
Benzene	13.4	12.4	8.1
Toluene	16.9	13.6	9.1
p-Xylene	14.0	14.4	10.1
Ethylbenzene	15.8	13.6	10.1
n-Propylbenzene	15.7	16.5	11.1
1,2-Dichloroethane	12.6	11.2	8.47
Fluorobenzene	14.8	11.5	8.27
1,1,2-trichloroethylene	14.7	11.4	8.5
Chlorobenzene	18.3	13.0	9.63
Bromobenzene	19.3	13.7	10.5
1,4-Dichlorobenzene	20.0	15.0	15.5
2-Butanone	13.4	8.73	8.3
2-Heptanone	19.7	15.0	--
4-Heptanone	19.0	15.3	--
Cyclohexanone	16.8	12.7	10.8
3-Methyl-2-butanone	14.5	10.8	8.82
3,3-Dimethyl-2-butanone	--	12.0	9.25
2,6-Dimethyl-4-heptanone	--	17.4	--
Acetophenone	18.4	15.8	13.4
n-Butylamine	12.6	10.4	7.8
n-Amylamine	15.0	12.5	--
n-Hexylamine	16.2	13.6	--
Benzylamine	15.0	17.2	--

Table 13 (continued)

Comparison of Differential Heats of Adsorption*, $\Delta\bar{H}_A$, for Adsorbates on Sorbent Resins with Heat of Liquefaction*, $\Delta\bar{H}_L$

Adsorbate	ΔH_A on Tenax-GC	ΔH_A on XAD-2	ΔH_L**
Di-n-butylamine	16.9	16.7	--
Tri-n-butylamine	16.7	--	--
Ethanol	9.2	10.0	10.1
n-Propanol	11.0	11.4	11.3
n-Butanol	13.7	10.7	12.5
2-Butanol	12.7	11.4	11.9
2-Methyl-2-propanol	9.8	9.7	11.1
2-Methyl-1-propanol	13.5	10.2	12.1
Phenol	16.9	15.8	16.4
o-Cresol	18.6	17.0	18.2
p-Cresol	18.9	17.0	17.7
m-Cresol	18.6	17.0	14.8
Acetic Acid	10.4	10.5	12.5
Propionic Acid	11.8	12.4	13.7
n-Butanoic Acid	11.8	11.9	15.2
n-Pentanoic Acid	15.8	13.0	16.6

---

[*] All values are negative and expressed in units of Kcal/mole.

[**] From J.D. Cox and G. Pilcher, "Thermochemistry of Organic and Organometallic Compounds," Academic Press, N.Y., 1970.

be indicative of the presence of strong polarization forces between Tenax-GC and the two Group B adsorbents. This enthalpy difference is not observed for any of the Group A or D adsorbates.

A comparison of the $\Delta\overline{H}_A$ value for all adsorbates on XAD-2 and Tenax-GC with $\Delta\overline{H}_L$ reveals that $\Delta\overline{H}_A$ exceeds $\Delta\overline{H}_L$ in all cases for the n-alkanes, aromatic and halogenated hydrocarbons, ketones and amines. However for three of Group D adsorbate classes: the phenols, alcohols and acids, $\Delta\overline{H}_L$ for a good number of the adsorbates exceeds $\Delta\overline{H}_A$. The magnitude of this difference is usually 0-1 Kcal/mole, indicative that there is not much intramolecular attraction between XAD-2 and Tenax-GC and the polar, Group D adsorbates.

The $\Delta\overline{H}_A$ values within a given sorbate class tend to increase with carbon number and/or molecular weight. This pattern has been observed in other adsorption studies (53). Overall, the $\Delta\overline{H}_A$ results indicate a predominance of adsorbate-adsorbent interactions, as judged by the general condition $\Delta\overline{H}_L < \Delta\overline{H}_A$, and that only for polar vapors is condensation in the resin matrix the predominant collection mechanism.

D. Frontal Analysis

The frontal analysis results discussed in this report were developed initially for two explicit purposes: to demonstrate that the elution analysis peak maximum correlated with the breakthrough curve on a short cartridge bed (as shown in Figure 1) and to determine adsorption isoterms applicable to potential sampling problems. Several additional factors such as difference in uptake, as measured by the adsorption and desorption branches of a frontal analysis, were also investigated.

Figure 32 presents an actual frontal chromatogram obtained from the Gow-Mac system using n-hexane vapor. This was obtained for a carrier gas phase concentration of ∿450 ppm (v/v), continuously infused via syringe. The initial plateau (A) is due to air in the syringe, a con-

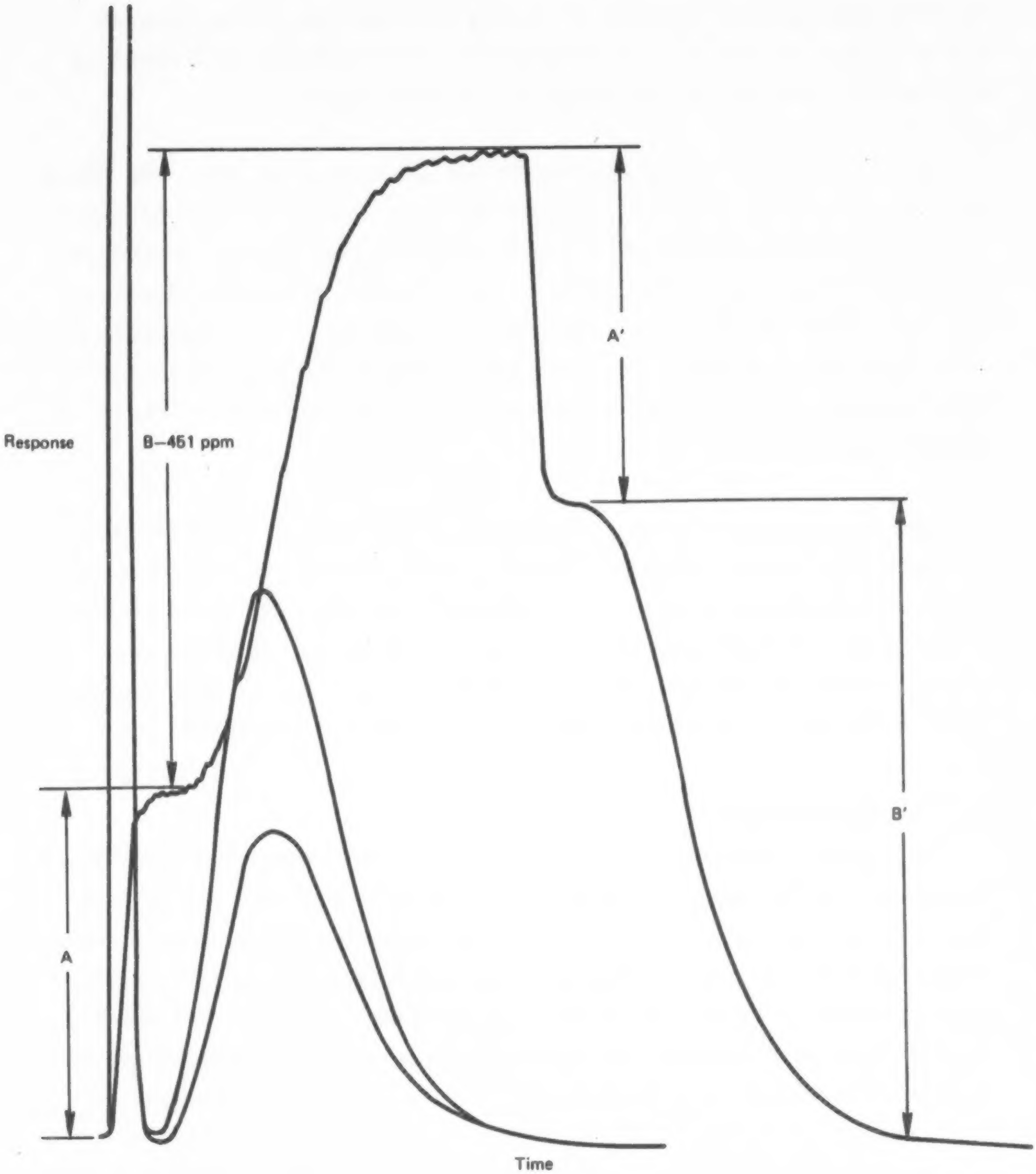

FIGURE 32 FRONTAL AND ELUTION CHROMATOGRAMS FOR n-HEXANE AT APPROXIMATELY 90°C ON XAD–2

taminant which is difficult to avoid during the sampling operation. The air plateau corresponds to the air peak in elution chromatography profiles using thermal conductivity detection and is useful to indicate the dead volume of the system.

Distance B is the plateau due to ~450 ppm (v/v) of n-hexane vapor. Termination of the infusion operation results in an immediate drop, the distance which corresponds to A', and since this is due to the air eluting from the sorbent cartridge, A=A'. The desorption of the n-hexane is the distance B'.

To confirm that these fronts corresponded to elution peaks in a comparable concentration range, the recorder chart was rewound, so that elution chromatograms would commence at the same starting time. Then discrete syringe injections of the same concentration were made.

Inspection of Figure 32 shows that the elution peak maxima correspond to the middle of the frontal profile. The two elution peaks in Figure 32 represent 0.5 mL and 0.25 mL injections of the same sample concentration used in the frontal experiments. There is a slight skew in both peaks which may indicate that the experiments are not in the Henry's Law region of adsorption but overall the results are gratifying.

Figure 33 is for the sorbate, n-octane, at a carrier gas concentration of ~100 ppm (v/v). Again the frontal chromatogram maintains essentially the same qualitative and quantitative features apparent in Figure 32. Note that the elution chromatogram run on the same chart paper at 1/2 height again shows good correspondence to the frontal profile.

Figures 34 and 35 are breakthrough curves for n-octane at two different challenge concentrations. Figure 35 was generated by using the same sampling bag concentration as in Figures 33 and 34, but changing

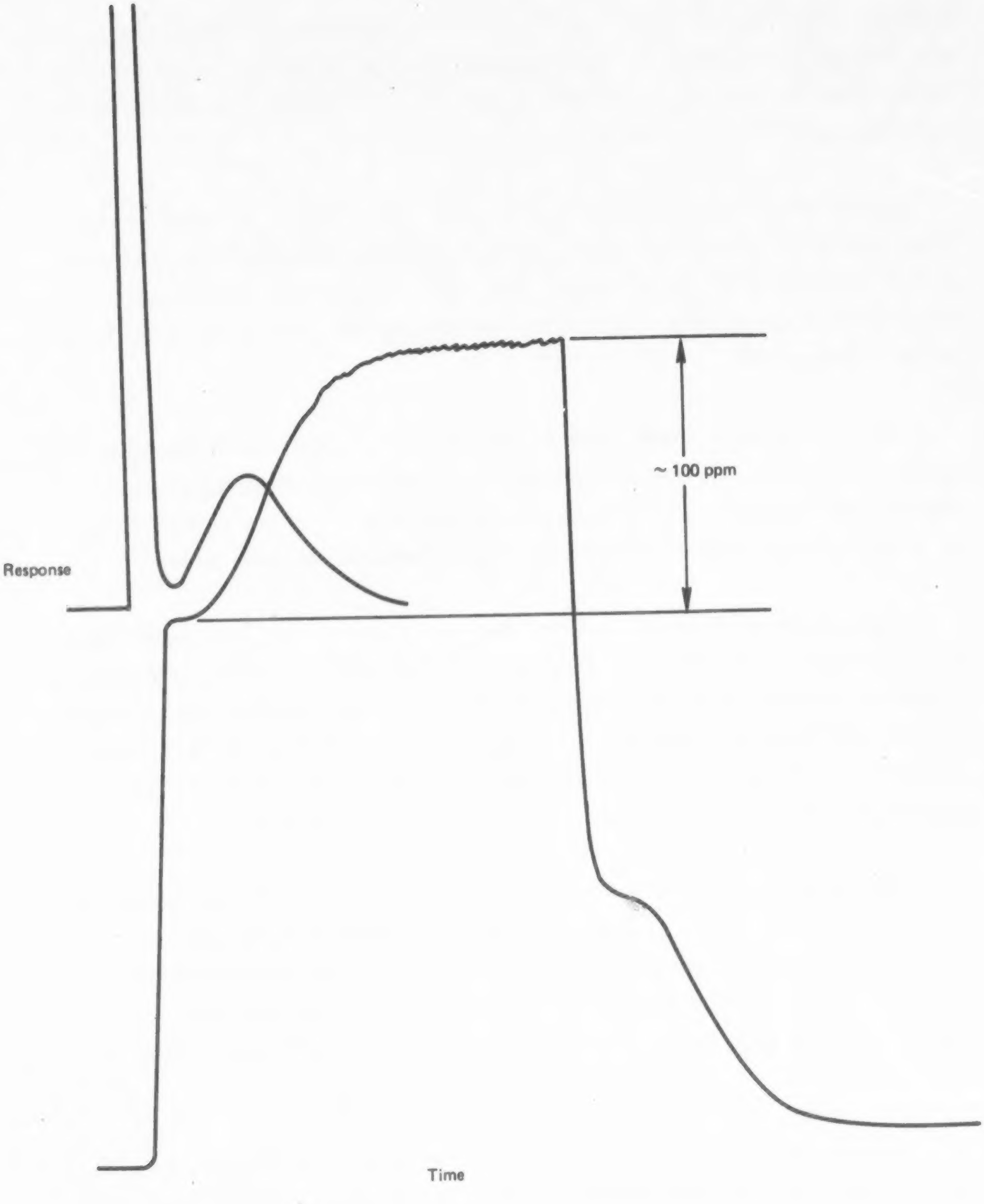

FIGURE 33 FRONTAL AND ELUTION CHROMATOGRAMS FOR n-OCTANE AT 94.7°C ON XAD–2

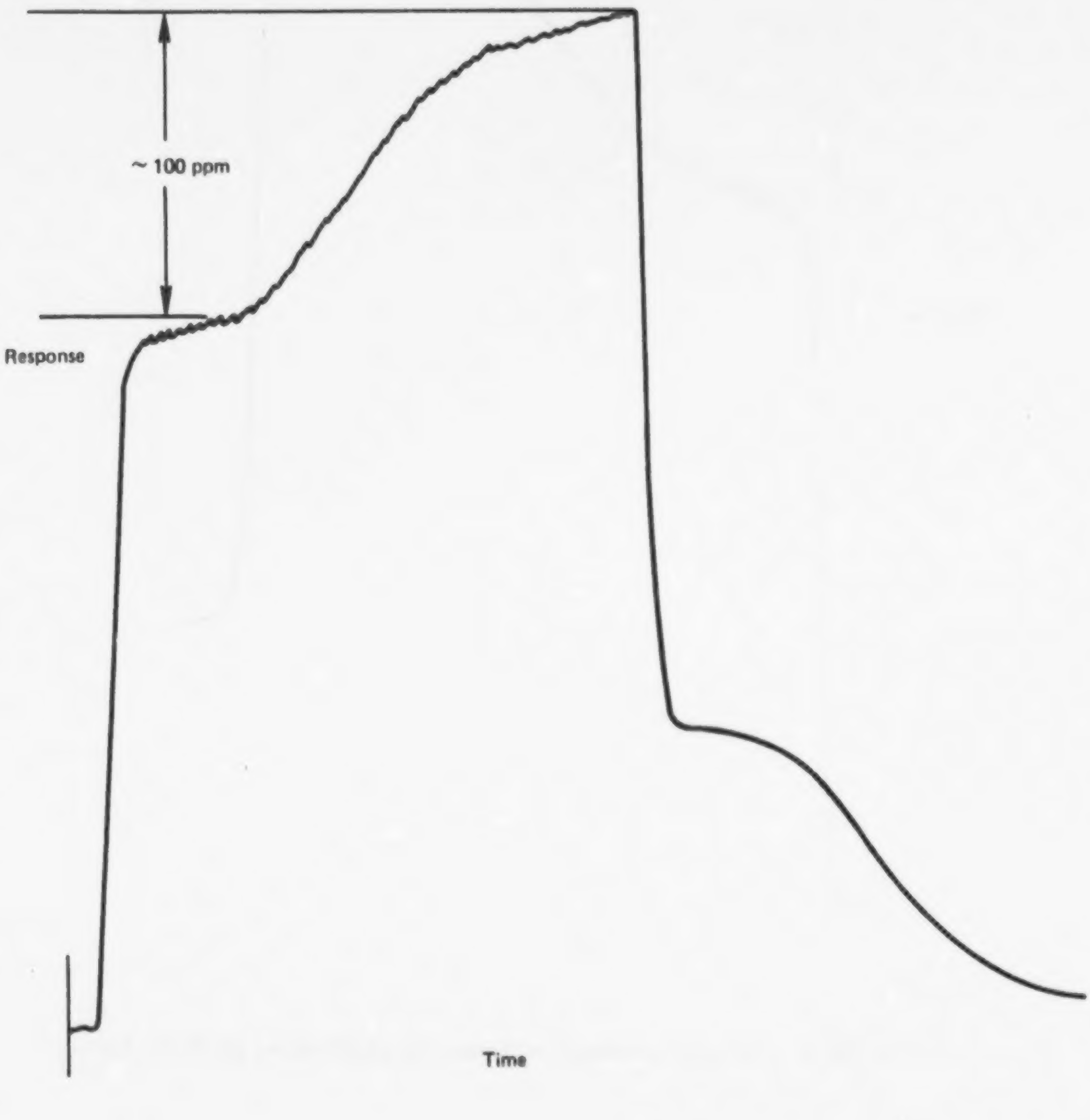

FIGURE 34 FRONTAL CHROMATOGRAMS FOR n-OCTANE AT 87.8°C ON XAD–2

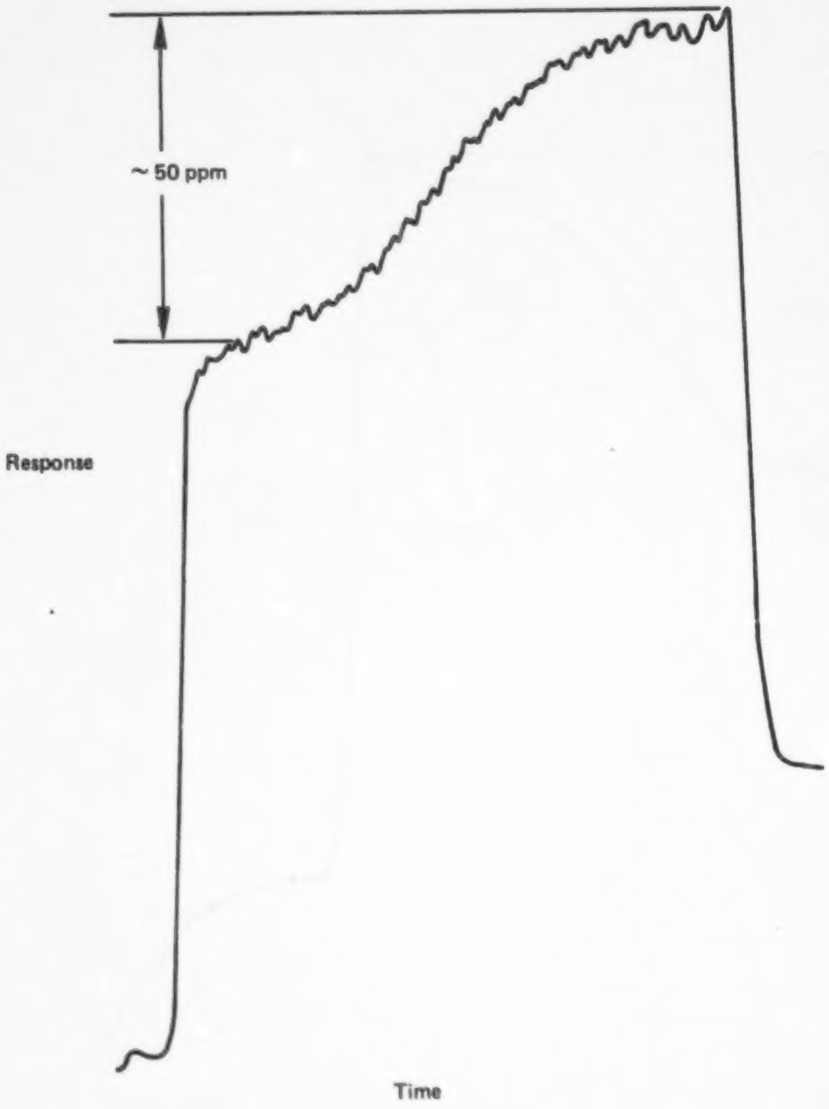

FIGURE 35 FRONTAL CHROMATOGRAMS FOR n-OCTANE AT 87.8°C ON XAD–2

to 50 ppm (v/v) in the carrier gas by altering the syringe infusion setting to reduce the delivery rate by one-half. Note that these curves are somewhat more diffuse than the curves at 94.7°C due to the lower temperature (87.8°). Since the lower challenge concentration curve would have been diminished in response by 1/2, the attenuation was also halved in recording it. Overlay of Figures 34 and 35 show that the curves are practically identical, in striking confirmation of the quantitative reproducibility of the technique.

Some additional data on the reproducibility and comparison of the specific retention volume determined from the mid-point of the frontal breakthrough curve to those obtained from elution peak maxima are given in Table 14. The average V_g^T for n-butylamine on XAD-2 at 93.2°C for the frontal technique is 507 mL/g, while for the elution technique the value is 489 mL/g. This is very good agreement and probably would be closer were it not for the one anomolously high value of 534 mL/g for the frontal technique. Certain kinetic contributions to the boundary profile in frontal analysis may distort the V_g^T value at one-half the plateau concentration unless corrections are made. Thus it is difficult to always obtain good agreement between V_g^T from the two experimental sources. Nonetheless, the results depicted in Figures 32-35 are encouraging and stand as evidence that the elution analysis peaks are an accurate measurement of breakthrough.

Table 15 summarizes the results for the frontal analysis studies, including values for q_g and V_g^T at 50% volumetric breakthrough in the desorption branch of the frontal analysis curve as well as the adsorption branch. The q_g values were determined by integration of the frontal analysis curves. The temperature and challenge concentration for the various adsorbates run are also listed. Most of the challenge concentrations are above 50 ppm (v/v), so that an adequate curve could be obtained for integration purposes.

Table 14

Comparison of Specific Retention Volumes Determined via Elution Chromatography with Those Determined by Frontal Analysis for n-Butylamine at 93.2°C on XAD-2

Frontal Analysis	
Run 1	534
Run 2	499
Run 3	481
Run 4	513
Avg. =	507

Elution Analysis	
Run 1	497
Run 2	485
Run 3	486
Avg. =	489

Table 15

Comparison of V_g^T and Weight Capacities for Sorbates on XAD-2 from Elution and Frontal Analysis (Gow-Mac)

				Frontal Analysis			
		Elution		Adsorption		Desorption	
Compound	Challenge Concentration (ppm)*	V_g^T (mℓ/g)	Column Temp. (°C)	V_g^T (mℓ/g)	Weight Capacity (g/g)	V_g^T (mℓ/g)	Weight Capacity (g/g)
Toluene	141	419	124.6	451	3.01×10^{-4}	428	2.98×10^{-4}
n-Butylamine	138	489	93.2	505	2.38×10^{-4}	502	2.55×10^{-4}
Ethanol	133	293	45.8	346	1.07×10^{-4}	363	0.955×10^{-4}
3,3-Dimethyl-2-butanone	72	587	111.7	650	2.36×10^{-4}	639	2.31×10^{-4}
n-Hexane	118	702	86.2	715	3.57×10^{-4}	708	3.53×10^{-4}
n-Octane	60	394	140.9	448	1.67×10^{-4}	410	1.42×10^{-4}

* ppm on volume/volume basis.

Column 2 in Table 15 lists the challenge concentrations studied for each sorbate. Since they vary from compound to compound, only derivation of an isotherm from each front allows a comparison to be made at equal concentration levels. However, n-hexane, n-butylamine, challenged the column at similar concentrations and temperatures. The order of adsorption is n-hexane > n-butylamine, which is consistent with the comparative V_g^T value determined earlier in elution experiments. The low affinity of the resin for alcohols, even when the column temperature for ethanol is ∿40°C less than for the other sorbates, is apparent in column 6.

Columns 5 and 7 tabulate the V_g^T values computed for 50% of the plateau concentration. These can be compared with the V_g^T for elution peaks generated at peak maxima concentrations in approximately the same range as 50% of the frontal plateau concentration. The elution values are in column 3. The agreement in general is very good, ranging from 3-15% difference. This definitely confirms that the frontal technique yields results equivalent to the elution data in the same concentration range.

It is interesting to note that two of the three adsorbates in most serious disagreement were at high challenge concentrations (133, 141 ppm v/v). Another sorbate, n-butylamine, showed excellent agreement at 130 ppm (v/v) challenge concentration. This latter case is possible if the sorption isotherm is linear over a large vapor phase concentration range. An example of this will be illustrated shortly.

Frontal chromatograms were easily generated for n-octane at a challenge level of ∿3 ppm (v/v) and were readily reproducible. In addition, triplicate elution chromatograms were determined for the same solute. These results with the data generated from frontal and elution analysis at higher concentrations are presented in Table 16. Included in this table are the n-octane results of Table 15 for direct comparison purposes.

Table 16

Comparison of V_g^T and Weight Capacities for n-Octane on XAD-2 From Elution and Frontal Analysis

				Frontal Analysis			
		Elution		Absorption		Desorption	
Detector	Challenge Concentration (ppm)*	V_g^T (mℓ/g)	Weight Capacity (g/g)	V_g^T (mℓ/g)	Weight Capacity (g/g)	V_g^T (mℓ/g)	Weight Capacity (g/g)
Thermal Conductivity	60	394		448	1.67×10^{-4}	410	1.42×10^{-4}
Flame Ionization	3.08	539	6.67×10^{-6}	926	1.62×10^{-5}	570	9.443×10^{-6}
Flame Ionization	70.4	522	1.80×10^{-4}	464	1.86×10^{-4}	550	2.219×10^{-4}

---

[*] ppm on a volume/volume basis.

A comparison of column 3 with columns 5 and 7 (V_g^T data) indicate good agreement between the elution V_g^T values and the frontal V_g^T values for the two high n-octane concentrations. Comparison of these values for n-octane at 3.08 ppm (v/v) challenge concentration shows some disagreement when comparing the frontal adsorption V_g^T value with the V_g^T from elution chromatography. Furthermore, there is some discrepancy between the V_g^T values estimated for the 70.4 ppm (v/v) concentration (run on the FID system) and those for the 60 ppm (v/v) concentration (done on the thermal conductivity gas chromatograph).

Weight capacities for the n-octane sorbing on XAD-2 are also presented in Table 16. Here again there are some significant differences; however the uptakes for n-octane at the 60 and 70 ppm (v/v) level agree quite well including the peak maximum uptake value in column 3. The most serious disagreement lies in the V_g^T and weight capacities of the n-octane (∿3 ppm v/v) for elution and frontal adsorption analysis results. In this case the V_g^T value on the adsorption trace is quite high and the skew lies in the adsorption branch. This is definitely opposite to the behavior observed for n-octane in evaluating its isotherm by the elution by characteristic point method (ECP), as will be shown later.

One reason for this discrepancy may lie in the possibility of some irreversible adsorption at the low challenge concentration levels which was not immediately apparent in the 50-150 ppm (v/v) challenge concentration range. It is pertinent to note that five out of the six adsorbates done on the thermal conductivity chromatograph at higher challenge concentration levels show reductions in the weight capacity of sorbate desorbed when compared to the initial adsorption uptake. This otherwise small difference is of the order which would appear significant at the 3 ppm (v/v) challenge concentration level.

To further examine this phenomena, additional frontal chromatograms were run for n-hexane, 3,3-dimethyl-2-butanone, and n-butylamine at low challenge concentrations. These were all run on the Varian flame ionization module at temperatures as close as possible to those previously employed on the thermal conductivity chromatograph at higher challenge concentrations (see Table 15). The resultant frontal chromatogram upon visual examination did not show significant difference between the adsorption and desorption traces as had been observed for the n-octane frontal analysis curve.

Computation of the 50% breakthrough V_g^T for both adsorption and desorption portions of the frontal chromatogram and the resultant weight capacities are listed in Table 17. Also included are V_g^T values obtained by elution analysis of bag samples at the same concentration used in the frontal analysis. In general, the same trends observed for n-octane hold for the additional three adsorbate vapors. Values of V_g^T from elution experiments correlate better with the V_g^T value from the desorption trace, rather than the adsorption trace. The V_g^T and weight capacities for the adsorption trace are slightly higher than those obtained from the desorption trace for the three new adsorbents at low challenge concentrations. However, in no case is the discrepancy as high as that observed with n-octane.

A comparison of the V_g^T values with those obtained at higher challenge concentrations show that for n-butylamine and 3,3-dimethyl-2-butanone, there is little difference in V_g^T outside of experimental error. This supports the earlier statement that even at 138 ppm (v/v), n-butylamine is in the Henry's Law region of its sorption isotherm. The same is true for the ketone and it, too, must be in the Henry's Law region, where V_g^T does not vary with challenge concentration (the weight capacity will change as shown in Tables 15 and 17). For the two n-alkanes, the V_g^T values increase with lower challenge concentration, indicative that the Henry's Law region has still not been totally reached

Table 17

Comparison of V_g^T and Weight Capacities for Sorbates on XAD-2 from Elution and Frontal Analysis (Varian)

				Frontal Analysis			
		------Elution-----		-----Adsorption----		-----Desorption----	
Compound	Challenge Concentration (ppm) *	V_g^T (mℓ/g)	Column Temp. (°C)	V_g^T (mℓ/g)	Weight Capacity, q_g (g/g)	V_g^T (mℓ/g)	Weight Capacity, q_g (g/g)
n-Butylamine	7.76	464	101.6	574	1.65×10^{-5}	467	1.47×10^{-5}
3,3-Dimethyl-2-butanone	8.21	549	115.0	629	3.21×10^{-5}	609	2.77×10^{-5}
n-Hexane	8.11	734	87.9	932	2.59×10^{-5}	799	2.54×10^{-5}
n-Octane	3.08	539	142.6	926	1.62×10^{-5}	570	9.44×10^{-6}
n-Octane	70.4	522	141.6	464	1.86×10^{-5}	550	2.22×10^{-4}

*ppm on a volume/volume basis

at 118 and 60 ppm (v/v) for n-hexane and n-octane, respectively.

The slight differences observed between the weight capacities (Table 17) derived from the adsorption and desorption traces of the chromatograms supports the earlier hypothesis based upon the results in Table 15 that some irreversible adsorption is occurring for higher boiling adsorbates and for those which show a greater affinity for XAD-2 (the n-alkanes). Again the differences are of the order of a few micrograms. The capacities are a factor of ten lower at 3 and 8 ppm (v/v) challenge concentrations compared to the higher values recorded in Table 15. The weight capacity is definitely a function of challenge concentration.

To determine whether irreversible adsorption is related to the temperature at which adsorption and desorption is taking place, the frontal analysis could be run at a higher temperature. Under these conditions, the irreversibility might be overcome and V_g^T and weight capacity should be identical from both traces. It is interesting to note that for the adsorbates in Table 15 the ratios for the V_g^T (adsorption)/ V_g^T (desorption) are approximately the same as the weight capacity (adsorption)/weight capacity (desorption) ratio (see Table 18). This shows how V_g^T and weight capacity are directly proportional in the Henry Law region and confirms that the V_g^T at 50% volumetric breakthrough measures the uptake of the resin for a symmetrical mass transfer front.

E. Adsorption Isotherms

As noted earlier, the evaluation of the sorption isotherm for a given adsorbate/adsorbent pair can be done by several chromatographic methods. The advantage of having the adsorption isotherm is obvious when q_g is a function of challenge concentration in that it permits weight capacities and breakthrough volumes to be calculated as a function of the same parameter. In addition, it sets the limits of K_A's applicability, indicates the affinity of resin for a sorbate and allows

Table 18

Comparison of the V_g^T (adsorption)/V_g^T (desorption) with Weight Capacity (adsorption)/Weight Capacity (desorption) Ratio

Adsorbate	V_g^T Ratio	Weight Capacity Ratio
n-Butylamine	1.23	1.12
3,3-Dimethyl-2-butanone	1.03	1.02
n-Hexane	1.16	1.15
n-Octane	1.62	1.71

the saturation capacity of the sorbent to be ascertained.

To determine the type of adsorption isotherm and its dependence on the nature of the adsorbate, frontal desorption chromatograms were analyzed by the characteristic point method (Appendix A). All the isotherms for n-octane, ethanol, toluene, 3,3-dimethyl-2-butanone, n-butylamine and n-hexane were Type I, Langmuir adsorption isotherms on XAD-2. The departure from linearity was slight in many cases. A typical isotherm derived from frontal analysis (in triplicate) is shown in Figure 36. The reproducibility is excellent between analyses. Type I isotherms have also been reported for n-butanol and diethyl ether on Chromosorb 102 (54).

Figure 37 shows the sorption isotherms for n-octane and n-butanol at 98.6°C on XAD-2 and a flow rate of 108 mL/min. It is obvious that the uptake of n-octane by the resin is considerably greater than for n-butanol. Attempts to gather data for lower temperature were difficult due to the failure of the decaying tail of the peak to return to baseline. Note that the sorption isotherm for n-octane is Type I and that for n-butanol, the isotherm is linear for a rather large challenge concentration range. These isotherms were determined by the elution by characteristic point method (Appendix A).

Since the ECP method is much simpler to run than frontal analysis, a rigorous comparison of the isotherms generated by these two techniques for a common sorbate at a common challenge concentration range would be of value. Isotherms for the two chromatographic techniques have been generated from the FID/GC results and are presented in Figures 38 and 39. For the higher challenge concentration range, curves I, II and III represent the frontal analysis generated isotherm, the elution curve generated isotherm without correction for kinetic band broadening (whose major contributors tend to be eddy and longitudinal diffusion and resistance to mass transfer from the resin bed), and the corrected

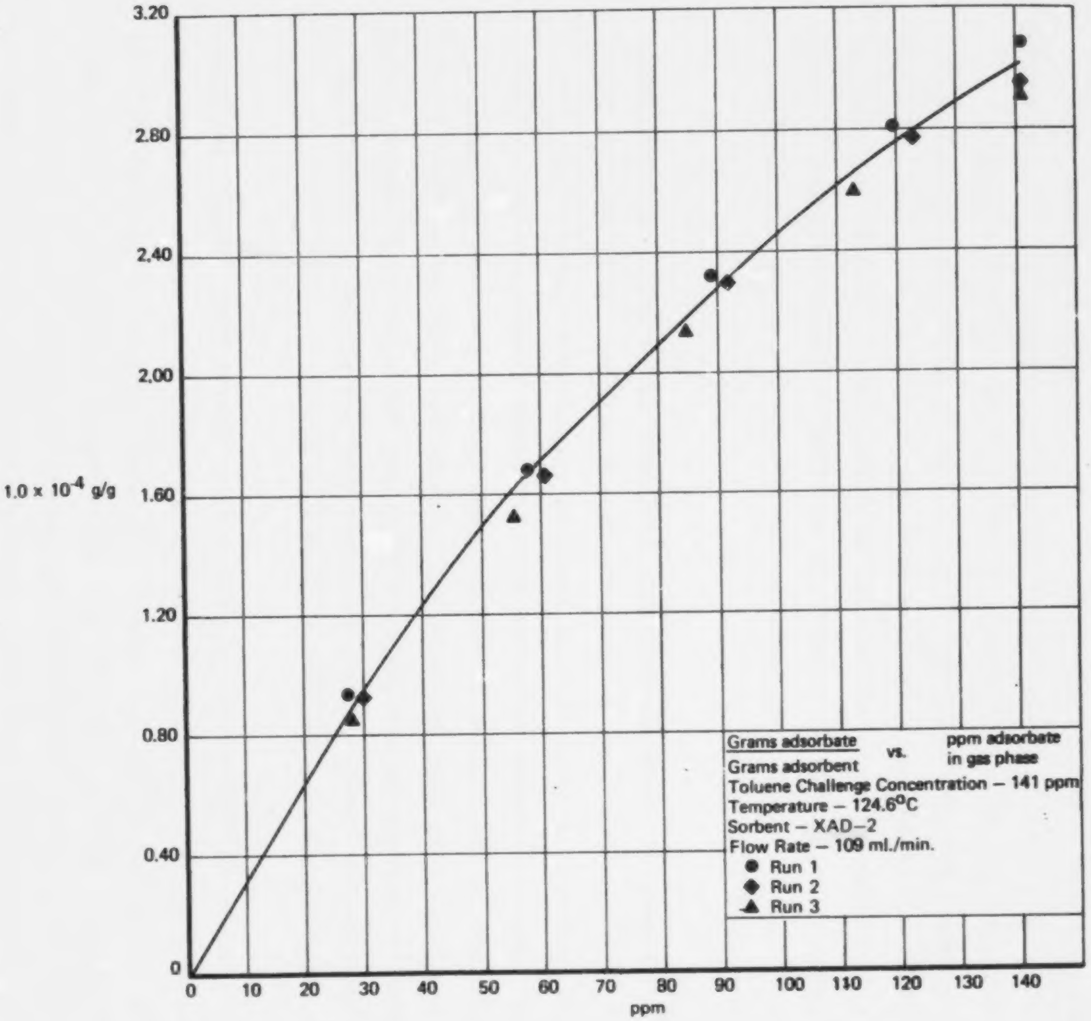

FIGURE 36 ADSORPTION ISOTHERM OF TOLUENE ON XAD–2 DERIVED FROM FRONTAL ANALYSIS RESULTS

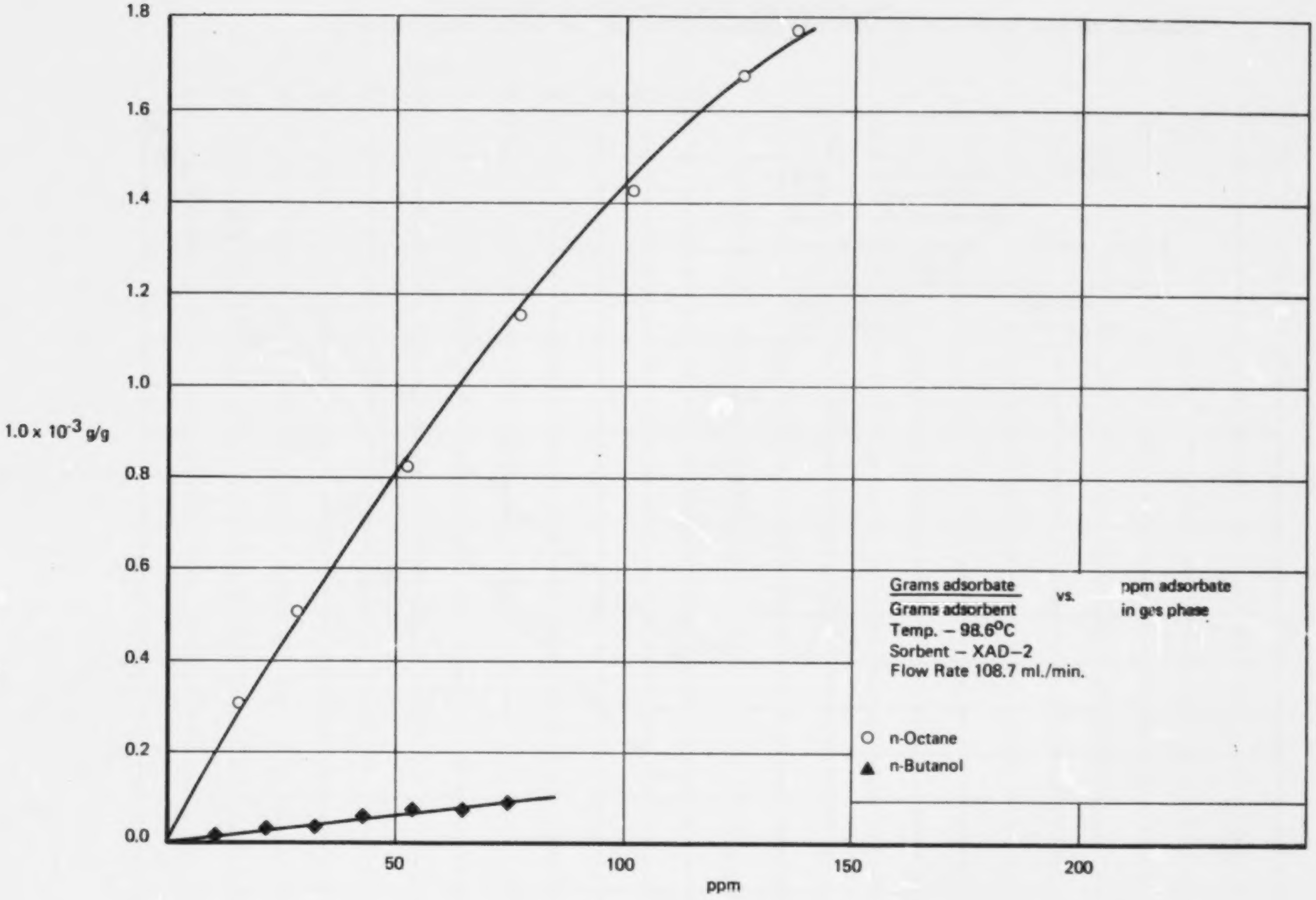

FIGURE 37 COMPARISON OF ADSORPTION ISOTHERMS FOR DIFFERENT TYPES OF ADSORBATES

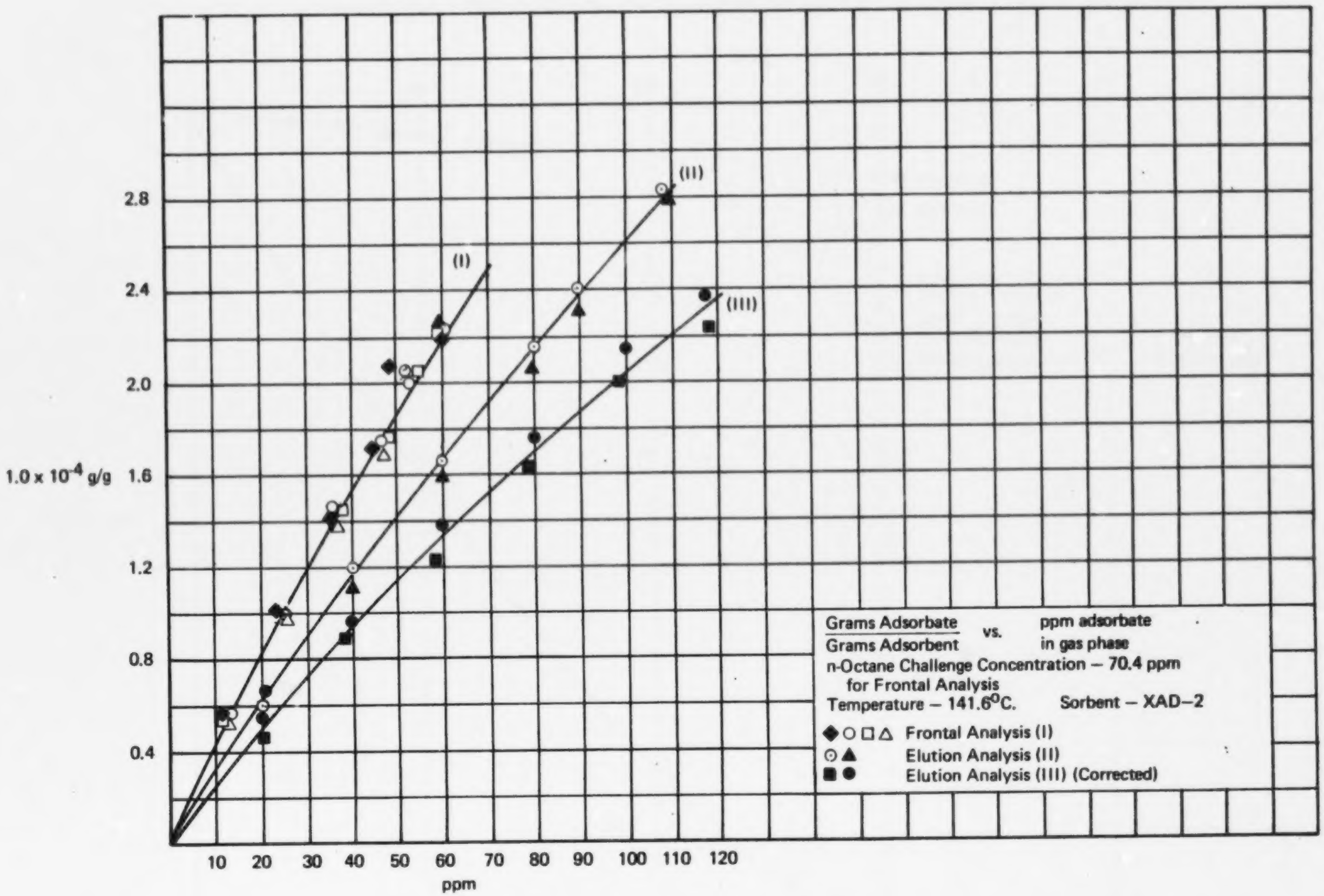

FIGURE 38 COMPARISON OF SORPTION ISOTHERMS GENERATED BY DIFFERENT CHROMATOGRAPHIC TECHNIQUES AT HIGH CHALLENGE CONCENTRATION

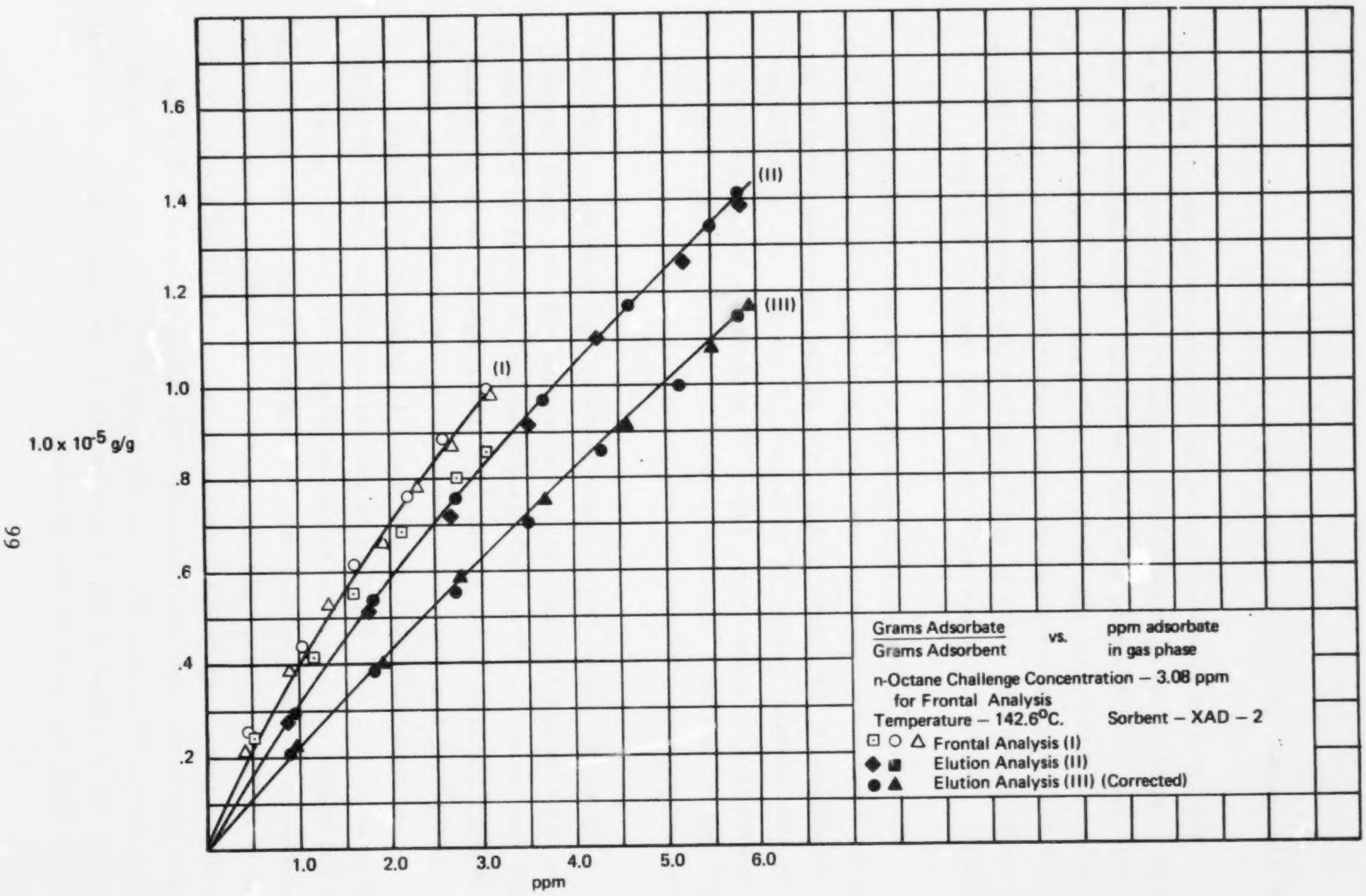

FIGURE 39 COMPARISON OF SORPTION ISOTHERMS GENERATED BY DIFFERENT CHROMATOGRAPHIC TECHNIQUES FOR LOW CHALLENGE CONCENTRATIONS

elution curve isotherm, respectively.

The isotherm generated by frontal analysis would tend to give a higher capacity for a given challenge concentration since there is no correction for diffusion, etc., in the method. Thus curves I and II should be similar, and they are. In addition, if one plots the isotherm for n-octane challenge concentration of 60 ppm (v/v) in Table 15, it exactly overlays curve II which confirms the equivalency of the two methods. Curve III of course is the "true" sorption isotherm.

The curves in Figure 39 correspond to the same sequence above except for a lower challenge concentration range. These results allow a comparison of the uptake by the resin by two independent isotherms. Take, for example, curve III in Figures 38 and 39. For a challenge concentration of 5 ppm (v/v), Figure 38 predicts an uptake of 1.2×10^{-5} g/g while Figure 39 yields a value of 1.0×10^{-5} g/g. This is excellent agreement between the two isotherms.

Figure 40 depicts the sorption isotherm for n-octane at different flow rates on XAD-2 resin. It is interesting that the resin uptake is very similar at the three flow rates examined, although at a challenge concentration level above 70 ppm (v/v) there appears to be a decrease in uptake with flow rate. The results from elution analysis V_g^T trends with flow rate would predict a decrease in uptake at 550 mL/min. (Figures 27-28), however, this is not discernible in Figure 40 except at the higher challenge concentration level. This points out the superiority of the V_g^T measurement for sorbate uptake in the Henry's Law region of the isotherm. One complementing fact obtained from Figure 40 is that slope of the n-octane isotherms as the challenge concentration tends toward zero are nearly equal. This slope is equal to K_A, the adsorption coefficient, hence the decrease in V_g^T with flow rate noted earlier for sorbates on XAD-2 must be due to the reduction in effective surface area available to the adsorbate.

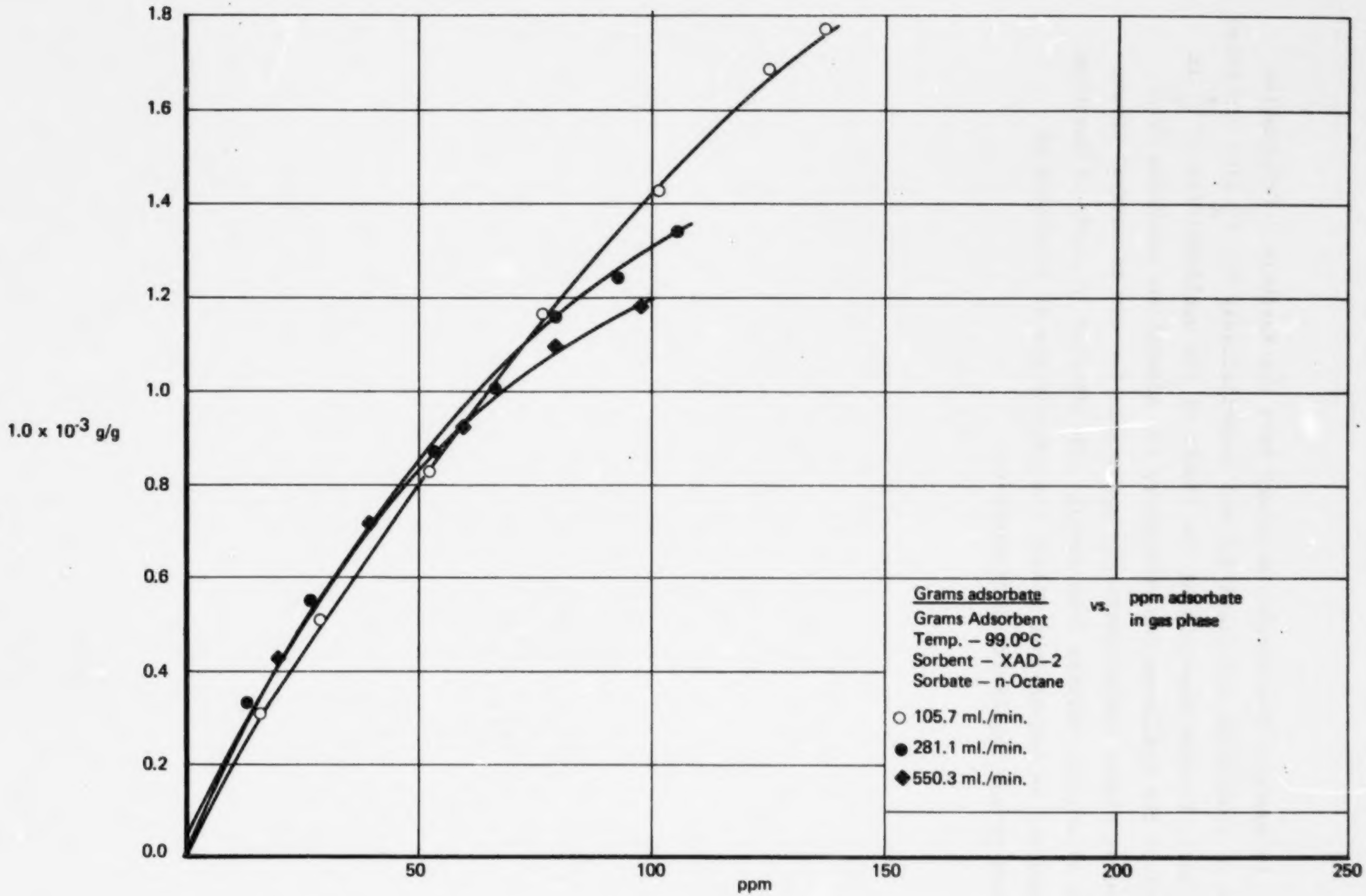

FIGURE 40 ADSORPTION ISOTHERM DEPENDANCE ON FLOW RATE OF CARRIER GAS

In summary, the results obtained from the isotherm determination tend to complement qualitatively and quantitatively the V_g^T data described earlier. Besides quantifying the limits of the applicability of V_g^T in terms of the challenge concentration, the adsorption isotherms determined at higher temperatures are applicable for use in thermal desorption of organic solutes from resins. In addition, a study of isotherm dependence on temperature allows the computation of breakthrough volume at any challenge concentration.

V. CONCLUSIONS AND RECOMMENDATIONS

The data presented in this report support the use of chromatographic elution data to characterize breakthrough and sorption capacity of sorbent cartridges containing synthetic resin. Specific retention volume data as a function of temperature, adsorbate type, and challenge concentration have been gathered on XAD-2 and Tenax-GC resin.

Complementary frontal analysis experiments indicate that the V_g^T values accurately measure breakthrough in relatively short sorbent cartridges. The quantity of V_g^T data have permitted correlations to be developed between adsorbate physical properties and V_g^T, which permit reliable estimation of V_g^T for other adsorbates without resorting to experimental measurement.

Selectivity toward non-polar organic species is shown by both resins, a trend supported by isotherm data of different sorbate types on both resins. Experiments conducted at high gas velocities show little variance in V_g^T with flow for Tenax-GC, but an apparent loss of 15-20% for several chemically dissimilar sorbates on XAD-2 at face velocities greater than 64 cm/sec. This in part may be attributed to mass transfer control of the sorbate in the microporous resin.

The experimental techniques and theory developed in the course of this program are generally applicable to characterizing any sorbent media. One of the principal advantages of the gas chromatographic technique is the ability to determine the required data with small quantities of sorbate. The gas chromatographic technique thus minimizes worker exposure to test chemicals, especially important for studies of suspected carcinogens, as well as saving time and money.

The data tabulated in this document also have application in analysis techniques requiring thermal desorption of organic matter from sorbent media. In theory the data are also useful for scale-up designs to enlarged industrial adsorption processes. However, in that case parameters such as $\Delta\bar{H}_A$ which are not of prime significance in this study, will be of greater importance.

Correlations have been observed between the specific retention (elution) volumes, V_g^T, of adsorbates on XAD-2 and Tenax-GC and their boiling points. These correlations may be used to extend the present data to other compounds of interest. The correlations are best when treated by specific compound classes.

Further studies in this area should include a survey of the effects of common combustion gases, such as CO_2 and H_2O, on the V_g^T values. The question of mutual interactions between two or more adsorbates, in the vapor state or on the adsorbent surface, also warrant careful study since the breakthrough and uptake characteristics may be mutually dependent. Additional extensions which warrant consideration are establishing V_g^T values on volatile metallic and organometallic species. Finally, the measurement of specific retention volume data on other adsorbents, such as charcoal, which would retain some of the species which are not retained on Tenax-GC or XAD-2 would be of value.

VI. REFERENCES

1. Locke, D.C., Physicochemical Measurements Using Chromatography in "Advances in Chromatography, Vol 14", J.C. Gidding, E. Grushka, J. Cazes, and P.R. Brown, eds., Marcel Dekker, Inc., N.Y., 1976, pp 87-198.

2. Kobayashi, R., H.A. Deans, and P.S. Chappelear, Physico-Chemical Measurements by Gas Chromatography in "Applied Thermodynamics", American Chemical Society, Washington, D.C., 1968, pp 227-246.

3. Novak, J., V. Vasak, and J. Janak, Anal. Chem., 37, 660 (1965).

4. Gelbicova-Ruzickova, J., J. Novak, and J. Janak, J. Chromatog., 64, 15 (1972).

5. Selucky, M., J. Novak, and J. Janak, J. Chromatog., 28, 285 (1967).

6. Wood, G.O., "Development of Air-Monitoring Techniques Using Solid Sorbents", LASL Project R-059, NIOSH-1A-75-31, LA-6513-PR Progress Report, September, 1976.

7. Snyder, A.D., F.M. Hodgson, M.A. Kemmer, and J.R. McKendree, "Utility of Solid Sorbents for Sampling Organic Emissions from Stationary Sources", EPA Report 600/2-76-201, July, 1976.

8. Janak, J., J. Ruzickova, and J. Novak, J. Chromatog., 99 689 (1974).

9. Butler, L.D., and M.F. Burke, J. Chromatog. Sci., 14, 117 (1976).

10. Adams, J., K. Menzies, and P. Levins, "Selection and Evaluation of Sorbent Resins for the Collection of Organic Compounds", EPA Report 600/7-77-044, April, 1977.

11. Conder, J.R., Physical Measurement by Gas Chromatography in "Progress in Gas Chromatography", J. H. Purnell, ed., Interscience, N.Y., 1968, p. 228.

12. Littlewood, A.B. "Gas Chromatography", Academic Press, N.Y., 1970, pp. 48-50.

13. Kiselev, A.V. and Y.I. Yashin, "Gas-Adsorption Chromatography", Plenum Press, N.Y., 1969, p. 20.

14. Ackerman, D.G., "Chromatographic Adsorption Studies Using a Computer-Controlled Data Acquisition System:, Ph.D. Thesis, Univ. of Arizona, 1973.

15. Steel, W.A., Adv. Colloid Interface Sci, 1, 3 (1967).

16. Dal Nogave, S., and R.S. Juvet, Jr., "Gas-Liquid Chromatography", Interscience, N.Y., 1962, p. 89.

References (continued)

17. Gregg, S.J., and R. Stock, Sorption Isotherms and Chromatographic Behavior of Vapours in "Gas Chromatography 1958", D.H. Desty, ed., Butterworths, London, 1958.

18. Kuge, Y., and Y. Yoshikawa, Bull. Chem. S oc., Japan, 38, 948 (1965).

19. Huber, J.F.K., and R.G. Gerritse, J. Chromatog., 58, 137 (1971).

20. Conder, J.R., and J.H. Purnell, Trans. Faraday Soc., 65, 824 (1969).

21. Cremer, E., and H.R. Huber, Agnew. Chem., 73, 461 (1961).

22. Sewell, P.A., and R. Stock, J. Chromatog., 50, 10 (1970).

23. Kiselev, A.V., and Y.I. Yashin, "Gas-Adsorption Chromatography", Plenum Press, N.Y., 1969, p. 114.

24. Cremer, E., and H.F. Huber, "Gas Chromatography," N. Brenner, J.E. Cullen, and M.D. Weiss, eds., Adademic Press, N.Y., 1962, p. 171.

25. Neumann, M.G., J. Chem. Ed., 53, 708 (1976).

26. Dear, D., A. Dillon, and A. Freedman, J. Chromatog., 137, 315 (1977).

27. Rappaport, S.M. et al, "Development of Sampling and Analytical Methods for Carcinogens," LASL Project R-219, LA-6387-PR, June, 1976.

28. Pellizzari, E.D., "Development of Analytical Techniques for Measuring Ambient Atmospheric Carcinogenic Vapors", EPA Report 600/2-75-076, November, 1975.

29. Dubnin, M.M., J. Colloid Interface Sci., 23, 487 (1967).

30. Kiselev, A.V., and Y.I. Yashin, "Gas-Adsorption Chromatography", Plenum Press, N.Y., 1969, pp. 11-16.

31. Lochmuller, C., Private Communication.

32. Ackman, R.G., J. Chromatog. Sci., 10, 506 (1972).

33. Gvosdovich, T.N., A.V. Kiselev, and Y.I. Yashin, Chromatographia, 6, 179 (1973).

34. Lange, N.A., ed., "Handbook of Chemistry", Handbook Publishers, Inc., Sandusky, Ohio, 1952.

35. Weast, R.C., ed., "Handbook of Chemistry and Physics - 44th Edition", Chemical Rubber Co., Cleveland, Ohio, 1964.

References (continued)

36. Kiselev, A.V., and Y.I. Yashin, "Gas-Adsorption Chromatography", Plenum Press, N.Y., 1969, p. 60.

37. Gearhart, H.L. and M.F. Burke, J. Chromatog. Sci., 11, 411 (1973)

38. Frontasev, V.P., and L.S. Shraiber, Russ. J. Phys. Chem., 43, 229 (1969).

39. LeFevre, R.J.W., and K.D. Steel, Chem. Ind., 670 (1961).

40. Applequist, J., J.R. Carl, and K. Fung, J. Amer. Chem. Soc., 94. 2952 (1972).

41. Batsanov, S.S. "Refractometry and Chemical Structure", D. Van Nostrand, Princeton, J.H., 1969.

42. Taterskii, V.M., V.A. Bonderskii, and S.S. Yavovoi, "Rules and Methods for Calculating the Physico-Chemical Properties of Paraffinic Hydrocarbons", Pergamon Press, N.Y., 1961.

43. Kiselev, A.V., and Y.I. Yashin, "Gas-Adsorption Chromatography", Plenum Press, N.Y., 1969, p. 58.

44. Rakshieva, N.R., S. Wicar, J. Novak and J. Janak, J. Chromatog., 91, 59 (1975)

45. Oberholtzer, J.E. and L.B. Rogers, Anal. Chem., 41, 1590 (1969).

46. Little, J.N., and W.J. Pauplis, Separation Sci., 4, 513 (1969).

47. Kelley, R.N., and F.W. Billmeyer, Jr., Anal. Chem., 42, 399 (1970).

48. Moreland, A.K., and L.B. Rogers, Separation Sci., 6, 1 (1971).

49. Rakshieva, N.R., J. Novak, S. Wicar and J. Janak, J. Chromatog., 91, 51 (1974).

50. Gaha, O.K., J. Novak and J. Janak, J. Chromatog., 84, 7 (1973).

51. Giddings, J.C., Gas Chromatography 1964 (A. Goldup, ed.) Elsevier, Amsterdam, 1965, p. 3.

52. DeLigny, C.L., J. Chromatog., 35, 50 (1968)

53. Hartkopf, A., and B.L. Karger, Accts. Chem. Res., 6, 209 (1973).

54. Kiselev, A.V., and Y.I. Yashin, "Gas-Adsorption Chromatography", Plenum Press, N.Y., 1969, p. 118.

55. Gvosdovich, T.N., A.V. Kiselev, and Y.I. Yashin, Chromatographia, 2, 234 (169).

References (continued)

56. Sakodinsky, K., Chromatographia, 1, 483 (1968).

57. Hamersma, J.W., S.L. Reynolds, and R. F. Maddalone, "IERL-RTP Procedures Manual: Level 1 Environmental Assessment", EPA Report 600/2-76-160a, June 1976.

APPENDIX A

Theoretical Considerations

Several chromatographic methods have been employed in this study to produce specific retention volume data, adsorption isotherms, etc. Each method, however, comes from one central theoretical derivation. The relationship between a chromatographic elution profile (whether it be frontal, elution, etc.) and a distribution coefficient, such as the adsorption coefficient, K_A, has been derived by Conder (11) as:

$$V_g^T = (1 - j\gamma)\left(\frac{dq}{dc}\right)_T A_s^\circ \qquad (1)$$

where j = pressure correction = $\frac{3}{2}\left[\frac{(P_i / P_o)^2 - 1}{(P_i / P_o)^3 - 1}\right]$

γ = mole fraction of the adsorbate in the gas phase

q = concentration of the adsorbate in the adsorbent in moles/cm^2 (better known as the surface excess, Γ)

c = concentration of the adsorbate in the gas phase in moles/cm^3

A_s° = specific surface area of the adsorbent in m^2/g

P_o = column outlet pressure

P_i = column inlet pressure.

In the studies reported here, γ is always smaller than 10^{-4}, hence equation (1) reduces to

$$V_g^T = \left(\frac{\partial q}{\partial c}\right)_T A_s^\circ$$

If the chromatographic experiment is being conducted in the low surface coverage region, Henry's Law applies and $\left(\frac{\partial q}{\partial c}\right)$ is a constant such as K_A^* so equation (2) becomes

$$V_g^T = K_A^* A_s^\circ \tag{3}$$

This equation is strictly applicable to the case of elution chromatography using an infinitely small sample (adsorbate) size. This situation frequently is approached in many of the environmental sampling cases. It is significant that in this Henry's Law region, V_g^T is independent of challenge concentration, c.

If $\frac{\partial q}{\partial c}$ is not constant, then V_g^T is input dependent, which means that V_g^T is dependent on c. To find the amount of sorbate captured by the sampling resin requires integration of equation (2) as

$$q = \frac{1}{A_s^\circ} \int_{c=C_o}^{c=C_B} V_g^T \; dc \tag{4}$$

This integration can be performed on an entire elution peak or frontal analysis profile, or if either profile approximates equilibrium, consecutive integrations may be performed for various values of C_B to yield q.

Equation (4) is equally applicable to elution analysis or frontal analysis for those cases where $\frac{\partial q}{\partial c}$ is either constant or not constant. However the following points must be considered:

(1) The primary difference in frontal and elution analysis is in the method of sample introduction. In elution analysis, a small quantity of adsorbate is injected onto the sorbent cartridge in an infinitesimally small time, t_e. For the frontal analysis case, the sample injection time (t_f) is very long (continuous until interrupted) hence the seal

difference in the two methods is in the inequality, $t_e \ll t_f$.

(2) The mode of sample introduction in no way affects the position of the frontal boundary curve or the elution peak maximum, since both are defined by equation (1) and theoretically should elute as pictured in Figure A-1. Figure A-1 is quite different from some of the chromatograms in standard chromatography texts illustrating the relationship between frontal and elution analysis, in that it notes that an elution peak maximum only coincides with the 50% volumetric breakthrough point in elution analysis if the input concentration is one-half that for the frontal plateau concentration.

(3) Both frontal and elution methods, even in the Henry's Law region may have kinetic effects superimposed on their profiles due to diffusional resistance or mass transfer effects. These phenomena account for the fact that real peaks and fronts are not straight lines and step functions, respectively, on the chromatogram. Such kinetic effects must be corrected for if accurate equilibrium isotherms are to be obtained from chromatographic experiments. They do, however, provide a valuable source of information with regard to maximizing the sampling efficiency, if they can be properly deconvoluted from the equilibrium profile. Kinetic effects are less difficult to handle for the Henry's Law region since the peak maximum does approximate equilibrium on the chromatographic profile.

A. Frontal Analysis

In the frontal analysis technique, a gas containing a specified concentration, C_B, of sorbate is continuously fed into the sorbent cartridge. The experimenter waits for the appearance of the boundary profile and continues to monitor the "breakthrough" of sorbate until it equilibrates with the cartridge for the challenge concentration specified. The equilibration stage is signaled by the onset of a concentration vs. time "plateau" which can be continued for as long as one wishes in a

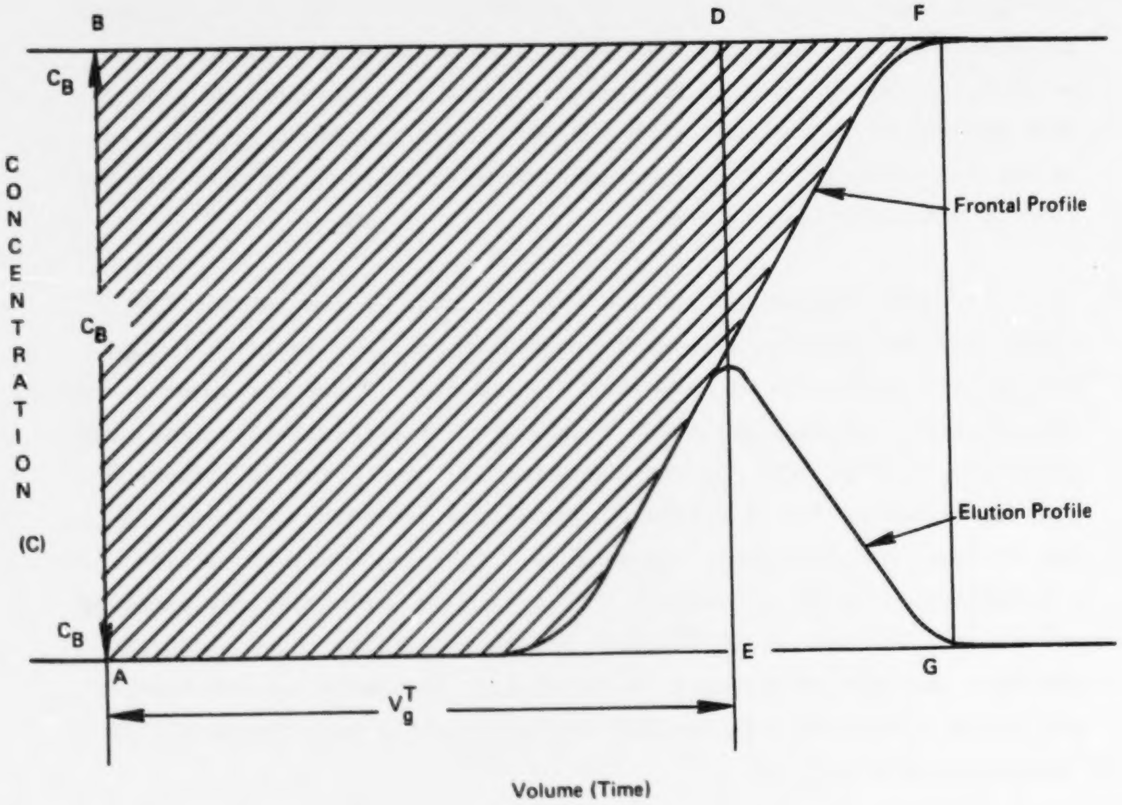
B
D
F
C_B
CONCENTRATION
(C)
C_B
C_B
Frontal Profile
Elution Profile
A
E
G
V_g^T
Volume (Time)

FIGURE A–1 RELATIONSHIP BETWEEN FRONTAL BREAKTHROUGH CURVE AND ELUTION PEAK "steady state" condition. If the breakthrough curve is sharp, or a symmetrical sigmoid profile, then q can be computed by

$$q = \frac{V_g^T C_B}{W_A} \qquad (5)$$

where V_g^T = volume of carrier gas passed to elute a symmetrical breakthrough curve at 0.5 C_B.

C_B = plateau, input, or challenge concentration

W_A = sorbent weight

For asymmetric boundary profiles, integration is required to obtain $\frac{1}{A_s^\circ} \int V_g^T \, dc$, so that

$$q = \frac{1}{A_s^\circ} \int_{C_0}^{C_B} V \, dc \qquad (6)$$

where V = volume of carrier gas passed to obtain completion of boundary profile.

which is the cross-hatched area in Figure A-1.

In Figure A-1, Point A marks the commencement of the frontal analysis, while distance AB represents the total challenge concentration presented to the sorbent bed. Distance AG is the total volume of gas containing sorbate at concentration, C_B, required to complete breakthrough. Hence, the ratio of the cross-hatched area (representing the adsorbate taken up by the adsorbent) to the area ABFG, times the total sorbate passed over the sorbent in V, volume of gas, gives the capacity of the sorbent bed at sorbate input, C_B.

The later sections of this report treat the use of frontal analysis in determining sorption isotherms. However, the basic theory presented here in equally applicable to isotherm determination.

B. Specific Retention (Elution) Volumes, V_g^T

The relationship of the specific retention (elution) volume (V_g^T) to measurable parameters in a gas chromatographic experiment has been derived in many standard treatises on gas chromatography (12). It is important to realize the V_g^T is the fundamental retention constant in gas chromatography and accounts for the effect of flow rate, pressure drop, temperature, column void volume, and stationary phase weight (volume or surface area) on the retention of an injected solute.

Knowledge of the value of V_g^T [frequently for convention corrected to 0°C (273°K)] allows one to estimate the retention volume of a solute at another temperature or for a different column length. Thus, V_g^T determined from conventional gas chromatographic columns can aid in the design of sorbent sampling modules.

The specific retention volume is also directly relatable to fundamental phase distribution constants, such as the partition coefficient, K_L or the adsorption coefficient, K_A. Thus, if certain physical characteristics of the stationary phase are known, such as A_s°, then K_A can be obtained. K_A then allows calculation of sorbate distribution for larger sorption systems than analytical scale devices.

Specific retention volumes, V_g^T, in this study were computed according to the following formula, and represent V_g^T at the temperature of the column oven in the chromatograph proper:

$$V_g^T = \frac{jF_c\ (t_r - t_a)}{W_A} \qquad (7)$$

where V_g^T = specific retention volume for the adsorbate at column (sorbent trap) temperature

$F_c = F_a\left(\frac{T_c}{T_a}\right)\left(1 - \frac{P_w}{P_a}\right)$ = flow rate of carrier gas at column temperature

F_a = flow rate of carrier gas at ambient temperature and pressure

T_c = column temperature

T_a = ambient temperature

P_a = ambient pressure

P_W = vapor pressure of water (at temperature of flow meter)

$$j = \frac{3}{2}\left[\frac{(P_i/P_o)^2 - 1}{(P_i/P_o)^3 - 1}\right]$$

t_r = peak maximum retention time

t_a = retention time for a completely non-sorbed solute

W_A = adsorbent weight

P_o = column outlet pressure

P_i = column inlet pressure.

C. Determination of Adsorption Coefficients (K_A)

The relationship between elution volume for an individual adsorbate and the equilibrium distribution of the adsorbate between the gas phase and the sorbent resin is described by:

$$v\left(\frac{\partial C_g}{\partial z}\right)_t + \left(\frac{\partial C_g}{\partial t}\right)_z + \left(\frac{\partial C_A}{\partial t}\right)_z = 0 \qquad (8)$$

where C_g = concentration of adsorbate in gas phase in moles/length of column

C_A = concentration of adsorbate in adsorbent in moles/length of column

v = average linear velocity of gas phase

z = distance from sorbent cartridge inlet

t = time

The three terms in the differential equation represent respectively, left to right, the adsorbate removed from the flowing gas stream, the increase of the adsorbate in the gas phase, and the increase of the adsorbate on the adsorbent.

In order to simplify this differential equation, one may integrate this equation for values with known limits, such as $0 \leq z \leq L$ and $0 \leq t \leq t_r$. Since the concentration of the adsorbate in the gas phase is a function of migration distance and time in the sorbent bed, these functions may be used to relate z and t by:

$$\frac{\frac{\partial C_g}{\partial t}}{\frac{\partial C_g}{\partial z}} = - \frac{dz}{dt} \qquad (9)$$

To make use of this relationship, equation (8) may be rearranged to

$$v \frac{\left(\frac{\partial C_g}{\partial z}\right)}{\left(\frac{\partial C_g}{\partial t}\right)} + 1 + \frac{\left(\frac{\partial C_A}{\partial t}\right)}{\left(\frac{\partial C_g}{\partial t}\right)} = 0 \qquad (10)$$

Or
$$- v \frac{dt}{dz} + 1 + \left(\frac{\partial C_A}{\partial C_g}\right) = 0 \qquad (11)$$

If one defines $\phi = \partial C_A / \partial C_g$, equation (11) becomes:

$$\frac{dz}{dt} = \frac{v}{1 + \phi} \qquad (12)$$

upon inverting both sides of the equation. Equation (12) is the differential equation describing the rate of motion of an adsorbate zone of concentration, C_g, in terms of v. Integration over the column length, L, and the time it takes for the peak maximum to elute, t_r, gives

$$v\int_o^{t_r} dt = (1 + \phi)\int_o^L dz \qquad (13)$$

Or

$$\frac{vt_r}{L} = 1 + \phi \qquad (14)$$

The velocity of the gas stream is determined by injection of adsorbate, a, with a $K_A = 0$, so that its residence time in the column is t_a, so

$$v = \frac{j F_c L}{V_a} \qquad (15)$$

$$C_g = \frac{P_A V_A}{LRT_c} \qquad (16)$$

$$C_A = \frac{\Gamma A_s W_a}{L} \qquad (17)$$

where Γ = concentration of adsorbate/m^2 of adsorbent (moles/m^2)

P_A = adsorbate partial pressure in the gas phase (mm Hg).

Thus

$$\phi = \left(\frac{\partial C_A}{\partial C_g}\right) = \left(\frac{W_A A_s RT_c}{V_A}\right) \left(\frac{\partial \Gamma}{\partial P_A}\right) \qquad (18)$$

which yields upon substitution into (14)

$$\frac{vt_r}{L} = 1 + \frac{W_A A_s RT_c}{V_A} \left(\frac{\partial \Gamma}{\partial P_A}\right) \qquad (19)$$

or when combined with (15)

$$\frac{j F_c t_r}{V_a} = 1 + \frac{W_A A_s R T_c}{V_a} \left(\frac{\partial \Gamma}{\partial P_A}\right) \tag{20}$$

which can be further simplified by multiplication of the equation by $\frac{V_a}{W_a}$ to

$$\frac{j F_c t_r - V_a}{W_A} = A_s R T_c \left(\frac{\partial \Gamma}{\partial P_A}\right) \tag{21}$$

where the left hand side of the equation is simply V_g^T (refer to equation 7). For the Henry's Law region of the absorption isotherm, V_g^T is constant, hence

$$V_g^T = A_s^\circ \; R T_c \left(\frac{\partial \Gamma}{\partial P_A}\right)_{p \rightarrow 0} \tag{22}$$

where A_s° is the limit of A_s as $p \rightarrow 0$, and the term in parentheses is known as Henry's Law adsorption coefficient, K_A. A knowledge of K_A at the temperature of adsorbate collection in a resin tube is valuable in establishing the quantity of adsorbate vapor which could be collected under conditions approaching equilibrium. This would then allow one to design traps of sufficient capacity to capture sufficient analyte for assay, aid in the choice of a sorbent resin, and in evaluating the collection of the sorbent resin.

Computation of K_A is readily facilitated by employing equation (23)

$$V_g^T = A_s^\circ \; R T_c K_A \tag{23}$$

The units of K_A in this case are moles/mm-m^2, thus V_g^T/A_s° is in ml/m^2, $R = 6.3 \times 10^4$ ml-mm/mole-°K, and T_c in °K. Note should be made that

K_A is proportional to q, since $K_A^* A_s^\circ = V_g^T$, thus the magnitude of V_g^T can serve as a quick guide as to sorbate affinity for the resin.

The specific surface area of the resins used in this study represents an average of several values determined by Micromeritics Instrument Corp., and literature values (10). The quantity V_g^T/A_s° is referred to as the retention volume/unit of surface area by Kiselev (13). In essence, this form is a form of "reduced V_g^T" in which the surface area dependence has been factored out of the specific retention volume. Thus tabulations of K_A can be used to compute breakthrough volumes on resins whose surface area characteristics vary between production lots. It is implicit in the calculation of K_A that the BET measured surface area is totally available to the adsorbate. Studies by Ackerman (14) refute this and, as will be shown later, high velocities through the adsorbent bed may limit the effective surface area available to the solute, particularly in the micropores of the resin.

The adsorption coefficient can be used to calculate q if the challenge concentration, c, is in the Henry's Law region of the adsorption isotherm. Figure A-2 indicates that K_A would be applicable to calculating q, if the vapor input is at a level c, in the gaseous eluent. In the non-Henry's Law region, use of K_A would lead to an erroneous value of q_2 at c_2, depending on the departure of the sorption isotherm from linearity. This is why the total adsorption isotherm can be of value over a wider concentration range than just covered by the Henry's Law region.

The concentration of the adsorbate in the adsorbent, q, can be calculated as grams of adsorbate/gram of sorbent by using the following equation

$$q_g = \frac{K_A A_s^\circ C_g (760 \text{ mm Hg}) (\text{MW})}{10^6} \qquad (24)$$

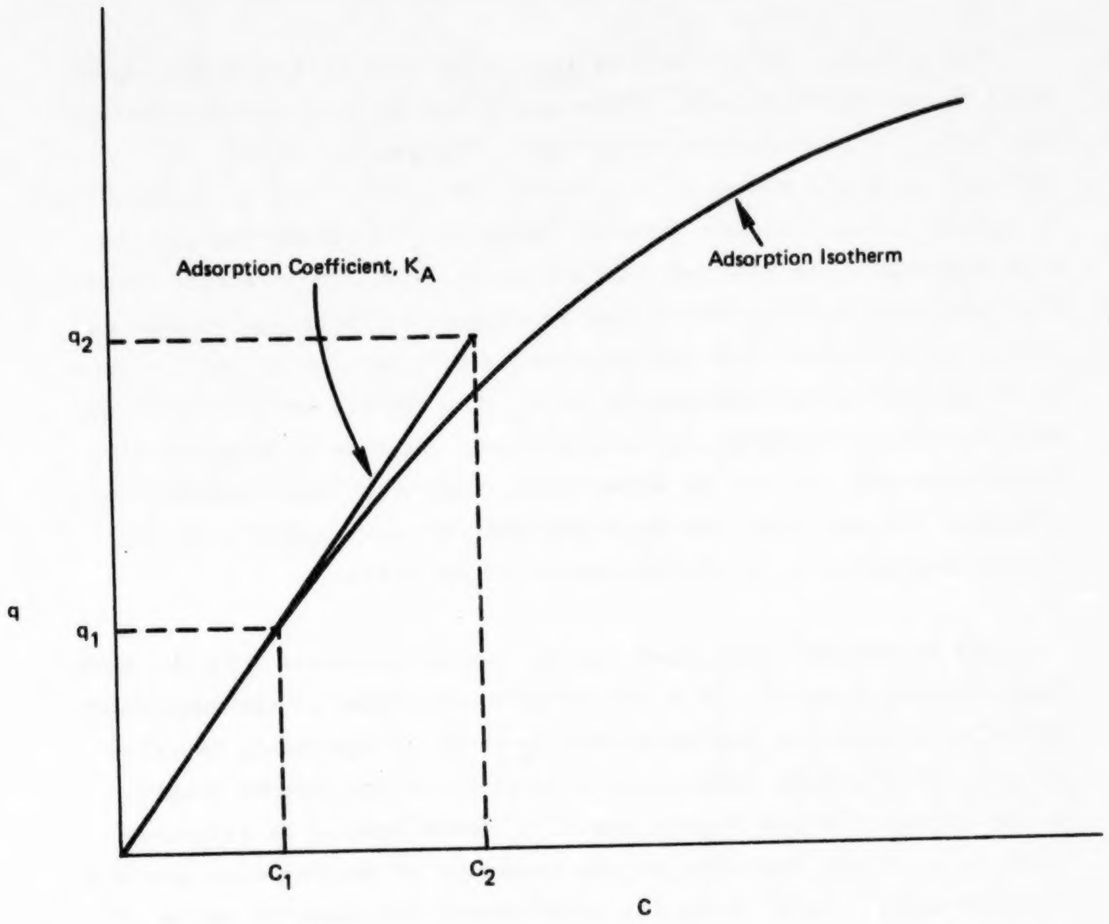
Adsorption Coefficient, K_A
Adsorption Isotherm
q_2
q_1
q
C_1
C_2
C

FIGURE A–2 RELATIONSHIP BETWEEN ADSORPTION ISOTHERM AND ADSORPTION COEFFICIENT, K_A

where C_g = gas phase concentration in ppm (v/v)

MW = molecular weight of the adsorbate

D. Thermodynamic Functions of Adsorption

Knowledge of the temperature dependence of K_A allows the computation of several thermodynamic functions of adsorption. Values of the molar free energy ($\Delta\bar{G}_A$), molar enthalpy of adsorption ($\Delta\bar{H}_A$), and molar entropy of adsorption ($\Delta\bar{S}_A$) may all be calculated.

The differential molar free energy of adsorption $\Delta\bar{G}_A$ is given by

$$\Delta\bar{G}_A = -RT \ln K_A \tag{25}$$

The logarithmic term usually contains a standard state defined for K_A in units consistent with a unitless logarithmic term. Unfortunately there is no universally accepted standard state of adsorption process, although several have been suggested (15).

The computation of $\Delta\bar{G}_A$ has not been pursued in this study since it primarily reflects the trends in K_A and hence ultimately is proportional to V_g^T. It lends little to the discussion of the experimental results, but could be of interest to theoretical surface chemists.

The differential molar enthalpy of adsorption, $\Delta\bar{H}_A$ is calculated as

$$\Delta\bar{H}_A = \partial\bar{\Delta}\, G_A/\partial(1/T_c) \tag{26}$$

or

$$\Delta\bar{H}_A = -2.302R \frac{\partial \log V_g^T}{\partial\, (1/T_c)} \tag{27}$$

Thus plots of log V_g^T vs. 1/T readily yield $\Delta\overline{H}_A$ for the temperature range of interest.

The differential molar enthropy of adsorption, $\Delta\overline{S}_A$, is calculated from the Gibbs-Helmholtz equation, where

$$\Delta\overline{S}_A = \frac{\Delta\overline{H}_A - \Delta\overline{G}_A}{T_c} \qquad (28)$$

$\Delta\overline{S}_A$ will contain both the error inherent in the determination of $\Delta\overline{G}_A$ and the slope measurement for $\Delta\overline{H}_A$ and hence frequently is of limited statistical significance.

The differential molar heat of adsorption is perhaps the parameter of most significance in this study since its magnitude and sign relative to the heat of liquefaction, $\Delta\overline{H}_L$, of the sorbate allows a qualitative assessment to be made of the strength of adsorbent/adsorbate interactions. Since $\Delta\overline{H}_L$ is negative, and $\Delta\overline{H}_A$ is negative if $\dfrac{\partial \log V_g^T}{\partial (1/T_c)}$ is positive, then $\Delta\overline{H}_L < \Delta\overline{H}_A$ is indicative of a strong enthalpic interaction between the sorbent and sorbate. If $\Delta\overline{H}_L \simeq \Delta\overline{H}_A$, then marginal interaction of the adsorbate with the resin is occurring, and the resin is merely serving as an inert surface allowing liquefaction of the adsorbate.

E. Determination of Adsorption Isotherms From Chromatographic Profiles

There is a direct relationship between the shape of a chromatographic profile (either in elution or frontal analysis) and the shape of the equilibrium adsorption isotherm. Figure A-3 illustrates this correspondence for three types of cases. The top set of graphs depict a linear, Langmuir, and anti-Langmuir isotherm, respectively. Beneath each type of isotherm is the resultant elution and then frontal profile, shown in the presence of kinetic band broadening of the chromatographic

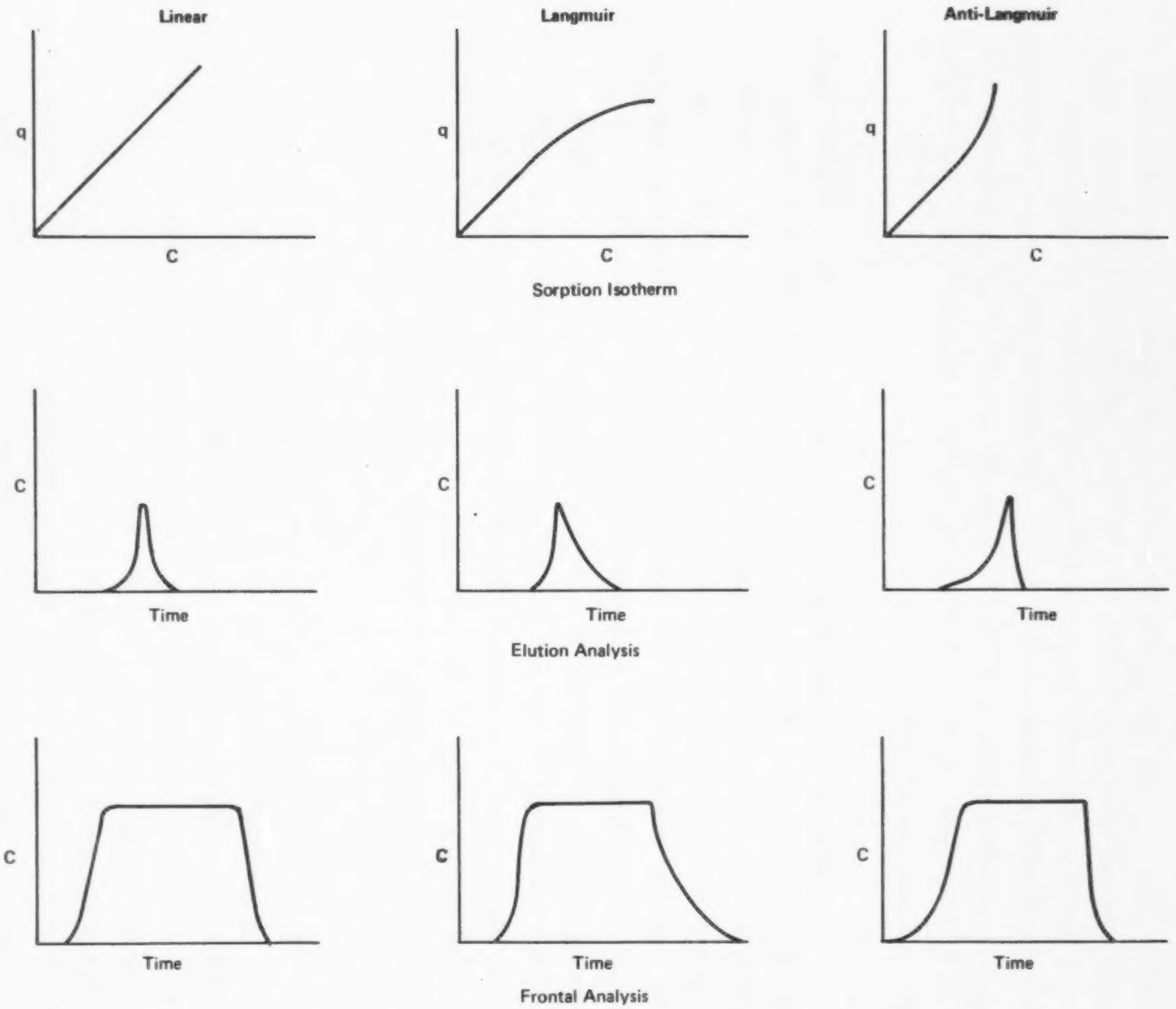
Linear
Langmuir
Anti-Langmuir
q
C
q
C
q
C
Sorption Isotherm
C
Time
C
Time
C
Time
Elution Analysis
C
Time
C
Time
C
Time
Frontal Analysis

FIGURE A–3 RELATIONSHIP BETWEEN ADSORPTION ISOTHERM, ELUTION ANALYSIS, AND FRONTAL ANALYSIS zone. Thus, if the skew factor on an elution peak is pronounced, one can immediately ascertain the type of sorption isotherm governing phase equilibrium. The same corollary holds true for the frontal analysis profiles shown in Figure A-3. For the linear isotherm case, the elution peak is assumed to be a symmetrical Gaussian distribution, likewise for the frontal case, both adsorption and desorption branches of the frontal profile are symmetrical.

In examining a chromatographic profile for skew one should be aware of several factors. For example, unfavorable adsorption/desorption kinetics can contribute to a skewed profile. Operating the chromatographic experiment at mobile phase flows far from the minimum in the van Deemter equation (16) can cause excessive band broadening, particularly in the high flow regime where resistance to mass transfer is maximized. It is also possible to start at an input concentration which corresponds to one section of an isotherm containing an inflection point. Thus a different input or challenge concentration may be in the other portion of the isotherm, and hence give a skew in the opposite direction from that encountered at the previous challenge concentration.

This is illustrated in Figure A-4 by some literature data representing the work of Gregg and Stock (17). The top half of Figure A-4 represents Langmuir isotherms with the associated frontal chromatogram for each case. For these cases, the skew in the desorption trace corresponds to the isotherm. For the second example pictured in the lower half of Figure A-4, the isotherm is concave to the pressure axis in one region of concentration and convex in the other region. The frontal chromatogram inserts show that depending on the input pressure (concentration) one of several frontal profiles could result. The same phenomena can be encountered in elution analysis (18).

Several chromatographic methods exist for isotherm determination, varying in their experimental complexity, attainment of equilibria, and

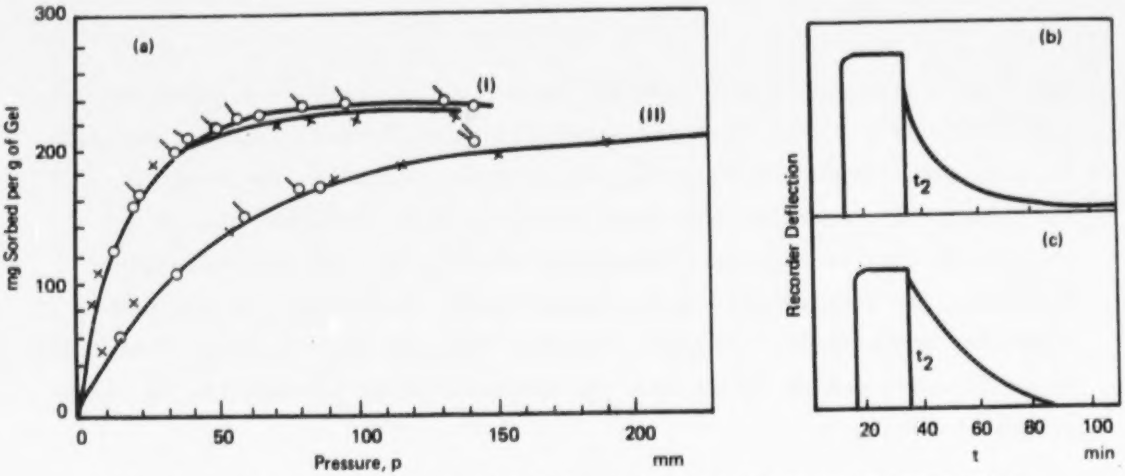

Systems showing Type I isotherms, on silica gel A. (a) Sorption isotherm for (i) n-hexane, (ii) n-pentane; circles, determined with the sorption balance; crosses, calculated from the chromatogram. (b) Chromatogram for n-hexane. (c) Chromatogram for n-pentane, t_2, time of change-over to pure nitrogen.

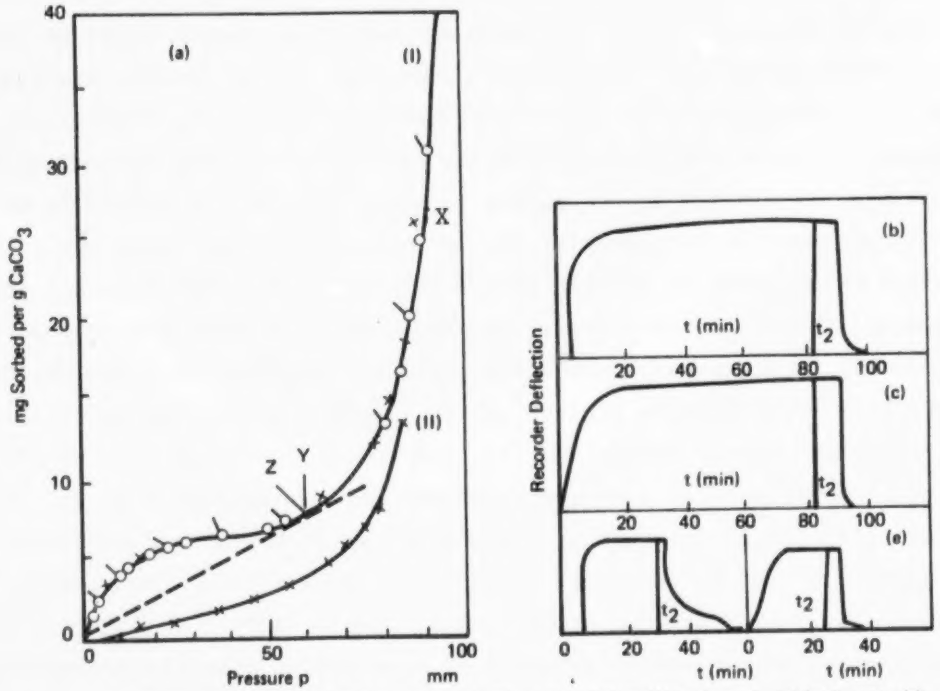

Cyclohexane on block-dried calcium carbonate (Type II and Type III isotherms). (a) Isotherms with the calcium carbonate: (i) in dry form, (ii) after treating with water; circles, determined with the sorption balance; crosses, calculated from the chromatograms. In (b) and (c) the column was saturated to a concentration corresponding to X and in (d) and (e) to a concentration corresponding to Y. t_2, time of change-over to pure nitrogen.

FIGURE A–4 COMPARISON OF ISOTHERM CURVATURE WITH FRONTAL CHROMATOGRAM – EXPERIMENTAL DATA (REFERENCE 17).

applicable adsorbate concentration range. Huber (19) has classified such techniques into equilibrium and nonequilibrium classes. The former class of techniques experimentally includes complex pneumatic instrumentation to produce concentration plateaus (frontal analysis) while the latter techniques involve elution pulses which are simpler to produce experimentally, but require extensive computational corrections in the higher adsorbate concentration ranges. Purnell (20) has advocated an alternative classification scheme based upon the method used to produce the chromatographic profile.

Elution by characteristic point (ECP) has been amply described in the literature (21, 22). Two basic methods exist in the ECP method for isotherm determination; one in which a series of peak maxima specific retention volumes, V_g^T, are determined, each yielding one point on the isotherm. These V_g^T volumes will be invariant in the Henry's Law region, but will show a variance in the nonlinear portion of the isotherm as the concentration of the adsorbate in the carrier gas stream decreases from the injected maximum concentration to zero. The second method involves the determination of a portion of the sorption isotherm from the locus of points on the diffuse profile of the elution pulse, implying that such a boundary for all ideal forms of chromatography represents a true equilibrium profile. Hence, a coincidence criterion is developed by which the diffuse edge of a large elution profile may be regarded as a summation of discrete peak maxima. Thus, as Kiselev (23) has noted, the proper choice of experimental conditions can assure a close approach to equilibrium, and the simplification of determining small portions of the total isotherm via a single peak (20) is realized. Figure A-5 shows several examples of elution by characteristic point, the isotherms derived from this method, and varying degrees of coincidence of peak maxima with the asymmetrical boundary profile.

In order to calculate the equilibrium adsorption isotherm, the chromatographic profile must be corrected for kinetic band broadening.

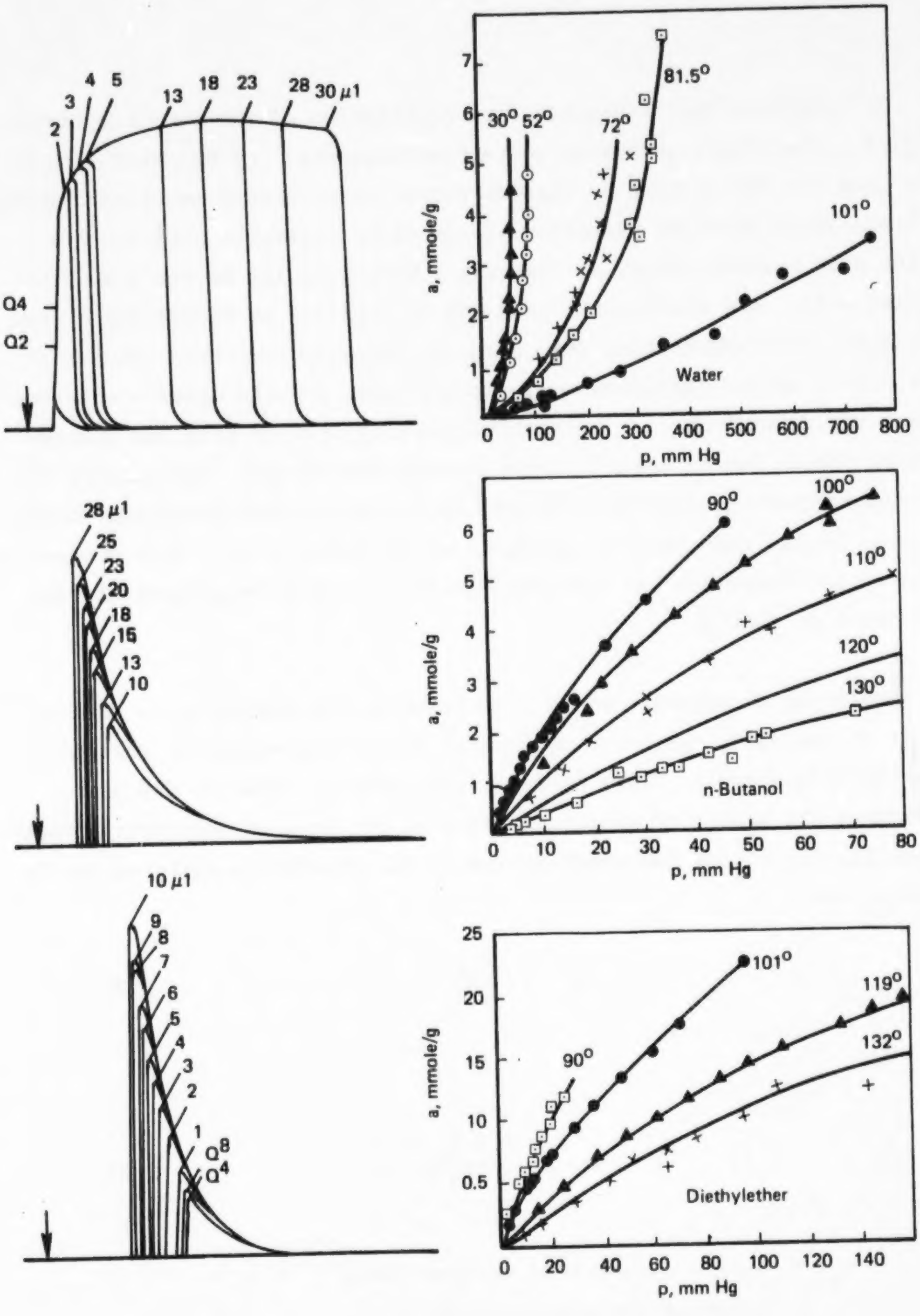

FIGURE A–5 EXAMPLES OF CHROMATOGRAMS FOR VARIOUS SAMPLE SIZES AND THE RESULTING ISOTHERMS FOR CHROMOSORB 102 USED AT VARIOUS TEMPERATURES WITH WATER, DIETHYL ETHER AND n-BUTANOL (REFERENCE 54)

To determine the divergence from equilibrium of the chromatographic profiles, the simple graphical correction suggested by Cremer (24) has been used for the elution by characteristic point method mentioned earlier. This procedure involves bisection of the chromatographic peak profile at its peak maximum value, by erecting a perpendicular to the base line (Figure A-6). The partitioned peak may be regarded as consisting of two sections: one representing the change in concentration with respect to time due to solute distribution nonequilibrium, and the other consisting of the solute distribution nonequilibrium contribution plus the concentration change due to equilibration between the phases. Subtraction of the nonequilibrium area from the area representing both processes yields the true equilibrium profile (dashed line in Figure A-6). This process is depicted in Figure A-6 for n-butanol (0.05 μl liquid injection) eluting from XAD-2 at ∿100°C.

Graphical integration at various heights (corresponding to various values of partial pressure of adsorbate) yields the amount of sorbate taken up by the resin. This cross-hatched area in front of the peak represents the amount of adsorbate adsorbed per gram of adsorbent. Mathematically, the values for construction of the adsorption isotherm can be obtained via

$$q_g = \frac{n\ A'}{A\ W_A} \tag{29}$$

and

$$p = \frac{R\ s\ T_c\ n'\ h}{Aj\ F_c} \tag{30}$$

where: q_g = weight capacity of sorbent resin

n = grams of sorbate injected

n' = moles of sorbate injected

A' = area corresponding to some partial pressure of sorbate, p

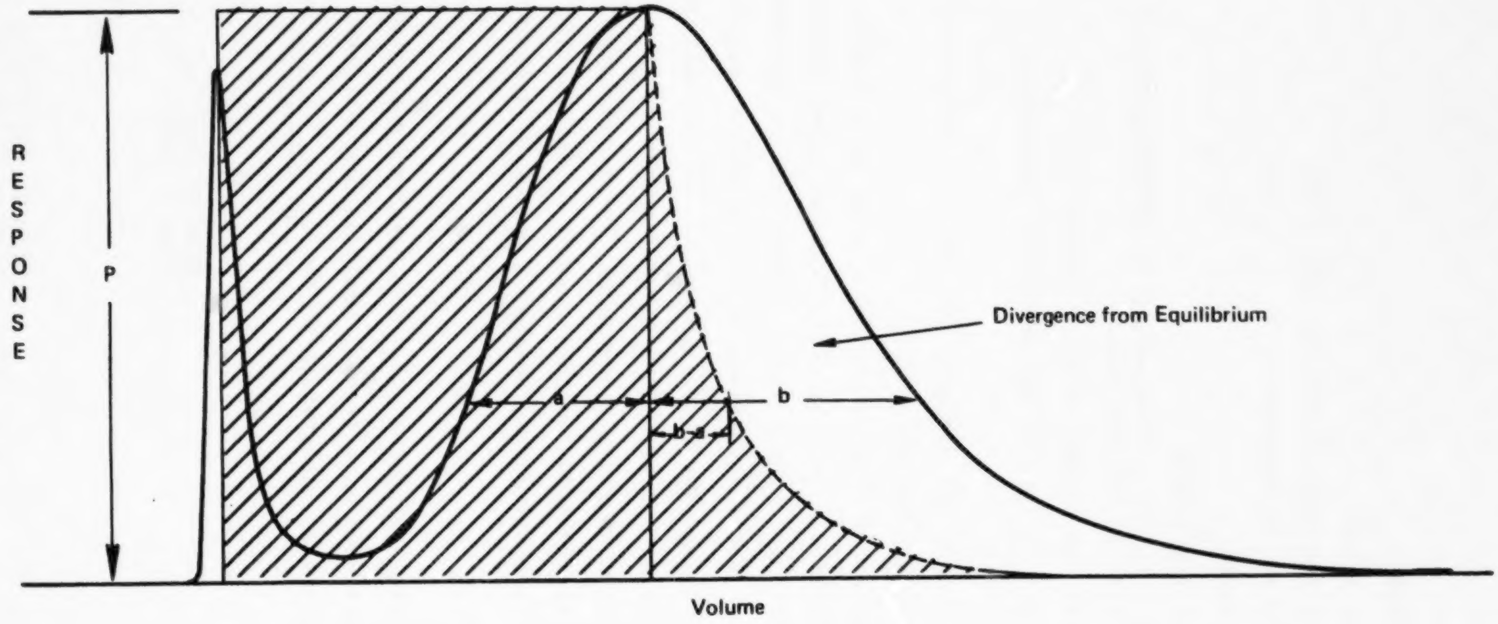

FIGURE A–6 CREMER METHOD FOR CORRECTING ELUTION PROFILE FOR KINETIC CONTRIBUTION (0.05 μl LIQUID INJECTION OF n-BUTANOL ON XAD–2 @ 100°C.)

A = peak area

W_A = sorbent weight

p = partial pressure of sorbate over resin

R = 6.232×10^4 mL-mm/mole -- °K

s = chart speed

T_c = column temperature

h = vertical height corresponding to partial pressure of sorbate in the gas phase

j = James-Martin compressibility factor

F_c = flow rate of carrier gas at column temperature

Equations (29) and (30) are directly derivable from equation (4) with a change in integration variables (25).

An analog similar to the elution case presented above exists for frontal analysis. Frontal analysis by characteristic point consists of calculating the equilibrium isotherm from a single diffuse boundary profile. Again it assumes that intermediate frontal analysis profiles coincide with the diffuse boundary profile. The resin bed is challenged with different concentrations of sorbate, thus several points on an adsorption isotherm can be determined as given in equation (6) and depicted in Figure A-7. The variable changing in this case is C_B in equation (6), hence determining the isotherm simply becomes a series of integrations at different values of C_B.

Figure A-7 shows the evaluation of q_g for both the desorption as well as the adsorption branch of a frontal analysis chromatogram. Here, q_g is determined by graphical integration so the $q_{g,\ \text{adsorption}}$ is given as

$$q_{g,\ \text{adsorption}} = \frac{\text{Area of ABDF}}{\text{Area of ABDEF}} V_{DE} C_B \tag{31}$$

and

$$q_{g,\ \text{desorption}} = \frac{\text{Area of A'B'D'F'}}{\text{Area of A'B'D'E'F'}} V_{A'F'} C_B \tag{32}$$

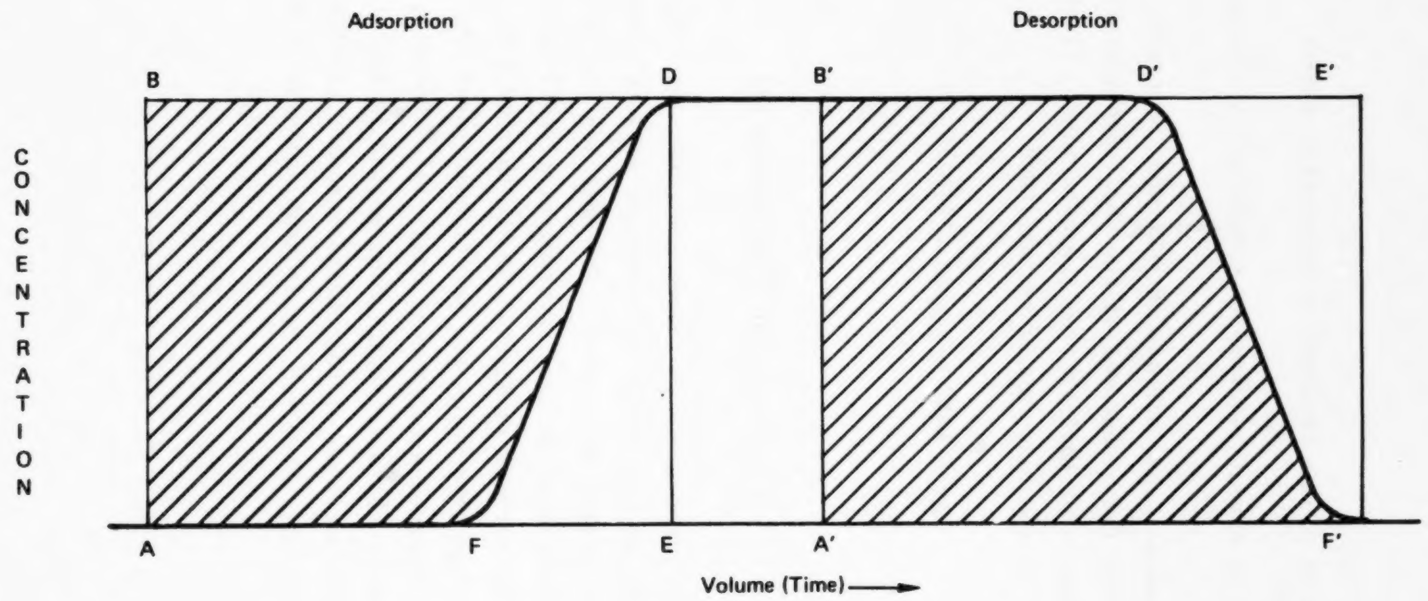
Adsorption
Desorption
B
D
B'
D'
E'
C O N C E N T R A T I O N
A
F
E
A'
F'
Volume (Time) ⟶

FIGURE A–7 GRAPHICAL EVALUATION OF q_g FROM FRONTAL ANALYSIS ADSORPTION AND DESORPTION CURVES where:

V_{DE} = volume of eluent required to completely adsorb sorbate

$V_{A'F'}$ = volume of eluent required to completely desorb sorbate

Point A marks the moment that sorbate is entering the sample cartridge while point B' marks the withdrawal of the challenge mixture and beginning of the dissipation of sorbate from the cartridge. If the experiment is performed in the Henry's Law region, then

$$\text{Area ABDF} = \text{Area A'B'D'F'}$$

and

$$q_{g,\ \text{adsorption}} = q_{g,\ \text{desorption}}$$

The two methods for determining isotherms described above each offer distinct advantages. The elution analysis technique of determining isotherms is experimentally simple and probably adequate for the challenge concentration ranges encountered in many environmental sampling situations. Unfortunately the sorbate is diluted by the carrier gas, limiting the concentration range over which the sorption isotherm can be determined (this is not a problem in frontal analysis). However, another advantage in the elution by characteristic point method is that the kinetic contribution to distortion of the chromatographic profile can be corrected with less difficulty than for the frontal analysis method.

APPENDIX B

Specific Retention Volume Data

Table B-1

Specific Retention Volumes (ml/g)

Resin: XAD-2

Adsorbate Class: Aliphatic Hydrocarbons

Adsorbate	V_g^T (ml/g)	Temperature (°C)	Slope	Intercept	Correlation Coefficient
n-Hexane	261	110.0	3.06580	-5.58655	0.99995
	740	89.7			
	1870	73.0			
n-Octane	693	130.4	3.77333	-6.51827	0.99973
	2280	108.7			
	7760	89.7			
n-Decane	1670	148.8	3.93204	-6.10014	1.00000
	4440	130.4			
n-Dodecane	7530	148.8			

Table B-2

Specific Retention Volumes (ml/g)

Resin: Tenax-GC

Adsorbate Class: Aliphatic Hydrocarbons

Adsorbate	V_g^T (ml/g)	Temperature (°C)	Slope	Intercept	Correlation Coefficient
n-Hexane	82.4	111.9	3.06668	-6.04832	0.99988
	266.0	89.2			
	778.0	69.9			
n-Octane	168.0	131.0	3.26578	-5.86329	0.99961
	430.0	110.9			
	144.0	89.2			
n-Decane	208.0	148.3	4.01717	-7.21373	0.99974
	562	130.5			
	1850	110.1			
n-Dodecane	684	148.3	5.30902	-9.76855	1.00000
	2380	130.8			

Table B-3

Specific Retention Volumes (ml/g)

Resin: XAD-2

Adsorbate Class: Aromatic Hydrocarbons

Adsorbate	V_g^T (ml/g)	Temperature (°C)	Slope	Intercept	Correlation Coefficient
Benzene	164	129.8	2.71260	-4.53329	0.9960
	329	110.3			
	858	90.0			
Toluene	204	150.3	2.97094	-4.72089	0.9970
	428	129.8			
	1100	110.3			
P-Xylene	458	150.3	3.14611	-4.77490	0.9998
	1060	130.0			
	2730	110.3			
Ethylbenzene	430	150.3	2.96535	-4.36304	0.9981
	1030	130.0			
	2190	111.5			
n-Propylbenzene	774	150.0	3.60543	-5.63485	1.0000
	1880	131.7			

Table B-4

Specific Retention Volume (ml/g)

Resin: Tenax-GC | **Adsorbate Class:** Aromatic Hydrocarbons

Adsorbate	V_g^T (ml/g)	Temperature (°C)	Slope	Intercept	Correlation Coefficient
Benzene	107	129.9	2.93478	-5.22599	0.98509
	313	109.8			
	657	90.7			
Toluene	109	149.9	3.69321	-6.70084	0.99983
	271	131.0			
	889	109.8			
o-Xylene	229	150.9	3.05239	-4.83089	0.99836
	552	131.0			
	1370	109.3			
Ethylbenzene	192	151.1	3.45687	-5.86934	1.00000
	483	131.0			
	1520	109.0			
n-Propylbenzene	372	150.8	3.42707	-5.50489	0.99790
	1000	131.0			
	2730	109.9			

Table B-5

Specific Retention Volumes (ml/g)

Resin: XAD-2

Adsorbate Class: Halogenated Hydrocarbons

Adsorbate	V_g^T (ml/g)	Temperature (°C)	Slope	Intercept	Correlation Coefficient
1,2-Dichloroethane	38.4	161.3			
	54.2	146.6	2.45466	-4.08429	0.99072
	96.9	132.4			
Fluorobenzene	50.9	161.3			
	75.0	146.6			
	132.0	132.4	2.52280	-4.11409	0.99523
1,1,2-Trichloroethylene	51.2	161.9			
	86.6	145.0	2.49480	-4.02811	0.99994
	141.3	130.9			
Chlorobenzene	60.6	192.8			
	108.6	174.5	2.84505	-4.32456	0.99994
	167.8	161.3			
Bromobenzene	107.7	192.8			
	188.3	174.5	2.98486	-4.38164	0.99872
	315.4	161.3			
1,4-Dichlorobenzene	164.9	192.8			
	301.3	174.5	3.28498	-4.84322	0.99803
	538.4	161.3			

Table B-6

Specific Retention Volumes (ml/g)

Resin: Tenax-GC

Adsorbate Class: Halogenated Hydrocarbons

Adsorbate	V_g^T (ml/g)	Temperature (°C)	Slope	Intercept	Correlation Coefficient
1,2-Dichloroethane	21.3	161.6	2.74521	-5.00108	0.99791
	31.2	148.3			
	75.5	126.5			
Fluorobenzene	22.8	161.6	3.23296	-6.08617	0.99975
	38.0	148.3			
	102.2	126.5			
1,1,2-Trichloroethylene	24.5	161.6	3.20783	-6.00053	0.99938
	39.9	148.3			
	108.1	126.5			
Chlorobenzene	27.0	186.0	3.99802	-7.26918	0.99774
	51.8	173.0			
	83.2	161.6			
Bromobenzene	51.1	186.0	4.22532	-7.49334	0.99967
	97.3	173.0			
	167.9	161.6			
1,4-Dichlorobenzene	69.2	186.0	5.36271	-7.64892	0.99454
	146.3	173.0			
	235.9	161.6			

Table B-7

Specific Retention Volumes (ml/g)

Resin: XAD-2 **Adsorbate Class**: Ketones

Adsorbate	V_g^T (ml/g)	Temperature (°C)	Slope	Intercept	Correlation Coefficient
2-Butanone	25.3	174.8	1.90864	-2.86767	0.99616
	39.5	153.0			
	69.4	133.0			
2-Heptanone	201.7	175.4	3.27760	-5.00653	0.99990
	480.4	153.0			
	1161.8	133.2			
4-Heptanone	175.6	175.4	3.33420	-5.19071	1.00000
	427.8	153.2			
	1034.6	133.4			
Cyclohexanone	185.4	175.6	2.78674	-3.94194	0.99995
	399.2	153.0			
	822.1	133.4			
3-Methyl-2-butanone	41.4	175.8	2.35244	-3.62170	0.99976
	78.9	153.6			
	146.3	133.4			
3,3-Dimethyl-2-butanone	67.3	176.2	2.62583	-4.02293	0.99883
	133.4	153.2			
	278.9	133.4			

continued....

Table B-7 (continued)

Adsorbate	V_g^T (ml/g)	Temperature (°C)	Slope	Intercept	Correlation Coefficient
2,6-Dimethyl-4-heptanone	519.0	175.8	3.80074	-5.75828	0.99953
	1415.5	153.0			
	3990.3	133.4			
Acetophenone	267.6	197.0	3.45276	-4.92004	0.99990
	626.6	174.6			
	1501.6	153.0			
	3808.0	133.4			

Table B-8

Specific Retention Volumes (ml/g)

Resin: Tenax-GC

Adsorbate Class: Ketones

Adsorbate	V_g^T (ml/g)	Temperature (°C)	Slope	Intercept	Correlation Coefficient
2-Butanone	17.5	152.8	2.92774	-5.64138	0.99917
	37.8	131.8			
	99.3	110.6			
2-Heptanone	146.7	152.8	4.31585	-7.97739	0.99969
	469.3	131.8			
	1902.6	110.6			
4-Heptanone	126.5	152.8	4.14677	-7.63681	0.99997
	406.8	131.8			
	1544.4	110.0			
Cyclohexanone	168.3	153.6	3.66388	-6.36534	0.99988
	476.8	131.8			
	1585.9	110.2			
3-Methyl-2-butanone	26.9	152.8	3.17976	-6.03588	0.99987
	66.6	131.8			
	183.6	110.0			
Acetophenone	88.5	196.6	4.01805	-6.61535	0.99906
	225.8	174.3			
	646.5	153.6			

Table B-9

Specific Retention Volumes (ml/g)

Resin: XAD-2

Adsorbate Class: Amines

Adsorbate	V_g^T (ml/g)	Temperature (°C)	Slope	Intercept	Correlation Coefficient
n-Butylamine	41.8	169.7	2.27928	-3.51956	0.99771
	76.0	150.7			
	126	131.3			
	276	109.7			
n-Amylamine	92.4	169.7	2.74263	-4.24533	0.98721
	175	150.7			
	298	131			
	895	110.1			
n-Hexylamine	183	169.7	2.96738	-4.44033	1.00000
	362	151.0			
	799	131.0			
Benzylamine	355	169.7	3.75608	-5.91593	0.97836
	597	160.8			
	876	150.3			
Di-n-Butylamine	447	169.7	3.64200	-5.58430	0.99810
	617	161.2			
	1060	150.3			

Table B-10

Specific Retention Volumes (ml/g)

Resin: Tenax-GC

Adsorbate Class: Amines

Adsorbate	V_g^T (ml/g)	Temperature (°C)	Slope	Intercept	Correlation Coefficient
n-Butylamine	19.6	170.0			
	31.9	150.9			
	64.9	130.6	2.75520	-4.97164	0.99535
	161	110.4			
	418	91.3			
n-Amylamine	35.5	170.0			
	64.8	150.9			
	150	130.8	3.28387	-5.90947	0.99637
	449	110.4			
	1360	91.3			
n-Hexylamine	61.2	170.2			
	135	150.9			
	313	130.8	3.55078	-6.24518	0.99508
	1120	110.4			
Benzylamine	257	170.2			
	562	150.9	3.27994	-4.98957	0.99998
	1350	130.9			
Di-n-butylamine	100	170.0			
	250	150.9	3.70514	-6.35624	0.99913
	647	130.9			
Tri-n-butylamine	33.3	170.0			
	64.3	150.9	3.65348	-6.77637	0.98674
	157	130.9			
	643	110.4			

Table B-11

Specific Retention Volumes (ml/g)

Resin: XAD-2 **Adsorbate Class**: Aliphatic Alcohols

Adsorbate	V_g^T (ml/g)	Temperature (°C)	Slope	Intercept	Correlation Coefficient
Ethanol	15.2	130.7	2.18956	-4.22468	0.99408
	31.8	111.1			
	60.7	90.7			
n-Propanol	43.7	130.9	2.48352	-4.50203	0.99903
	96.5	110.6			
	211	90.5			
n-Butanol	74.0	150.3	2.34307	-3.67715	0.99593
	128	130.6			
	275	110.7			
2-Butanol	54.4	149.7	2.49183	-4.19021	0.99449
	88.2	130.9			
	194	110.6			
	485	90.5			
2-Methyl-2-propanol	16.4	130.8	2.12922	-4.06001	0.99990
	30.2	111.1			
	62.5	90.7			
2-Methyl-1-propanol	60.7	150.1	2.22674	-3.48989	0.99632
	101	130.9			
	210	110.7			

Table B-12

Specific Retention Volumes (ml/g)

Resin: Tenax-GC

Adsorbate Class: Aliphatic Alcohols

Adsorbate	V_g^T (ml/g)	Temperature (°C)	Slope	Intercept	Correlation Coefficient
Ethanol	21.9	110.1	2.01955	-3.93050	0.99999
	41.0	91.4			
	86.0	71.3			
n-Propanol	67.6	110.1	2.39945	-4.42767	0.99935
	147	91.4			
	344	71.3			
1-Butanol	70.4	130.2	2.99335	-5.57235	0.99968
	175	110.4			
	437	91.3			
2-Butanol	48.2	129.9	2.76500	-5.16541	0.99876
	120	110.1			
	267	91.3			
	719	71.5			
2-Methyl-2-propanol	12.9	111.5	2.15199	-4.49011	0.99964
	25.6	91.4			
	58.5	71.1			
2-Methyl-1-propanol	49.5	130.2	2.95273	-5.61303	0.99582
	131	110.4			
	296	91.6			

Table B-13

Specific Retention Volumes (ml/g)

Resin: XAD-2

Adsorbate Class: Phenols

Adsorbate	V_g^T (ml/g)	Temperature (°C)	Slope	Intercept	Correlation Coefficient
Phenol	137.9	196.6	3.44622	-5.18973	0.99837
	221.2	185.0			
	337.4	173.0			
o-Cresol	228.5	196.6	3.71282	-5.53959	0.99918
	374.7	185.0			
	593.7	173.2			
p-Cresol	261.6	196.6	3.70588	-5.46240	0.99763
	439.2	185.0			
	684.9	173.0			
m-Cresol	262.1	196.6	3.71874	-5.49053	0.99842
	436.1	185.0			
	688.3	173.0			

Table B-14

Specific Retention Volumes (ml/g)

Resin: Tenax-GC

Adsorbate Class: Phenols

Adsorbate	V_g^T (ml/g)	Temperature (°C)	Slope	Intercept	Correlation Coefficient
Phenol	68.4	185.2	3.70378	-6.24066	0.99956
	131.9	170.3			
	269.1	153.8			
o-Cresol	103.6	185.2	4.05497	-6.83084	1.00000
	206.1	170.3			
	463.3	153.8			
p-Cresol	118.8	185.2	4.12943	-6.93879	0.99977
	231.7	170.3			
	545.1	153.2			
m-Cresol	116.7	185.2	4.06926	-6.80843	0.99993
	235.6	170.3			
	525.0	153.8			

Table B-15

Specific Retention Volume (ml/g)

Resin: XAD-2

Adsorbate Class: Aliphatic Acids

Adsorbate	V_g^T (ml/g)	Temperature (°C)	Slope	Intercept	Correlation Coefficient
Acetic Acid	50.0	131.1	2.29043	-3.96313	0.99923
	107	109.9			
	238	88.0			
Propionic Acid	117	131.4	2.70997	-4.64209	0.99867
	262	109.9			
	746	88.0			
n-Butanoic Acid	148	151.4	2.59865	-3.97513	0.98817
	263	130.7			
	681	109.8			
n-Pentanoic Acid	289	151.4	2.83271	-4.20089	0.98691
	441	142.2			
	640	130.7			

Table B-16

Specific Retention Volumes (ml/g)

Resin: Tenax-GC

Adsorbate Class: Aliphatic Acids

Adsorbate	V_g^T (ml/g)	Temperature (°C)	Slope	Intercept	Correlation Coefficient
Acetic Acid	25.6	131.3	2.27624	-4.25864	0.99523
	47.1	110.7			
	97.6	90.7			
Propionic Acid	34.4	150.9	2.58210	-4.57032	0.99769
	61.2	131.3			
	149	110.7			
	338	90.7			
n-Butanoic Acid	70.4	150.9	3.01511	-5.26958	0.99988
	156	130.6			
	390	110.7			
	1050	90.7			
n-Pentanoic Acid	127	150.9	3.44349	-6.00272	0.99647
	363	130.6			
	1000	108.9			